



University of Calgary

PRISM: University of Calgary's Digital Repository

Graduate Studies

The Vault: Electronic Theses and Dissertations

2017

Wind Farm Layout Optimization Considering Commercial Turbine Selection and Hub Height Variation

Abdulrahman, Mamdouh Ahmad

Abdulrahman, M. A. (2017). Wind Farm Layout Optimization Considering Commercial Turbine Selection and Hub Height Variation (Unpublished doctoral thesis). University of Calgary, Calgary, AB. doi:10.11575/PRISM/28711
<http://hdl.handle.net/11023/4118>
doctoral thesis

University of Calgary graduate students retain copyright ownership and moral rights for their thesis. You may use this material in any way that is permitted by the Copyright Act or through licensing that has been assigned to the document. For uses that are not allowable under copyright legislation or licensing, you are required to seek permission.

Downloaded from PRISM: <https://prism.ucalgary.ca>

UNIVERSITY OF CALGARY

Wind Farm Layout Optimization Considering Commercial Turbine Selection and Hub Height

Variation

by

Mamdouh Ahmad Abdulrahman

A THESIS

SUBMITTED TO THE FACULTY OF GRADUATE STUDIES
IN PARTIAL FULFILMENT OF THE REQUIREMENTS FOR THE
DEGREE OF DOCTOR OF PHILOSOPHY

GRADUATE PROGRAM IN MECHANICAL AND MANUFACTURING ENGINEERING

CALGARY, ALBERTA

SEPTEMBER, 2017

© Mamdouh Ahmad Abdulrahman 2017

Abstract

New aspects were added to the wind farm layout optimization problem; commercial turbine selection, generic realistic representation for the thrust coefficient, investigating the power-cost of energy trade-off range, and introducing the wind farm layout upgrade optimization problem. A range of commercial turbines was selected and the manufacturers' power curves were used to evaluate the power developed by each turbine using the effective wind speed. The classical Jensen's wake model was implemented to simulate the wake and wake interference within the farm in an analytic and accurate way. A simple field-based cost model was developed to evaluate the cost of any layout in terms of the turbine rated power and hub height. For the upgrade cases, the cost model included an area factor to account the upgraded area to the original farm area. A Genetic Algorithm was used for optimization throughout this dissertation. A technique called Random Independent Multi-Population Genetic Algorithm was used in some cases to accelerate the optimization.

The results showed that co-operative optimization is superior over the selfish one. The turbine aerodynamic efficiency was found to magnify the difference between the two optimization strategies. A wide range of commercial turbines was selected and a useful range of power-cost of energy trade-off was obtained. The optimization was found to be more efficient in offshore cases because of the low entrainment coefficient in the wake model. The Random Independent Multi-Population technique caused a significant reduction in the speed of the optimization. It is likely that most farms can be efficiently and practically upgraded with a wide range of power-cost of energy trade-offs, using the proposed upgrade layout and the optimization objective.

Keywords: Wind farm layout optimization, Layout upgrade optimization, Commercial turbine selection, Hub height variation, Multi-population genetic algorithm, Thrust coefficient, Aerodynamic efficiency, Co-operative optimization, Selfish optimization.

Preface

This thesis collects the research conducted by the candidate under the supervision of Professor D.H. Wood in the field of Wind Farm Layout Optimization (WFLO). Chapter 3, Chapter 4, and Chapter 5 have been published, the citations are:

- Kiani, A., Abdulrahman, M., Wood, D. (2014). Explicit solutions for simple models of wind turbine interference. *Wind Engineering*, 38(2), pp. 167-180.
- Abdulrahman, M., Wood, D. (2015). Some effects of efficiency on wind turbine interference and maximum power production. *Wind Engineering*, 39(5), pp. 495-506.
- Abdulrahman, M., Wood, D. (2017). Investigating the power-COE trade-off for wind farm layout optimization considering commercial turbine selection and hub height variation. *Renewable Energy*, 102 (B) (2017) 267-516.

Chapter 6 has revised and resubmitted to Renewable Energy and is under review:

- Abdulrahman, M., Wood, D. (2017). Large wind farm layout upgrade optimization.
Revised and Submitted on July, 31st 2017 to Renewable Energy.

The candidate has done the computation and the editing for Chapter 4, Chapter 5, and Chapter 6. Professor Wood has done the academic supervision, consultation, and revision.

In Chapter 3, the idea and the formulation were due to Professor Wood, the literature review was done by the candidate, the editing was done mainly by Dr. Kiani, and the revisions were done by the three authors. Although the candidate did not make the major contribution to this work, it is included in the thesis as it provides the background to the subsequent chapters.

Acknowledgements

This research is part of a program of work on renewable energy funded by the Natural Science and Engineering Council (NSERC) and the ENMAX Corporation. The candidate acknowledges the Egyptian Government and Al-Azhar University for providing financial support during the early (and the important) part of this work.

The candidate wants to express his gratefulness to Prof. David Wood for being an exceptional supervisor. David was exceptionally available even in weekends and holidays. He was exceptionally patient during the idle periods of this research. The exceptional supervisor has offered all kinds of support (academic, technical, financial, and spiritual) that any grad student needs to accomplish his/her degree.

The very first brain storming led to this research was attained with the great Professor Faisal El-Refaie, Ex-Dean of the Faculty of Engineering, Al-Azhar University.

The very first steps, problem formulation, and the early supervision were done by the candidate's Godfather in research, Professor El-Adl El-Kady, the current Dean of the Faculty of Engineering, Al-Azhar University.

Dedication

To:

My Mother ... *My Founder* ...

The Memory of My Father ...

The Memory of My Father In-Law ...

My Mother In-Law ... *My Co-Mother* ...

My Wife ... *My Life* ...

My Elder Sister ... *My Younger Mother* ...

My Brother ... *My Father after My Father* ...

My Younger Sister ... *My First Daughter* ...

My Children ... *My Present & Future* ...

Table of Contents

Abstract.....	ii
Preface.....	iv
Acknowledgements	v
Dedication	vi
Table of Contents	vii
List of Tables.....	x
List of Figures and Illustrations	xi
List of Symbols, Abbreviations and Nomenclature	xiv
Chapter 1 : Background.....	1
1.1 Wind Energy.....	1
1.2 Wind Turbines	2
1.3 Wind Turbine Wake and Wake Modelling	4
1.4 Wind Farm Cost Breakdown	6
1.5 The Wind Farm Layout Optimization Problem	8
1.5.1 Design variables.	8
1.5.2 Constraints.....	8
1.5.3 Optimization technique.	9
1.5.4 Optimization objectives.....	10
1.6 Thesis Outline.....	10
1.7 References.....	12
Chapter 2 : Literature Review	16
2.1 Introduction.....	16
2.2 Early Studies.....	17
2.3 Recent Studies	18
2.4 Motivation and Research Objectives	21
2.5 References.....	22
Chapter 3 : Explicit Solutions for Simple Models of Wind Turbine Interference.....	27
3.1 Introduction.....	28
3.2 The Basic Model of Turbines In Line	31
3.3 Optimization of the Power Output.....	32
3.3.1 Selfish optimization.....	32
3.3.2 Co-operative optimization.....	33
3.4 Optimization with Wake Recovery	35
3.4.1 Selfish optimization with wake recovery.....	36
3.4.2 Co-operative optimization with wake recovery.	37
3.5 Optimization Examples and Numerical Simulation	37
3.6 Modeling Turbines In Line with Changing Wind Speed	42
3.7 Conclusions.....	46
3.8 References.....	48
Chapter 4 : Some Effects of Efficiency on Wind Turbine Interference and Maximum Power Production.....	50

4.1	Introduction.....	51
4.2	Wake Model.....	53
4.3	Determining the Induction Factor.....	54
4.4	Details of the Simulations.....	56
4.5	Results and Discussion.....	58
4.6	Conclusions.....	62
Appendix to Chapter 4: The technical specifications for the 8 commercial turbines.		64
4.7	References	66
Chapter 5 : Investigating the Power-COE Trade-Off for Wind Farm Layout Optimization Considering Commercial Turbine Selection and Hub Height Variation		
5.1	Introduction.....	70
5.2	Literature Review	71
5.3	Methodology	73
	5.3.1 Wake model and interference calculations.....	74
	5.3.2 Commercial Turbines and Power Calculations	77
	5.3.3 Commercial Turbine Coefficients	78
	5.3.4 Hub Height Variation.....	80
	5.3.5 Simple Cost Model	81
	5.3.6 Test cases.....	83
	5.3.7 Optimization	85
	 5.3.7.1 <i>Design Variables.</i>	85
	 5.3.7.2 <i>Constraints</i>	86
	 5.3.7.3 <i>Optimization objectives</i>	87
	 5.3.7.4 <i>Optimization technique</i>	87
5.4	Results, and Discussion.....	88
5.5	Conclusions.....	99
5.6	References	101
Chapter 6 : Large Wind Farm Layout Upgrade Optimization		107
6.1	Introduction.....	108
6.2	Horns Rev 1: Background and Reasons for Its Selection	110
6.3	Upgrade Methodology	113
	 6.3.1 Proposed upgraded layouts.....	113
	 6.3.2 Wake model and interference calculations.....	115
	 6.3.3 Commercial turbines and AEP calculations.....	117
	 6.3.4 Hub height variation.....	119
	 6.3.5 Modified simple cost model.....	120
	 6.3.6 Optimization.....	122
6.4	Results and Discussion.....	124
6.5	Conclusions.....	131
6.6	References	133
Chapter 7 : Conclusions and Suggestions for Further Investigations		139
7.1	Introduction.....	139

7.2 Findings from “Explicit Solutions for Simple Models of Wind Turbine Interference”	139
7.3 Findings from “Some Effects of Efficiency on Wind Turbine Interference and Maximum Power Production”.....	140
7.4 Findings from “Investigating the Power-COE Trade-Off for Wind Farm Layout Optimization Considering Commercial Turbine Selection and Hub Height Variation”	141
7.5 Findings from “Large Wind Farm Layout Upgrade Optimization”	142
7.6 Suggestions for Further Investigations	145

List of Tables

Table 5.1: Technical data for the six most selected turbines in decreasing order.	98
Table 6.1: Code, rated power, rotor diameter, and rated speed for the turbines included in the selection.	118
Table 6.2: Illustration of the three objective functions.	122

List of Figures and Illustrations

Figure 1.1: Global wind power cumulative capacity (2001-2016) [2].	1
Figure 1.2: C_P and C_T vs. a , according to the ADT equations.....	3
Figure 1.3: C_T - C_P relation according to the ADT equations, up to the Betz-Joukowsky limit.	4
Figure 1.4: Wind turbine wake structure [11].....	5
Figure 1.5: Capital cost breakdown for a typical onshore wind power project [20].	7
Figure 1.6: Capital cost breakdown for a typical offshore wind power project [20].....	7
Figure 1.7: Flowchart for Genetic Algorithm [29].	10
Figure 2.1: Normalized power curve for GE-1.5 xle-82.5, as developed by Chowdhury et al. [34] and generalized for all turbines as long as the rated power, P_r , the rated speed, U_r , and the cut-in speed, U_{in} , are defined.....	20
Figure 3.1: Total power output from co-operative (symbols) and individual (solid lines) optimization as a function of b . The number of turbines in the line is indicated on the Figure.....	38
Figure 3.2: Ratio of total power output from co-operative optimization to individual optimization. Lines for visual aid only. The number of turbines in the line is indicated on the Figure.	39
Figure 3.3: Wake induction factors for $b = 0.5$. Individual optimization for $N = 12$, shown by diamonds. Other results for co-operative optimization for N indicated by last symbol.....	40
Figure 3.4: Induction factors for co-operative optimization for $N = 5$ as a function of b	40
Figure 3.5: Individual turbine power output for $N = 6$ and b as indicated for co-operative (top Figure) and individual (bottom Figure) optimization. Value of b indicated in legend.....	41
Figure 3.6: Maximum power output of two turbines for selfish (solid lines) and co-operative (dotted lines) optimization for a range of k . The value of b is indicated on each curve. The heavy dashed line indicates the power output with the first turbine shut down.	46
Figure 4.1: C_T vs U for the 8 wind turbines described in the Appendix compared with Equation (4.9) and $C_T = 0.88$	55
Figure 4.2: C_T vs C_P for the 8 wind turbines described in the Appendix compared to that from Equations (4.10) and (4.11).....	56
Figure 4.3: Comparison of the two efficiencies for turbines 1-3. The left Figure shows η_a and the right η_c	57

Figure 4.4: The local aerodynamic power coefficient for co-operative and selfish cases. From the top left Figure the values of η_a are 0.75, 0.80, and 0.85. From the bottom left Figure the values of η_a are 0.90, 0.95, and 1.0.....	58
Figure 4.5: The local blade axial induction factor for co-operative and selfish cases. From the top left Figure the values of η_a are 0.75, 0.80, and 0.85. From the bottom left Figure the values of η_a are 0.90, 0.95, and 1.0	59
Figure 4.6: The global aerodynamic power coefficient for co-operative and selfish cases. From the top left Figure the values of η_a are 0.75, 0.80, and 0.85. From the bottom left Figure the values of η_a are 0.90, 0.95, and 1.0	60
Figure 4.7: The sum of the global power coefficients for the co-operative cases.	60
Figure 4.8: The sum of the global power coefficients for the selfish cases.....	61
Figure 4.9: The ratio of selfish to co-operative total power.	61
Figure 5.1: A front view (parallel to wind direction) illustrates the overlap of the upwind turbine wake (the dashed circle) with the downwind turbine rotor (the solid circle). The Y co-ordinate is into the page.	74
Figure 5.2: Validation of Jensen wake model against data from Horns Rev 1 offshore wind farm.	77
Figure 5.3: General representation for the thrust coefficient, C_T , vs the aerodynamic and the electric power coefficients, $C_{P,a}$ and $C_{P,e}$, respectively, compared with $C_T - C_{P,a}$ curves obtained for NREL 5 MW reference turbine at different values of pitch angle, β	80
Figure 5.4: Reference TIL, array, and staggered SWF layouts.	85
Figure 5.5: Flowchart for Genetic Algorithm.	88
Figure 5.6: Normalized P and TCI to the reference layout for onshore TIL as a function of S . ..	91
Figure 5.7: Normalized P and TCI to the reference layout for offshore TIL as a function of S ... Figure 5.8: Normalized P and TCI to the reference layout for onshore SWF as a function of S	92
.....	95
Figure 5.9: Normalized P and TCI to the reference layout for offshore SWF as a function of S	96
Figure 5.10: Frequency of turbine and H selection for TIL cases.	97
Figure 6.1: The percentage global cumulative installed wind capacity, relative to 2015, adapted from Ref. [2].	109

Figure 6.2: Frequency of occurrence, f , of wind speed and direction at hub height for Horns Rev 1, adapted from Ref. [23].	112
Figure 6.3: Proposed upgraded layouts for Horns Rev 1 wind farm. (a): inside. (b): outside. The existing turbines are numbered from 1 to 80 (in black), while the added turbines are numbered from 81 (in red).	114
Figure 6.4: A front view (parallel to wind direction) illustrates the overlap of the upwind turbine wake (the dashed circle) with the downwind turbine rotor (the solid circle). The Y co-ordinate is into the page [22].	116
Figure 6.5: H_{max} , H_{max} , and HHR as function of D in the investigated range.	120
Figure 6.6: Normalized AEP, TCI, and COEI for single turbine layouts.....	126
Figure 6.7: Normalized AEP, TCI, and COEI for multi-turbine layouts.....	128
Figure 6.8: Rated power distribution for the selected turbines for all multi-turbine cases.....	129
Figure 6.9: Coefficient of height, C_H , distribution for all multi-turbine cases.	129
Figure 6.10: Frequency of turbine selection for multi-turbine cases.	130
Figure 6.11: Frequency of C_H selection for multi-turbine cases, with bin width = 0.05.	130
Figure 7.1: TCCI vs NCOEI.	144
Figure 7.2: TCCI dependence on P_r and D	144

List of Symbols, Abbreviations and Nomenclature

Abbreviations

Abbreviation	Definition
ADT	Actuator Disk Theory
AEP	Annual Energy Production
AF	Area Factor
CC	Capital Cost
CCI	Capital Cost Index
CF	Capacity Factor
COE	Cost Of Energy
COAEI	Cost Of Added Energy Index
COTEI	Cost Of Total Energy Index
GA	Genetic Algorithm
HAWT	Horizontal-Axis Wind Turbine
HHR	Hub Height Range
LCOE	Localized Cost Of Energy
MGC	Minimum Ground Clearance
MTH	Maximum Tip Height
NAEP	Normalized Annual Energy Production
NCOEI	Normalized Cost Of Energy Index
NTCI	Normalized Total Cost Index
ObjFun	Objective Function

O&M	Operation and Maintenance
PS	Population Size
RIM-GA	Random Independent Multi-Population Genetic Algorithm
SWF	Small Wind Farm
TC	Total Cost
TCI	Total Cost Index
TCIOP	Total Cost Index per Output Power
TCCI	Turbine Cost of energy Comparison Index
TIL	Turbine In Line
TolFun	Tolerance Function
WFLO	Wind Farm Layout Optimization
WFLUO	Wind Farm Layout Upgrade Optimization

Subscripts

Subscript	Definition
a	Aerodynamic
a	Ambient
b	Blade
exp	Expansion
H	Height
i	Upwind turbine

j	Downwind turbine
k	Counter
o	Original
o	Free stream
P	Power
$nominal$	Nominal rotor diameter
r	Rated
ref	Reference
T	Thrust
w	Wake
x	Crosswind distance
y	Downwind distance

English Symbols

Symbol	Definition
A	Rotor area
A_{ij}	Overlap area
a	Blade axial induction factor
b	Wake recovery factor
C_P	Power coefficient
C_H	Coefficient of height
C_T	Thrust coefficient

c_{ik}	Polynomial coefficient
D	Rotor diameter
D_{exp}	Expansion diameter
$D_{w,ij}$	Wake diameter
$D_{nominal}$	Nominal diameter
f	Frequency of occurrence
G, g	Number of generations
H	Hub height
H_{ref}	Reference height
i, j, k, m, n	Counters
I	Inside upgraded layout
K	Degree of polynomial
k	Wind speed factor
k	Wake expansion coefficient
L	Line length
M	Number of added turbines
N	Number of existing turbines
n	Number of independent initial populations
O	Outside upgraded layout
P	Power
P_r	Rated power
p	Pressure
p_a	Ambient pressure

R	Rotor radius
R_{exp}	Expansion radius
$R_{w,ij}$	Wake radius of the
S	Turbine spacing multiplier
T	Thrust force
U, V	Local wind speed
U_a, V_a	Ambient wind speed
U_b	Wind speed at blade section
U_i	Effective wind speed
U_{in}	Cut-in speed
U_o	Free stream wind speed
U_r	Rated speed
U_{ref}	Reference wind speed
U_w	Wind speed within the wake
Y	Main wind direction
z_o	Roughness length

Greek Symbols

Symbol	Definition
α	Wake expansion coefficient
β	Pitch angle
Δn	sum of the power coefficients from terms

	involving a_n
Δx_{ij}	Crosswind distance
Δy_{ij}	Downwind distance
δU_{ij}	Single wake velocity deficit
δU_i	Multiple wake velocity deficit
η	Turbine efficiency
θ	Wind direction angle

Chapter 1 : Background

1.1 Wind Energy

Wind energy is one of the most promising and fastest growing sources of renewable energy worldwide. It has become one of the most competitive sources of electricity, not only among renewable energy sources but also compared with conventional fossil fuels [1]. The global cumulative installed wind capacity exceeded 486 GW by the end of 2016 [2]. Wind power represents about 6 % of the global electricity capacity [3] and about 3.7 % of the global electricity generation [1,4] of all energy sources. Among renewable energy sources, wind energy capacity is more than 23% and 55% of the worldwide renewable installed capacity (with and without the hydropower, respectively) [1]. Wind energy also is the second highest growing renewable energy source (after solar photovoltaics) [1]. Figure 1.1 shows the global wind power cumulative capacity from 2001 to 2016.

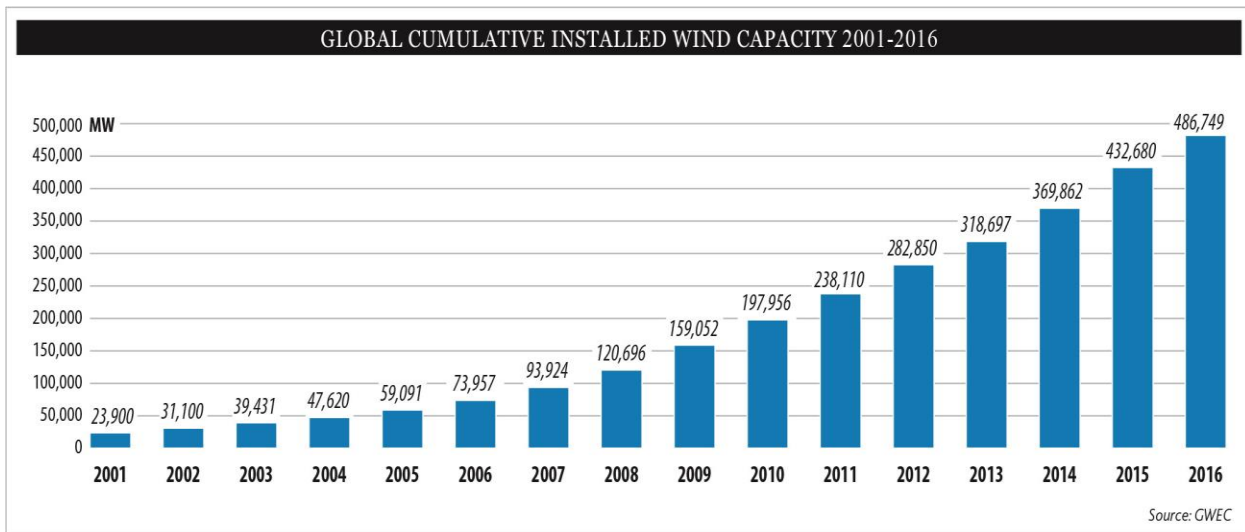


Figure 1.1: Global wind power cumulative capacity (2001-2016) [2].

1.2 Wind Turbines

Wind turbines convert a fraction of the wind's kinetic energy into mechanical energy by direct contact with its blades. Wind turbines are classified according to the direction of the axis of rotation into two categories: horizontal-axis wind turbines and vertical-axis wind turbines. The former is the most widely used and it is also the type considered in the proposed work, so reference will only be made to "wind turbine(s)" or even "turbine(s)" throughout this thesis.

Wind turbines are specified by geometrical and operational parameters as well as performance curves. The main geometrical parameters are the number of blades, the rotor diameter, D , and the hub height, H . The major operational parameters are the power coefficient, C_P , the thrust coefficient, C_T , which are defined as

$$C_P = \frac{\text{output power}}{\text{available power}} = \frac{P}{0.5\rho AU^3} \quad (1.1)$$

$$C_T = \frac{\text{thrust force}}{\text{dynamic force}} = \frac{T}{0.5\rho AU^2} \quad (1.2)$$

where ρ is the average air density (kg/m^3), A is the rotor area (m^2), and U is the wind speed (m/s) ahead of the turbine.

These two dimensionless parameters, C_P and C_T , as well as the blade axial induction factor, a , are mutually dependent. The basic Actuator Disk Theory (ADT) [5] provides the theoretical relations:

$$C_P = 4a(1 - a)^2 \quad (1.3)$$

$$C_T = 4a(1 - a) \quad (1.4)$$

The blade axial induction factor, a , is defined as the axial wind velocity deficit at the rotor, which expressed mathematically in terms of the upwind speed, U , and that at the rotor, U_b , as

$$a = \frac{U - U_b}{U} = 1 - \frac{U_b}{U} \quad (1.5)$$

Figure 1.2 provides graphical representation for Equations (1.3) and (1.4), while Figure 1.3 shows the C_T - C_P curve according to the ADT analysis. Compared with commercial turbines, Equations (1.3) and (1.4) overestimate C_P for a particular C_T (or underestimate C_T for a particular C_P), as will be proven later in Chapter 4 and Chapter 5. ADT also indicates that no more than 16/27 of the kinetic energy that possessed by the air passing through a wind turbine rotor can be converted into mechanical energy. This value is the maximum theoretical C_P for a wind turbine (known as the Betz- Joukowsky limit), when $a = 1/3$ and $C_T = 8/9$, as indicated in Figure 1.2 by the dashed vertical line.

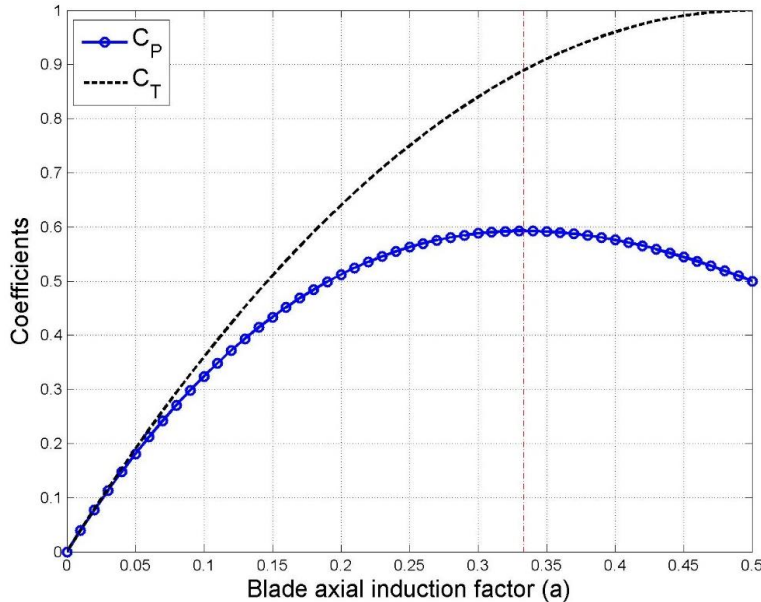


Figure 1.2: C_P and C_T vs. a , according to the ADT equations.

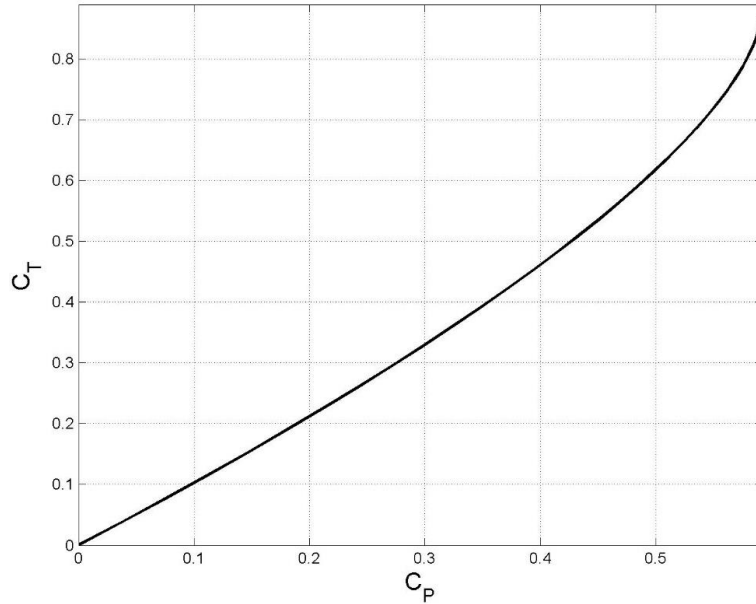


Figure 1.3: C_T - C_P relation according to the ADT equations, up to the Betz-Joukowsky limit.

1.3 Wind Turbine Wake and Wake Modelling

By absorbing part of the wind's kinetic energy, the wake behind the turbine rotor is characterized by decreased wind speed and increased turbulence. The entrainment of the ambient (undisturbed) air into the wake eventually leads to recovery so that far from a turbine the wind speed and turbulence will have effectively returned to the undisturbed values. Wind turbine wake modelling consists of characterizing the air flow (mainly the velocity and the turbulence level) downstream of the rotor.

The wake behind a wind turbine has two main regimes: near wake, and far wake, e.g. [6,7]. The near wake, dominated by the tip and hub vortices, extends a few rotor diameters downstream, where which the velocity deficit at the centerline reaches its maximum and the pressure equals the free stream value [8]. On the other hand, the far wake is the region in which the actual rotor shape is less important, but the focus lies on wake modeling, wake interference, turbulence modelling

and topographic effects, e.g. [6,9]. A third region may be considered between near and far wakes, called transition, e.g. [8,9,10], or intermediate wake [11]. Figure 1.4 illustrates the flow structure of a typical wind turbine wake.

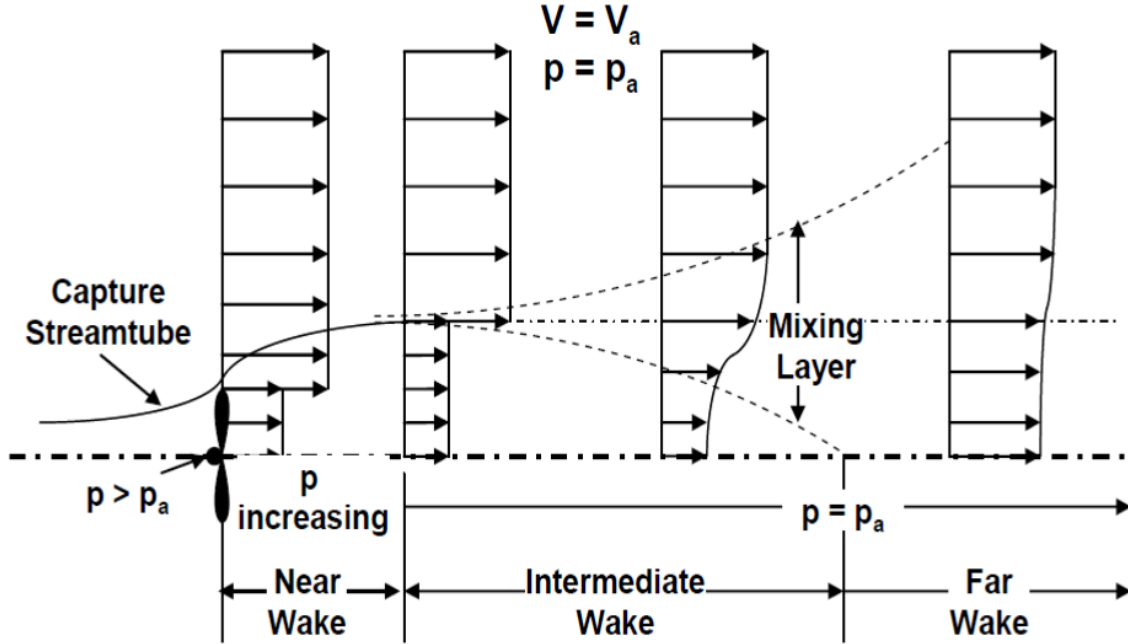


Figure 1.4: Wind turbine wake structure [11].

Many wake models have been developed over the past five decades, extensive details can be found in the review articles, e.g. [12,10,9,6,13]. For the present purposes, the aerodynamics of wind turbines can be divided into two principal domains [14]:

- I. The prediction of rotor performance (focusing only on the near wake).
- II. The study of the wake (mainly the far wake) to evaluate the influence of wind turbines in farms (which is the aspect of relevance to the current research).

The output power from a single wind turbine is limited (up to few MW), so wind turbines are commonly installed in groups (wind farms) to increase the energy production. Any wind turbine

in a wind farm is affected by the wake(s) of the upwind turbine(s). Wake overlap (interference) significantly affects the performance of the whole farm, especially downstream the first few upwind rows, e.g. [10,15,16,17,18,19], after which their multiple wakes are merged [17].

1.4 Wind Farm Cost Breakdown

Although the wind is blowing freely, the conversion of wind's kinetic energy into useful electrical power is not free. The wind power Cost Of Energy (COE) significantly varies over time and location and it also affected by the wind resources and the farm size, e.g. [20,21]. The major cost of a wind power project is due to the initial capital cost, which represents more than 70 % and up to 89 % of the total cost over the life span [22]. The operations and maintenance costs can be represented globally as 11 - 30 % of the total cost over the life span [22] or annually as 1.5 - 3 % of the initial capital cost [23].

The capital cost, in turn, is due to turbines, balance of the system, and financial costs [20]. The turbine cost represents the major part for onshore projects, while the balance of the system cost is the major part of the offshore ones, as shown in Figure 1.5 and Figure 1.6, respectively.

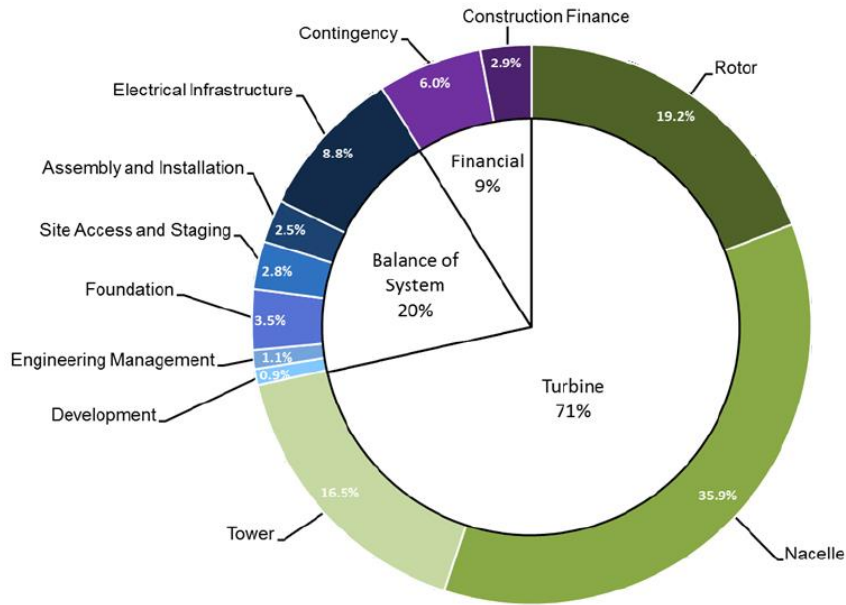


Figure 1.5: Capital cost breakdown for a typical onshore wind power project [20].

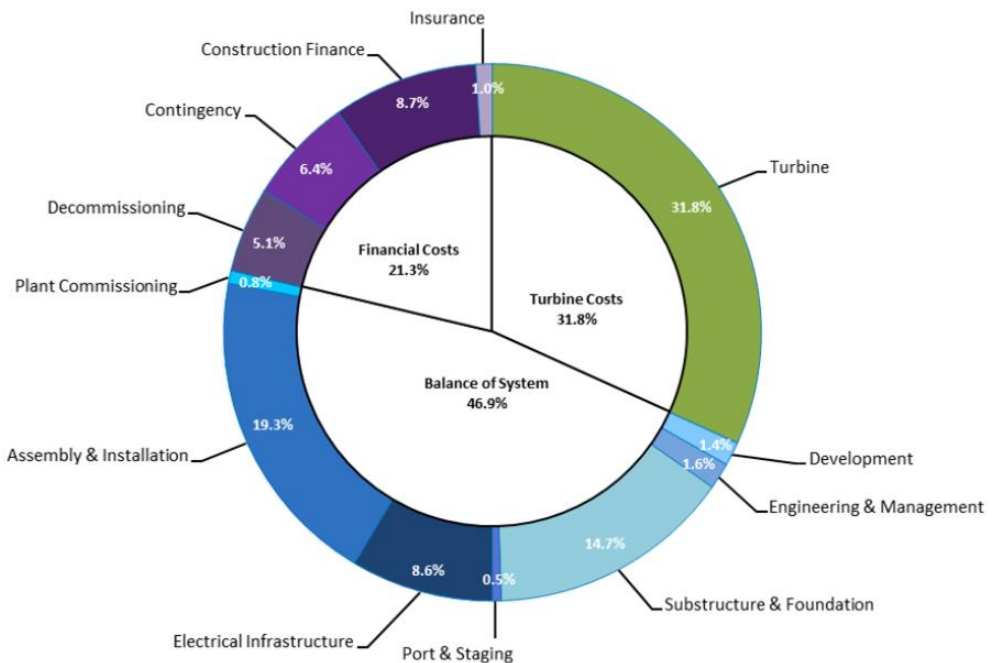


Figure 1.6: Capital cost breakdown for a typical offshore wind power project [20].

1.5 The Wind Farm Layout Optimization Problem

As the wind power market expands, it faces increasing challenges, which can be classified into three main categories: technical, financial, and environmental. For example, to produce more power from a wind farm, the number of turbines should increase and the turbines should be larger. Besides, the turbines should be spaced further apart in order to reduce the wake interference. On the other hand, larger turbines and/or larger wind farm area mean more cost (turbines, land, roads, cables, etc.). Moreover, many restrictions have been put on wind farm installations because of their environmental impact regarding noise, visual effects, flight paths, and even birds' seasonal immigration routes. All these factors increase the need for Wind Farm Layout Optimization (WFLO), which investigates the ways to design wind farms so that the power is maximized while the cost as well as the unwanted environmental impacts are minimized.

Any optimization problem, including the WFLO, consists of the four fields described in the following sub-sections, e.g. [24,25]:

1.5.1 Design variables.

The design (or decision) variable is the parameter that needs to be determined (adjusted) in order to achieve the optimum solution, e.g. [38,26,1]. The design variables must have upper and lower limits within which the feasible solutions are obtained.

1.5.2 Constraints.

Optimization problems are usually subjected to restrictions (constraints), and hence not all solutions are feasible. The upper and lower limits for the design variables are the simplest form of constraints, and the integer constraint is another example, in which one (or more) of the design

variables, such as number of turbines, is (are) necessarily integer. Both upper and lower limits as well as the integer constraints are linear, moreover, most the engineering optimization problems are subjected to other constraints (linear and/or nonlinear) according the physics of the problem. In the WFLO, the minimum turbine spacing is the most common nonlinear constraint on turbine siting inside the farm is restricted.

1.5.3 Optimization technique.

The best optimization technique depends mainly on the nature of the problem as well as the constraints. The present optimization problem is discrete, non-linear, non-convex, high-dimensional, and mixed integer. Genetic algorithms (GAs) have been proven a powerful tool for such complex problems, e.g. [27]. For this reason, GAs were implemented in most the WFLO literature, although they are slow compared with the other optimization methods [26,1]. GAs are computer programs that mimic the processes of biological evolution in order to solve problems and to model evolutionary systems [28]. The solution is obtained by moving from one population of chromosomes (feasible solutions) to a new population by using a kind of natural selection (random search) together with the genetics-inspired operators of crossover, mutation, inversion, etc. Each chromosome consists of a number of genes that are the possible values of the design variables. The selection operator chooses those chromosomes in the population that will be allowed to reproduce, and on average the fitter chromosomes produce more offspring than the less fit ones [28]. A flowchart for GA used in the present work [29] is given in Figure 1.7.

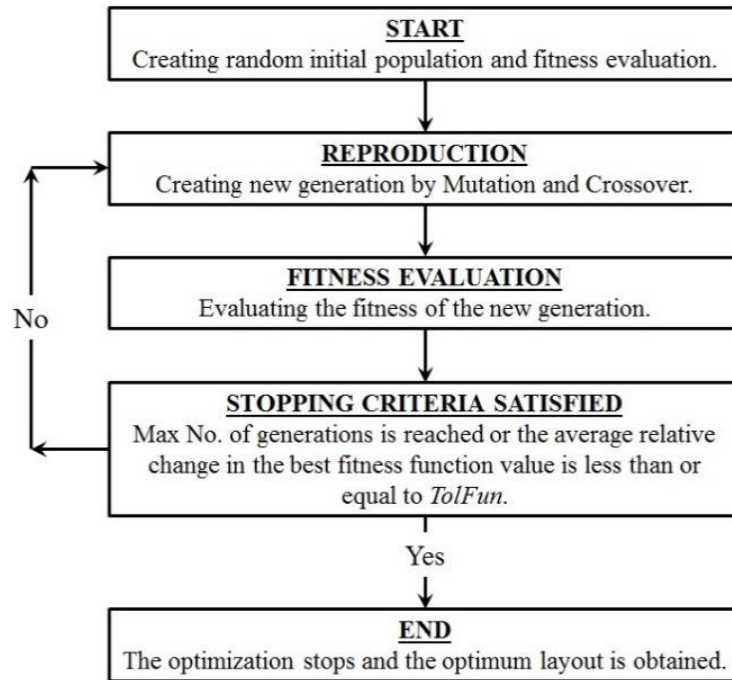


Figure 1.7: Flowchart for Genetic Algorithm [29].

1.5.4 Optimization objectives.

An objective (fitness) function is simply the function that its value is to be optimized (maximized or minimized), e.g. [26,1]. The objective in most of the WFLO literature is to maximize energy production, minimize cost of energy, COE, maximize profit, or a combination of them [19].

1.6 Thesis Outline

An introduction to the topic of this thesis is given in this chapter. A literature review for the WFLO problem followed by the motivation and research objectives are provided in Chapter 2. The rest of the thesis is arranged as follows:

The selfish (individual) and the co-operative (collective) control alternatives for wind farms are the topic of Chapter 3. The arrangement of Turbines In Line (TIL) is considered, as it gives the maximum wake interference. The effect of wake recovery and topology are investigated.

The different efficiencies of commercial wind turbines relative to the ADT is introduced in Chapter 4. The effect of the aerodynamic efficiency on the maximum power production is investigated for both selfish and co-operative optimization strategies.

In Chapter 5, the power-COE trade-off is investigated. Selection among 61 commercial turbines and common range of hub height variation are considered. The optimization is carried out on two simple wind farm arrangements; 6 TIL and a 6-by-3 matrix of turbines.

Wind Farm Layout Upgrade Optimization (WFLUO) for existing farms is introduced in Chapter 6. The famous large offshore wind farm (Horns Rev 1) is taken as case study. The power-COE trade-off for both inside and outside upgrades are investigated. Commercial turbine selection and turbine-specific hub height variation are employed. The cost model is modified and the GA is improved by using Random Independent Multi-Population technique.

Finally, in Chapter 7, the chapters are concluded and the logical sequence of the different chapters as one unit is explained.

1.7 References

1. REN21. 2016. Renewables 2016 Global Status Report (Paris: REN21 Secretariat). ISBN 978-3-9818107-0-7.
2. Global Wind Statistics 2016 (2017). Global Wind Energy Council GWEC.
3. <http://www.tsp-data-portal.org/Breakdown-of-Electricity-Capacity-by-Energy-Source#tspQvChart> [last accessed: Dec. 2016].
4. <http://www.gwec.net/global-figures/wind-in-numbers/> [last accessed: Dec. 2016].
5. Froude, R. E. (1889). On the part played in propulsion by difference in pressure. Transaction of the Institute of Naval Architects, 30, pp. 390-423.
6. Sanderse, B. (2009). Aerodynamics of wind turbine wakes: literature review. ECN-e--09-016.
7. Rathmann, O., Frandsen, S., Barthelmie, R. (2007). Wake modelling for intermediate and large wind farms. Wind Energy Conference and Exhibition, Paper BL3.199.
8. Ecen, P.J., Bot, E.T.G., (2010). Improvements to the ECN wind farm optimisation software "FarmFlow". ECN-M--10-055 , Presented at European Wind Energy Conference and Exhibition, Warsaw, Poland.
9. Vermeer, L.J., Sørensen, J.N., Crespo, A. (2003). Wind turbine wake aerodynamics. Progress in Aerospace Sciences, 39, pp. 467–510.
10. Crespo, A., Hernandez, J., Frandsen, S. (1999). Survey of modelling methods for wind turbine wakes and wind farms. Wind Energy, 2, pp. 1-24.
11. Werle, M.J. (2008). A new analytical model for wind turbine wakes. FloDesign Inc. Wilbraham MA, REPORT No. FD 200801.

12. Bossanyi, E. A., Maclean, C., Whittle, G. E., Dunn, P. D., Lipman, N. H., Musgrove, P. J. (1980). The efficiency of wind turbine clusters. Proceedings of the 3rd International Symposium on Wind Energy Systems, Lyngby, pp. 401-416.
13. Sanderse, B. (2011). Review of computational fluid dynamics for wind-turbine wake aerodynamics. *Wind Energy*, 14, pp. 799–819.
14. El Kasmi, A., Masson, C. (2008). An extended $k - \epsilon$ model for turbulent flow through horizontal-axis wind turbines. *Journal of Wind Engineering and Industrial Aerodynamics*, 96, pp. 103–122.
15. Katic, I., Hojstrup, J., Jensen, N.O. (1986). A simple model for cluster efficiency. In Proceedings of the European Wind Energy Association Conference and Exhibition, pp. 407–410.
16. Frandsen, S., Chacon, L., Crespo, A., Enevoldsen, P., Gomez-Elvira, R., Hernandez, J., Højstrup, J., Manuel, F., Thomsen, K., Sørensen, P. (1996). Measurements on and modelling of offshore wind farms. Editor: Frandsen, S., Risø-R-903(EN), 100 p.
17. Frandsen, S., Barthelmie, R., Pryor, S., Rathmann, O., Larsen, S., Højstrup, J., Thøgersen, M. L. (2006). Analytical modelling of wind speed deficit in large offshore wind farms. *Wind Energy*, 9, pp. 39–53.
18. Kiani, A., Abdulrahman, M., Wood, D. (2014). Explicit solutions for simple models of wind turbine interference. *Wind Engineering*, 38(2), pp. 167-180.
19. Tesauro, A., Réthoré, P-E, Larsen, G.C. (2012). State of the art of wind farm optimization. Proceedings of European Wind Energy Conference & Exhibition, European Wind Energy Association (EWEA 2012), Copenhagen, Denmark.

20. Mone, C., Hand, M., Bolinger, M., Rand, J., Heimiller, D., Ho, J. (2017). 2015 Cost of Wind Energy Review. Technical Report, NREL/TP-6A20-66861, Revised May 2017. [<https://www.nrel.gov/docs/fy17osti/66861.pdf>]
21. REN21. 2016. Renewables 2016 Global Status Report. (Paris: REN21 Secretariat). ISBN 978-3-9818107-0-7.
22. Schwabe, P., Lensink, S., Hand, M. (2011). IEA wind task 26: multi-national case study of the financial cost of wind energy. Work Package 1, Final Report, NREL Report No. TP-6A20-48155.
23. Manwell, J.F., McGowan, J.G., Rogers, A.L. (2009) Wind energy explained: Theory, Design and Application, Second Edition, John Wiley & Sons, Ltd, Chichester, UK.
24. Boyd, S., Vandenberghe, L. (2009). Convex Optimization. Cambridge University Press, New York.
25. Baldick, R. (2008). Applied Optimization, Formulation and algorithms for engineering systems. Cambridge University Press, New York.
26. Samorani, M. (2010). The wind farm layout optimization problem. Technical Report, Leeds School of Business, University of Colorado.
27. Kwong P., Zhang P.Y., Romero D.A., Moran J., Morgenroth M., Amon C.H. (2012). Wind farm layout optimization considering energy generation and noise propagation. In Proceedings of the ASME International Design Engineering Technical Conferences.
28. Melanie, M. (1999). An introduction to genetic algorithms. 5th Printing, MIT Press, Cambridge, Massachusetts, USA.

29. Abdulrahman, M., Wood, D. (2017). Investigating the power-COE trade-off for wind farm layout optimization considering commercial turbine selection and hub height variation. Renewable Energy, 102 (B), pp. 267-516.

Chapter 2 : Literature Review

2.1 Introduction

As mentioned in section 1.5; the WFLO is the problem of designing wind farms so that the power is maximized while the cost as well as the unwanted environmental impacts are minimized. The interest in WFLO increased over the time as the installation of new large wind farm faces technical, financial, and environmental challenges. WFLO is relatively new area of research; in 1994, Mosetti et al. [1] studied this problem for the first time. They considered 10x10 square cells of length 200 m, in which the 40 m rotor diameter turbines were possibly centered. Identical turbines with constant thrust coefficient, $C_T = 0.88$, as well as simple cubic power curve were considered.

Three cases were studied:

- (1) uniform wind direction with constant wind speed,
- (2) multi-directional wind with constant mean wind speed, and
- (3) multi-directional wind with variable speeds.

The analytical Jensen's wake model [2,3] was used to evaluate the wake behind the turbines. A GA was implemented to maximize a combined objective function including the total power and the inverse of the COE, using arbitrary weighting factors.

For the following decade, no significant contribution was added to WFLO. New aspects were then added; either to the design variables, constraints, objective functions, and/or to the optimization methodology.

Many researchers have analyzed the problem proposed by [1] in order to obtain better layouts and/or reduce the computational time; either with some improvements to the GA, e.g. [4,5,6,7] or by implementing other optimization strategies, e.g. [8,9,10,11,12].

2.2 Early Studies

Ozturk et al. [13] introduced a heuristic methodology to find layouts that maximize profit, which is the product of the cost efficiency of the turbines and the total power output from the wind farm. To evaluate their solution methodology, they constructed six test problems with different siting area sizes.

Şişbot et al. [14] employed a multi-objective GA approach to optimize the layout for a particular wind farm in order to maximize the power production while constraining the cost of installed turbines.

Many other biologically-inspired algorithms have been also applied successfully for WFLO. As examples: Particle Swarm Optimization [15,16], Ant Colony Optimization [17], Coral Reef Optimization [18], and Viral Based Optimization [19].

Mixed Integer Programming (MIP) was proved to be a powerful tool in WFLO [20]. Many Linear and Nonlinear MIP models have been developed and improved to find optimum layouts as well as reducing the computational time, e.g. [21,22,23,20,24]. Monte Carlo Simulation [8,25] and Simulated Annealing [26,27] were also successfully implemented for WFLO.

Landowner decisions and participation rates have been modeled as design variables and their impact on WFLO has been investigated in series of publications by Chen and MacDonald [28,7,29].

Recently, noise propagation has been added to the problem. Fagerfjäll [30] and Zhang et al. [31] considered the noise level as a constraint in their optimization using Mixed Integer Programming. Kwong et al. [32] considered noise level minimization as a second objective function (beside the power production maximization) in their multi-objective optimization using the Non-dominated Sorting Genetic Algorithm-II (NSGA-II) algorithm.

Very few studies have considered using different turbines and hub heights; these will be reviewed in more detail in the next subsection.

2.3 Recent Studies

Herbert-Acero et al. [26] maximized the power production by a line of turbines in the wind direction, using both Simulated Annealing and a Genetic Algorithm implemented in MATLAB. This arrangement maximizes the power loss by interference. They used the technical data for REpower, MD77 (rotor diameter, $D = 77$ m). Two values of hub height (H) were used, 50 m and 85 m, to reduce the effect of wake interference. The design parameters were the number of turbines, their location, and the individual H while fixing the line length at 1,550 m. The results showed that the placement of wind turbines with different heights could increase the power generation in a straight line layout for a single wind speed and two opposite wind directions along the line.

Chowdhury et al. [33,16] applied their Unrestricted Wind Farm Layout Optimization to optimize the farm layout, simultaneously with the appropriate selection of turbines in terms of D (while fixing H), in order to maximize the total power generation. Three different layout optimization cases were considered:

- (1) Wind farm with identical turbines,
- (2) Wind farm with differing D , and
- (3) Wind farm with identical turbines that can adapt to wind conditions (variable a depending on the wind speed) as in the case of commercial turbines.

They found that an optimal combination of wind turbines with differing rotor diameters can appreciably increase the farm power generation. They mentioned that a more practical wind farm

optimization requires the treatment of rotor diameters as discrete design variables, as there is only a limited choice of commercial wind turbines.

Chowdhury et al. [34] significantly improved their method, enabling it to simultaneously optimize the placement and the selection of turbines for commercial-scale wind farms to minimize the COE. The number of turbines and the farm size were assumed to be fixed at the values for the particular wind farm that they studied. They used the GE 1.5 xle-82.5 as the reference turbine and normalized the manufacturer's power curve with respect to the general specifications (rated power (P_r), cut-in and rated speeds, U_{in} and U_r , respectively). This curve was assumed to hold for all commercial turbines and scaled back to represent the power curve for any turbine (in the rated power range from 0.6 to 3.6 MW) as long as the general specifications are defined, as shown in Figure 2.1.

The results showed significant increase in energy production by simultaneous optimization of the layout and the turbine selection compared with layout optimization alone. The optimum layout contained turbines with rated power from 1.8 to 3 MW, with rotor diameters from 90 to 110 m, and hub heights from 80 to 120 m.

Chen et al. [35] investigated the use of different H in a small wind farm layout optimization using the GA function in MATLAB. They first conducted the layout optimization of a 500 m square wind farm. Enercon E40-600kW turbines were used in the analysis with two values of hub height, 50 and 78 m, and the minimum spacing was set as 100 m. Then a larger wind farm (2800 m x 1200 m) with larger wind turbine (GE 1.62-100) was analyzed to further examine the benefits of using different hub heights (80 and 100 m) in more realistic conditions. The minimum spacing was set as 400 m. Different cost models were used in the analysis, and results showed that different hub height wind turbines can increase the power production and/or reduce the COE.

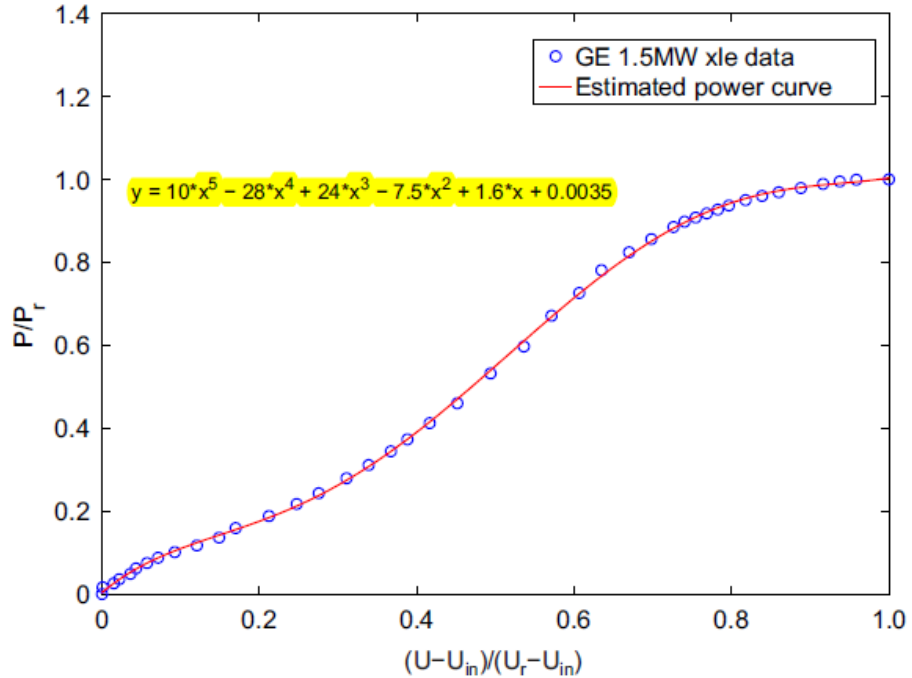


Figure 2.1: Normalized power curve for GE-1.5 xle-82.5, as developed by Chowdhury et al. [34] and generalized for all turbines as long as the rated power, P_r , the rated speed, U_r , and the cut-in speed, U_{in} , are defined.

Tong et al. [36], based on their previous work [16,37,38,34], have proposed a bi-level multi-objective optimization framework considering the capacity factor and the land use as objective functions. The capacity factor (CF) of a wind farm can be defined as the ratio of the actual (or expected) output of the farm over a time period and the potential output if the farm was operating at full nameplate capacity throughout that time period, e.g. [34]. Identical turbines were assumed, and the design variables were the turbine locations, the land area, and the nameplate or rated capacity. The model aimed to investigate the trade-off between the CF and the land use and its effect on the optimum capacity.

2.4 Motivation and Research Objectives

By reviewing the WFLO literature, some deficiencies can be identified. The proposed work aims to fill these gaps by adding the following dimensions to WFLO, which are considered also the novelties of the presented work:

- (1) The selection among a range of actual (commercial) turbines,
- (2) The realistic evaluation of the turbine C_T , and hence the wake development, and
- (3) Investigating the power-COE trade-off for WFLO, and
- (4) Exploring the possibility and the feasibility for existing wind farms to be upgraded either by extra turbines within the original farm area or outside that area.

2.5 References

1. Mosetti, G., Poloni, C., Diviacco, B. (1994). Optimization of wind turbine positioning in large wind farms by means of a genetic algorithm. *Journal of Wind Engineering and Industrial Aerodynamics*, 51, pp. 105-116.
2. Jensen, N.O. (1983). A note on wind generator interaction. Risø-M-2411, Risø National Laboratory.
3. Katic, I., Hojstrup, J., Jensen, N.O. (1986). A simple model for cluster efficiency. In *Proceedings of the European Wind Energy Association Conference and Exhibition*, pp. 407-410.
4. Grady, S.A., Hussaini, M.Y., Abdullah, M.M. (2005). Placement of wind turbines using genetic algorithms. *Renewable Energy*. 30(2), pp. 259-270.
5. Hou-Sheng, H. (2007). Distributed genetic algorithm for optimization of wind farm annual profits. *International Conference on Intelligent Systems Applications to Power Systems*, ISAP 2007, Kaohsiung, Taiwan.
6. Emami, A., Noghreh, P. (2010). New approach on optimization in placement of wind turbines within wind farm by genetic algorithms. *Renewable Energy*, 35, pp. 1559-1564.
7. Chen, L., MacDonald, E. (2012). Considering landowner participation in wind farm layout optimization. *Journal of Mechanical Design*, 134, 084506-1:6.
8. Marmidis, G., Lazarou, S., Pyrgioti, E. (2008). Optimal placement of wind turbines in a wind park using monte carlo simulation. *Renewable Energy*, 33, pp. 1455–1460.
9. González, J.S., Gonzalez Rodriguez, A.G., Mora, J.C., Santos, J.R., Payan, M.B. (2010). Optimization of wind farm turbines layout using an evolutive algorithm. *Renewable Energy*, 35(8), pp. 1671-1681.

10. Ituarte-Villarreal, C.M., Espiritu, J.F. (2011). Wind turbine placement in a wind farm using a viral based optimization algorithm, *Procedia Computer Science*, 6, pp. 469–474.
11. Turner, S.D.O., Romero, D.A., Zhang, P.Y., Amon, C.H., Chan, T.C.Y. (2014). A new mathematical programming approach to optimize wind farm layouts. *Renewable Energy* 63(c), pp. 674–680.
12. Zhang, P.Y., Romero, D.A., Beck, J.C., Amon, C.H. (2014). Solving wind farm layout optimization with mixed integer programming and constraint programming. *EURO Journal on Computational Optimization*, 2(3), pp. 195-219.
13. Ozturk, U.A, Norman B.A. (2004). Heuristic methods for wind energy conversion system positioning. *Electric Power Systems Research*, 70, pp. 179–185.
14. Şişbot, S., Turgut, Ö., Tunç1and, M., Çamdalı, Ü. (2010). Optimal positioning of wind turbines on gökçeada using multi-objective genetic algorithm. *Wind Energy*, 13(4), pp. 297–306.
15. Wan, C., Wang, J., Yang, G., Zhang, X. (2010). Optimal micro-siting of wind farms by particle swarm optimization. In: *Advances In Swarm Intelligence*, Berlin, Heidelberg, pp. 198-205.
16. Chowdhury, S., Zhang, J., Messac, A., Castillo, L. (2012). Unrestricted wind farm layout optimization (UWFLO): Investigating key factors influencing the maximum power generation. *Renewable Energy*, 38(1), pp. 16–30.
17. Eroğlu, Y., Seçkiner S.U. (2012). Design of wind farm layout using ant colony algorithm. *Renewable Energy*, 44, pp. 53-62.

18. Salcedo-Sanz, S., Gallo-Marazuela, D., Pastor-Sánchez, A., Carro-Calvo, L., Portilla-Figueras, A., Prieto L. (2014). Offshore wind farm design with the coral reefs optimization algorithm. *Renewable Energy*, 63, pp. 109-115.
19. Ituarte-Villarreal, C.M., Espiritu, J.F. (2011). Wind turbine placement in a wind farm using a viral based optimization algorithm. *Procedia Computer Science*, 6, pp. 469–474.
20. Donovan, S. (2006). An improved mixed integer programming model for wind farm layout optimization. In: Proceedings of the 41st annual conference of the Operations Research Society, Wellington.
21. Turner, S.D.O., Romero, D.A., Zhang, P.Y., Amon, C.H., Chan, T.C.Y. (2014). A new mathematical programming approach to optimize wind farm layouts. *Renewable Energy* 63(c), pp. 674–680.
22. Zhang, P.Y., Romero, D.A., Beck, J.C., Amon, C.H. (2014). Solving wind farm layout optimization with mixed integer programming and constraint programming. *EURO Journal on Computational Optimization*, 2(3), pp. 195-219.
23. Donovan, S. (2005). Wind farm optimization, In: Proceedings of the 40th annual conference of the Operations Research Society, Wellington.
24. Archer, R., Nates, G., Donovan, S., Waterer, H. (2011). Wind turbine interference in a wind farm layout optimization mixed integer linear programming model. *Wind Engineering*, 35, pp. 165-178.
25. Brusca, S., Lanzafame, R., Messina M. (2014). Wind turbine placement optimization by means of the monte carlo simulation method. *Modelling and Simulation in Engineering* Volume 2014.

26. Herbert-Acero, J-F., Franco-Acevedo, J-R., Valenzuela-Rendon, M., Probst-Oleszewski, O. (2009). Linear wind farm layout optimization through computational intelligence. Proceedings of 8th Mexican International Conference on Artificial Intelligence, pp. 692–703.
27. Rivas, R.A., Clausen, J., Hansen, K.S., Jensen, L.E. (2009). Solving the turbine positioning problem for large offshore wind farms by simulated annealing. Wind Engineering, 33, pp. 287–297.
28. Chen, L., MacDonald, E. (2011). A New Model for Wind Farm Layout Optimization with Landowner Decisions, In: Proceedings of the ASME 2011 International Design Engineering Technical Conferences and Computers and Information in Engineering Conference, pp. 303-314.
29. Chen, L., MacDonald, E. (2014). A system-level cost-of-energy wind farm layout optimization with landowner modeling. Energy Conversion and Management, 77, pp. 484-494.
30. Fagerfjäll, P. (2010). Optimizing wind farm layout: More bang for the buck using mixed integer linear programming. MSc Thesis, Chalmers University of Technology and Gothenburg University.
31. Zhang, P.Y., Romero, D.A., Beck, J.C., Amon, C.H. (2014). Solving wind farm layout optimization with mixed integer programming and constraint programming. EURO Journal on Computational Optimization, 2(3), pp. 195-219.
32. Kwong P., Zhang P.Y., Romero D.A., Moran J., Morgenroth M., Amon C.H. (2012). Wind farm layout optimization considering energy generation and noise propagation. In Proceedings of the ASME International Design Engineering Technical Conferences.

33. Chowdhury, S., Messac, A., Zhang, J., Castillo, L., Lebron, J. (2010). Optimizing the unrestricted placement of turbines of differing rotor diameters in a wind farm for maximum power generation. ASME 2010 International Design Engineering Technical Conferences and Computers and Information in Engineering Conference, Paper No. DETC2010-29129, pp. 775-790.
34. Chowdhury, S., Zhang, J., Messac, A., Castillo, L. (2013). Optimizing the arrangement and the selection of turbines for wind farms subject to varying wind conditions. *Renewable Energy*, 52, pp. 273-282.
35. Chen, Y., Li, H., Jin, K., Song, Q. (2013). Wind farm layout optimization using genetic algorithm with different hub height wind turbines. *Energy Conversion and Management*, 70, pp. 56–65.
36. Tong, W., Chowdhury, S., Mehmani, A. Messac, A. (2013). Multi-objective wind farm design: Exploring the trade-off between capacity factor and land use. 10th World Congress on Structural and Multidisciplinary Optimization, Orlando, Florida.
37. Chowdhury, S., Tong, W., Messac, A., Zhang, J. (2012). A mixed-discrete particle swarm optimization algorithm with explicit diversity-preservation. *Structural and Multidisciplinary Optimization*, 47(3), pp. 367-388.
38. Chowdhury, S., Zhang, J., Messac, A., Castillo, L. (2012). Characterizing the influence of land area and nameplate capacity on the optimal wind farm performance. In ASME 2012 6th International Conference on Energy Sustainability, San Diego, pp. 1349-1359.

Chapter 3 : Explicit Solutions for Simple Models of Wind Turbine Interference

Abstract

Wind turbine interference - the reduction in output power of a turbine downwind of any others - is a major problem for wind farm optimization and control. With interference, it is well-known for specific cases that co-operative optimization of power output yields more power than does the selfish optimization of individual turbines. This paper develops explicit solutions for simple models of interference for the general case of any number of turbines in line with the wind. For the simplest case of no wake recovery, analytical solutions for co-operative and selfish optimization are derived. They show that co-operative optimization nearly always yields more power and never yields less. Adding a simple form of wake recovery for equally spaced turbines precludes analytical solutions, but numerical solutions are developed to find the power to any required level of accuracy. Again, co-operative optimization is superior in nearly all cases. These simple solutions should be useful for demonstrating the importance of interference and for testing methods for optimizing wind farm layout and operation. It is shown that the maximum benefit from co-operative operation occurs at turbine spacing comparable to that commonly used in wind farms. The analysis is then extended to include topographical effects modeled as changes in wind speed along the line. Explicit solutions are obtained for two turbines in line. Co-operative optimization remains the best strategy. In particular, when the wind speed increases, it quickly becomes optimal to shut down the first turbine.

3.1 Introduction

Wind energy is usually harvested by wind farms that consist of multiple wind turbines located in a particular layout over a substantial stretch of land (onshore) or water (offshore). It has been shown in the literature (see [1,2,3,4,5]) that the total power extracted by a wind farm is often significantly less than the simple product of the power extracted by a stand-alone turbine and the number of turbines in the farm. The loss in energy is due mainly to interference on any downwind turbines due to the wake of the upwind machines [6].

Given the primary effect of the wake in the reduction of the wind farm power, an analytical wake model is an important tool to study and particularly mitigate interference. The Park wake model, originally developed by Jensen [7] and later completed by Katic et al. [8], is one of the most popular analytical wake models used in wind farm modeling. The modified Park wake model and the Eddy Viscosity wake model are other standard wake models [6]. The Park model includes wake recovery, the entrainment of the external flow into the turbine wake to re-energize it. Recently, Hancock [9] analyzed turbines in a line by an extension of the one-dimensional analysis using conservation of mass, momentum, and energy, that leads to the Betz-Joukowsky limit for a single turbine⁽¹⁾. Hancock extended his model to include a simple form of wake recovery that we will also use in this paper.

The loss of output power due to interference depends primarily on the geometric arrangement of multiple wind turbines in relation to the important wind directions. Hence, an optimal layout of turbines that ensures maximum output power is expected to improve the economics of a wind farm project (see [2,3,4]).

(1) Okulov & van Kuik [10] recently argued that the commonly-termed Betz limit should be attributed to Joukowsky as well.

Another factor that plays an important role in increasing wind farm power in the presence of interference is the co-ordination of the control of power output among the turbines in the wind farm. There should be a close interaction between layout design and operational control which is not addressed in this paper. We assume that the wind farm layout is given and the goal of this paper is to provide a collective adjustment of the power output of multiple wind turbines in line to maximize the total output power. Following Hancock [9], we consider the extreme case of the interaction within a farm that occurs when turbines form a straight line in the wind direction, as this minimizes the energy available to the downwind turbines.

Studies of control methodologies by Herbert-Accro et al. [11], Madjidian & Rantzer [12], and Marden et al. [13] show that co-operative optimization produces more power than does selfish optimization of the individual turbines. This paper considers co-operative and selfish optimization for simple wake models. It starts with Hancock's basic model to develop a closed form maximization of the power output from N identical turbines in line with no wake recovery. Hancock's second model with wake recovery reduces to the first as a special case but cannot generally be solved in closed form. However, we describe an iterative solution which can be made arbitrarily accurate for any N . Power optimization is done for two cases. In the first, the N turbines are individually maximized which is an N -dimensional problem. In the second case, a simpler one-dimensional optimization of the collective or co-operative power is considered. We demonstrate explicitly and numerically that the maximum co-operative power is never less than the sum of the maximum individual powers, and in many cases, it is considerably higher. For simplicity, we assume that the turbines are equi-spaced.

Finally, we consider some effects of topography, modeled as a change in wind speed along the line of turbines. Because this change is likely to be different for each turbine, we do not attempt

to solve the general problem. Analytic solutions are developed for selfish and co-operative optimization of two turbines in line with wind speed changes. Again, co-operative optimization is superior. In particular, we find a special case of co-operative optimization, “sacrificial” optimization in which power output is maximized if the first turbine is shut down when the wind speed increases from the first to second. Sacrificial optimization is valid even for small increases in the wind speed from the first to second turbine.

The main contributions of this paper are:

- (1) A simple analysis which shows the advantage of co-operative turbine operation when there is no wake interference with and without topographical effects.
- (2) A more sophisticated analysis that includes a form of wake recovery. The equations can be solved iteratively to arbitrary accuracy. Co-operative optimization is shown to be most beneficial at turbine spacing typical of modern wind farms.
- (3) In all cases, the co-operative maximum power was shown to be greater than the sum of the maximum individual powers. This result is proved for the first simple model for an arbitrary number of turbines, and demonstrated numerically for the second model. The superiority of co-operative optimization is established analytically for wake recovery for two turbines in line, with wind speed changes between them.

This paper is organized as follows. In the next section, we derive the equation for the power output of N turbines in line without wake recovery. This is largely a restatement of the analysis of Hancock [9]. In Section 3.1, we analyze the case where each turbine maximizes its power extraction. Then in Section 3.2, we will present the results for maximization of the overall output. A simplified form of the Park model which modifies the induction factor of the wake is presented

in Section 3.4. Following this, numerical simulations are provided in Section 3.5. Topographical effects are considered in Section 3.6. Concluding remarks are made in Section 3.7.

3.2 The Basic Model of Turbines In Line

Denote the induction factor in the wake of the n^{th} turbine as a_n , the wind speed by U and turbine area by A . a_n is defined relative to U and there is no compounding of a_n for the downwind turbines. We assume that the N turbines in line are identical. From Hancock's formulation of the momentum equation, the thrust of the n^{th} turbine, T_n , in the presence of the wake of the $(n - 1)^{th}$ turbine can be written as

$$T_n = \rho U(1 - a_{b,n})A[U(1 - a_{n-1}) - U(1 - a_n)] \quad (3.1)$$

or

$$T_n = \rho U^2 A(1 - a_{b,n})(a_n - a_{n-1}) \quad (3.2)$$

where $a_{b,n}$ is the induction factor at the blades of turbine n . The pressure difference across the rotor can be found using Bernoulli's equation for the upwind and downwind flow for each turbine:

$$P_+ - P_- = \frac{1}{2}\rho U^2(1 - a_{n-1})^2 - \frac{1}{2}\rho U^2(1 - a_n)^2 \quad (3.3)$$

From Equation (3.3), the thrust of turbine n is

$$\begin{aligned} T_n &= (P_+ - P_-)A = \frac{1}{2}\rho U^2 A[(1 - a_{n-1})^2 - (1 - a_n)^2] \\ &= \frac{1}{2}\rho U^2 A(a_n - a_{n-1})(2 - a_n - a_{n-1}) \end{aligned} \quad (3.4)$$

Comparing Equation (3.2) with Equation (3.4), it follows that

$$a_{b,n} = \frac{(a_n + a_{n-1})}{2} \quad (3.5)$$

From the energy equation, the power output of turbine n is

$$P = \frac{1}{2} \rho U^3 A (1 - a_{b,n}) [(1 - a_{n-1})^2 - (1 - a_n)^2] \quad (3.6)$$

Defining $C_{P,n}$ as the power coefficient of the n^{th} turbine in the normal manner allows Equation (3.6) to be combined with Equation (3.5) to give

$$C_{P,n} = \frac{P}{\frac{1}{2} \rho U^3 A} = \frac{1}{2} (a_n - a_{n-1})(2 - a_n - a_{n-1})^2 \quad (3.7)$$

Now consider two different cases: in the first case designated as “selfish” optimization, each individual $C_{P,n}$ is maximized. The second case of “co-operative” optimization, maximizes $\sum_{n=1}^N C_{P,n}$. As with the common derivation of the Betz–Joukowsky equation, optimization is based on selecting the value of a_n to maximize the power.

3.3 Optimization of the Power Output

3.3.1 Selfish optimization.

To maximize the power for each individual turbine from Equation (3.7), we set

$$\frac{\partial C_{P,n}}{\partial a_n} = \frac{1}{2} (3a_n - a_{n-1} - 2)(a_n + a_{n-1} - 2) = 0 \quad (3.8)$$

Since $a_n, a_{n-1} < 1$,

$$3a_n = a_{n-1} + 2 \quad (3.9)$$

Given $a_0 = 0$, it follows that

$$a_1 = \frac{2}{3} \quad (3.10)$$

which is the Betz-Joukowsky value. By extension to the downwind turbines, we obtain

$$a_2 = \frac{1}{3} \left(\frac{2}{3} + 2 \right) = \frac{2}{3^2} + \frac{2}{3} \text{ and } a_3 = \frac{1}{3} \left[\frac{1}{3} \left(\frac{2}{3} + 2 \right) \right] = \frac{2}{3^3} + \frac{2}{3^2} + \frac{2}{3} \quad (3.11)$$

Generalizing Equation (3.11) gives a_n as

$$a_n = 2 \sum_{i=1}^n \frac{1}{3^i} = 1 - 3^{-n} \quad (3.12)$$

It is easy to interpret Equation (3.12) as showing that each turbine operates at the Betz–Joukowsky limit with the “wind” speed equal to the wake velocity of the immediately upwind turbine. For n sufficiently large, $a_n \rightarrow 1$. Using Equation (3.12), the sum of the power coefficients can be calculated as

$$\begin{aligned} \sum_{n=1}^N C_{P,n} &= \frac{1}{2} \sum_{n=1}^N (2 - a_n - a_{n-1})^2 (a_n - a_{n-1}) \\ &= \frac{1}{2} \sum_{n=1}^N (3^{-n} + 3^{-n+1})^2 (3^{-n} + 3^{-n+1}) \end{aligned} \quad (3.13)$$

Summing Equation (3.13), we obtain

$$\sum_{n=1}^N C_{P,n} = \frac{8}{13} \left(1 - \frac{1}{3^{3N}} \right) \rightarrow \frac{8}{13} \text{ as } N \rightarrow \infty \quad (3.14)$$

Equation (3.14) gives the maximum power obtainable from N turbines in line if each maximizes its power. For $N = 1$, Equation (3.14) reduces to the Betz-Joukowsky limit which is only 3.8 % less than the maximum possible power coefficient, $8/13$, for an infinite line of turbines.

3.3.2 Co-operative optimization.

From Equation (3.7), the contribution to the sum of the power coefficients from terms involving a_n is

$$\begin{aligned} \Delta_n &= C_{P,n} + C_{P,n+1}, \text{ for } 1 < n < N \\ &= \frac{1}{2} [(2 - a_n - a_{n-1})^2(a_n - a_{n-1}) + (2 - a_{n+1} - a_n)^2(a_{n+1} - a_n)] \end{aligned} \quad (3.15)$$

To find the a_n that maximizes the sum of the power from the turbines up to $N - 1$, we set

$$\begin{aligned} \frac{\partial \Delta_n}{\partial a_n} &= 0, \text{ or} \\ \frac{1}{2} [(3a_n - a_{n-1} - 2)(a_n + a_{n-1} - 2) + (3a_{n+1} - a_n - 2)(a_{n+1} + a_n - 2)] &= 0 \end{aligned} \quad (3.16)$$

It follows that

$$a_n = \frac{(a_{n-1} + a_{n+1})}{2}, \text{ for } 1 < n < N \quad (3.17)$$

Obviously, Equation (3.17) does not apply to the last turbine which must be considered separately.

Given that $a_0 = 0$, it follows that $a_2 = 2a_1$, and $a_3 = 3a_1$. It is easy to use induction to establish the general result that

$$a_n = na_1, \text{ for } 1 < n < N \quad (3.18)$$

The N^{th} turbine must operate according to Equation (3.9) with $n = N$. Substituting Equation (3.18) into Equation (3.7) and evaluating the sum gives

$$\begin{aligned} \sum_{n=1}^N C_{P,n} &= \frac{a_1}{2} \sum_{n=1}^{N-1} (2 - 2na_1 + a_1)^2 + \frac{16}{27} [1 - (N - 1)a_1]^3 \\ &= \frac{N - 1}{6} [12a_1 - 12(N - 1)a_1^2 + 4a_1^3(N - 1)^2] + \frac{16}{27} [1 - (N - 1)a_1]^3 \end{aligned} \quad (3.19)$$

Equation (3.19) shows the power output of all N turbines now depends only on a_1 . The maximum total power occurs when

$$\frac{\partial \sum_{n=1}^N C_{P,n}}{\partial a_n} = \frac{N}{18} [4 - 8Na_1 - (4N^2 - 9)a_1^2] = 0 \quad (3.20)$$

Solving Equation (3.20) yields

$$a_1 = 1/\left(N + \frac{1}{2}\right) \quad (3.21)$$

When $N = 1$, Equation (3.21) gives $a_1 = 2/3$ and when N tends to infinity, $a_1 \rightarrow 1/N$. Using Equation (3.21), the maximum total power for N turbines is

$$\sum_{n=1}^N C_{P,n} = \frac{2N(N+1)}{3\left(N + \frac{1}{2}\right)^2} \rightarrow \frac{2}{3} \text{ as } N \rightarrow \infty \quad (3.22)$$

The asymptotic result is a small increment (12.5%) above the Betz-Joukowsky limit for a single turbine. Nevertheless, co-operative optimization always gives the same or more power than selfish optimization. Let $\delta(N)$ denote the difference in the sum of power outputs between N co-operative turbines and N selfish turbines. Equations (3.14) and (3.22) give

$$\delta(N) = \frac{8}{39} \left(3^{1-N} + \frac{N^2 + N - 3}{(1 - 2N)^2} \right) \quad (3.23)$$

$\delta(1) = 0$ obviously, but $\delta(N) > 0$ for any $N > 1$.

3.4 Optimization with Wake Recovery

We now use a simplified form of the Park model which modifies the induction factor of the wake of the $(n-1)^{th}$ turbine before that wake reaches the n^{th} turbine in an equi-spaced line. The upwind induction factor of the n^{th} turbine is $a'_{n-1} = ba_{n-1}$, where, as before, a_{n-1} is the wake induction factor for the $(n-1)^{th}$ turbine, and $b \leq 1$. The factor b is identical to f used by Hancock [9]. It allows for some wake recovery by entrainment of external air at higher wind speed. Thus,

$$C_{P,n} = \frac{1}{2}(2 - a_n - ba_{n-1})^2(a_n - ba_{n-1}) \quad (3.24)$$

We now extend the results in Sections 3.3.1 and 3.3.2 to include b .

3.4.1 Selfish optimization with wake recovery.

Modifying Equation (3.8), using the wake recovery model in Equation (3.24), we have

$$\frac{\partial C_{P,n}}{\partial a_n} = \frac{1}{2}(3a_n - ba_{n-1} - 2)^2(a_n + ba_{n-1} - 2) = 0$$

Since $b \leq 1$, the second term can never be zero and therefore

$$a_n = \frac{(ba_{n-1} + 2)}{3}, \text{ for } 1 \leq n \leq N \quad (3.25)$$

Thus for $b \leq 1$,

$$a_0 = 0, \quad a_1 = \frac{2}{3}, \quad a_2 = \frac{1}{3}\left[\frac{2b}{3} + 2\right] = \frac{2b}{3^2} + \frac{2}{3}$$

and, in general,

$$a_n = 2 \sum_{i=1}^n \frac{b^{i-1}}{3^i} = \frac{2 - 2\left(\frac{b}{3}\right)^n}{3 - b} \quad (3.26)$$

Substituting Equation (3.26) in Equation (3.24), we obtain

$$\sum_{n=1}^N C_{P,n} = 2 \sum_{n=1}^N \left[\frac{2 - 2b + 4\left(\frac{b}{3}\right)^n}{3 - b} \right]^3 \quad (3.27)$$

When the turbines are far enough apart, $b \rightarrow 0$. In this case, Equation (3.27) implies that

$$\sum_{n=1}^N C_{P,n} = \frac{16}{27}N \quad (3.28)$$

which shows that each turbine operates at the Betz-Joukowsky limit. When $b = 1$, we recover the simple model result, Equation (3.14). It should be noted that from Equation (3.27) does not have a compact summation as did Equation (3.14). It is probably better to evaluate the sum directly for each N .

3.4.2 Co-operative optimization with wake recovery.

The contribution to the overall power coefficient from the $(n - 1)^{th}$ and n^{th} turbines denoted in Equation (3.15) becomes

$$\Delta_n = (2 - a_n - ba_{n-1})^2(a_n - ba_{n-1}) + (2 - a_{n+1} - ba_n)^2(a_{n+1} - ba_n)$$

As in Section 3.3.2, the maximum power occurs when

$$\begin{aligned} \frac{\partial \Delta_n}{\partial a_n} &= 4 + b(a_{n+1}^2 - ba_{n-1}^2 - 4) - 3(b^3 - 1)a_n^2 + \\ &+ 2a_n[b(a_{n-1} - ba_{n+1} + 4b) - 4] = 0 \end{aligned} \quad (3.29)$$

Rewriting Equation

(3.29) to make a_n the subject gives

$$\overline{a_n} = \frac{4 + b(a_{n+1}^2 - ba_{n-1}^2 - 4) - 3(b^3 - 1)a_n^2}{2[4 - b(a_{n-1} - ba_{n+1} + 4b)]} \quad (3.30)$$

where $\overline{a_n}$ indicates that the equation can be used to iterate for a_n as solving the quadratic equations for every n would also have to be done iteratively. Again $a_0 = 0$ independent of b .

The form of Equation (3.30) suggests an analytic solution is possible only when $b = 1$ or 0 . When $b = 0$, Equation (3.30) does not require iteration and $a_n = 2/3$ from Equation (3.10). When $b = 1$, Equation (3.30) reduces to Equation (3.17), again without iteration. For the N^{th} turbine, $a_{N+1} = 0$ so a_N is given by Equation (3.25) and the power output of the last turbine is

$$C_{P,N} = (2 - a_N - ba_{N-1})^2(a_N - ba_{N-1}) \quad (3.31)$$

3.5 Optimization Examples and Numerical Simulation

Figure 3.1 and Figure 3.2 compare the maximum co-operative power output to the individually optimized power. As $b \rightarrow 0$, the turbines become far enough apart to operate independently and

the co-operative and individual optimizations yield the same total power. For all other b , co-operative optimization produces more power, with the biggest improvement around $b = 0.7$. In this version of the Park model we can approximate

$$b = (1 + 2kx)^{-2} \quad (3.32)$$

where the empirical factor k has the value of 0.075 in the well-known software WAsP, and x is the distance between the turbines of diameter D . Thus, $b = 0.4$ corresponds to turbines spaced four diameters apart, which is about the minimum distance used in practice.

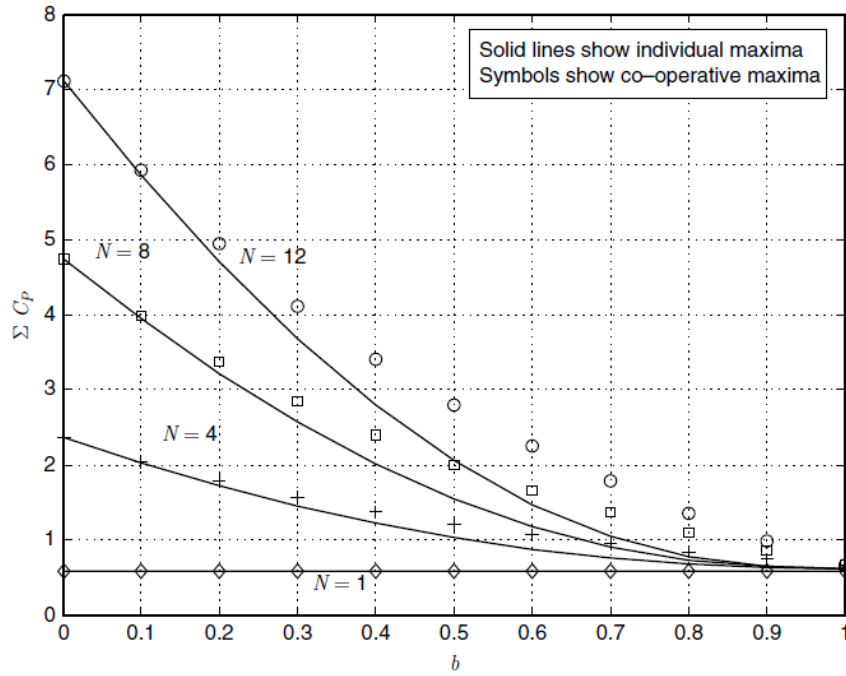


Figure 3.1: Total power output from co-operative (symbols) and individual (solid lines)

optimization as a function of b . The number of turbines in the line is indicated on the Figure.

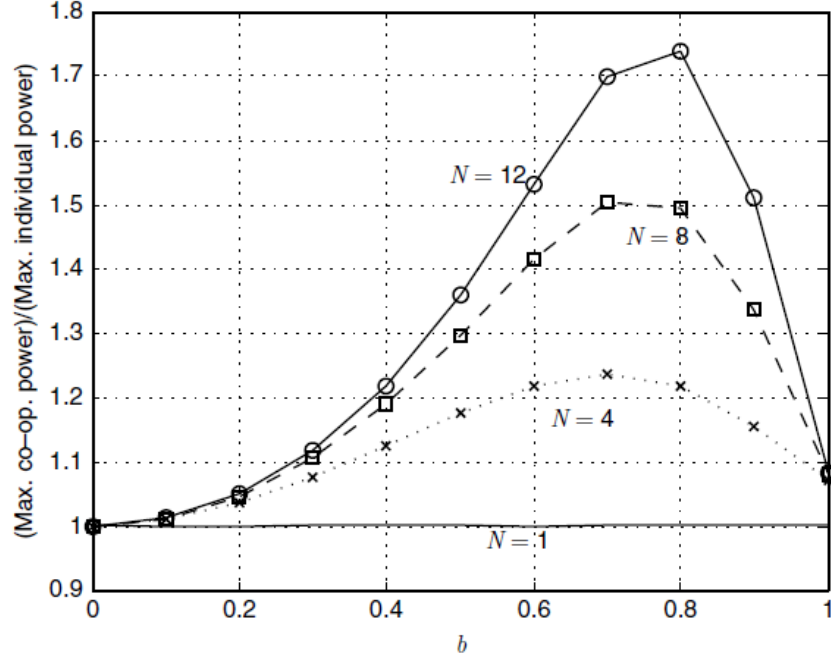


Figure 3.2: Ratio of total power output from co-operative optimization to individual optimization. Lines for visual aid only. The number of turbines in the line is indicated on the Figure.

The assumption of constant b is an approximation to the Park model because no account is taken of the interaction of successive wakes when $N > 2$.

Figure 3.3 shows the induction factors for selfish ($N = 12$) and co-operative optimization for $N = 3, 6, 9, \text{ and } 12$. The difference in operation between the two types of optimization is much more obvious in a_n than in the power output. Figure 3.4 shows the variation in a_n with n for $N = 5$ and varying b for co-operative optimization. For the extreme case of $b = 0$ ($a_n = 2/3$) all turbines operate at the Betz-Joukowsky limit. With no wake recovery, $b = 1$ and $a_n = \frac{n}{N+0.5}$ from Equation (3.18) and Equation (3.21)).

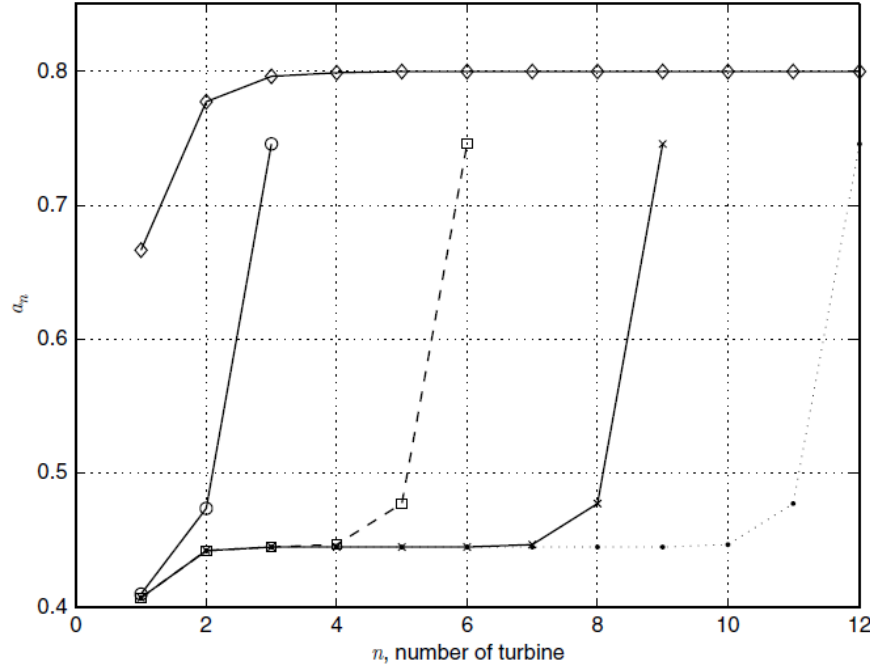


Figure 3.3: Wake induction factors for $b = 0.5$. Individual optimization for $N = 12$, shown by diamonds. Other results for co-operative optimization for N indicated by last symbol.

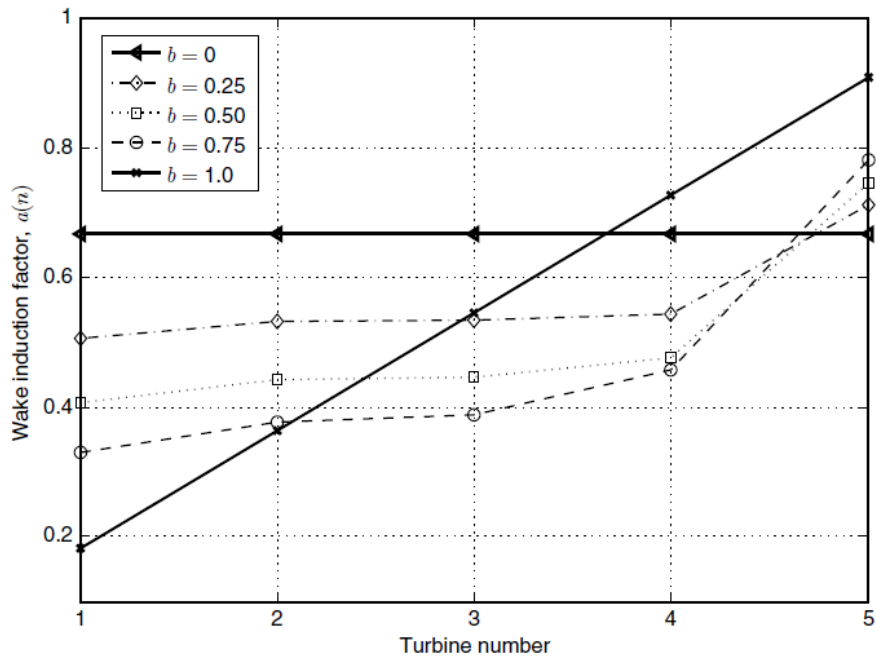


Figure 3.4: Induction factors for co-operative optimization for $N = 5$ as a function of b .

Both Figures show that the interior turbines ($1 < n < N$) tend to operate at constant a_n for co-operative optimization.

The individual turbine power outputs for $N = 6$ and $0 \leq b \leq 1$ for both optimization schemes is shown in Figure 3.5. Note that the first turbine always performs at the Betz-Joukowsky limit for the selfish case. For small b , there is little difference between the outputs from the two cases, but as $b \rightarrow 1$ the middle turbines produce significantly more when co-operating. The trend of the first turbine producing significantly more than the rest for realistic values of b is typical of wind farm practice, e.g. Hancock [9] and Crasto & Castellani [14].

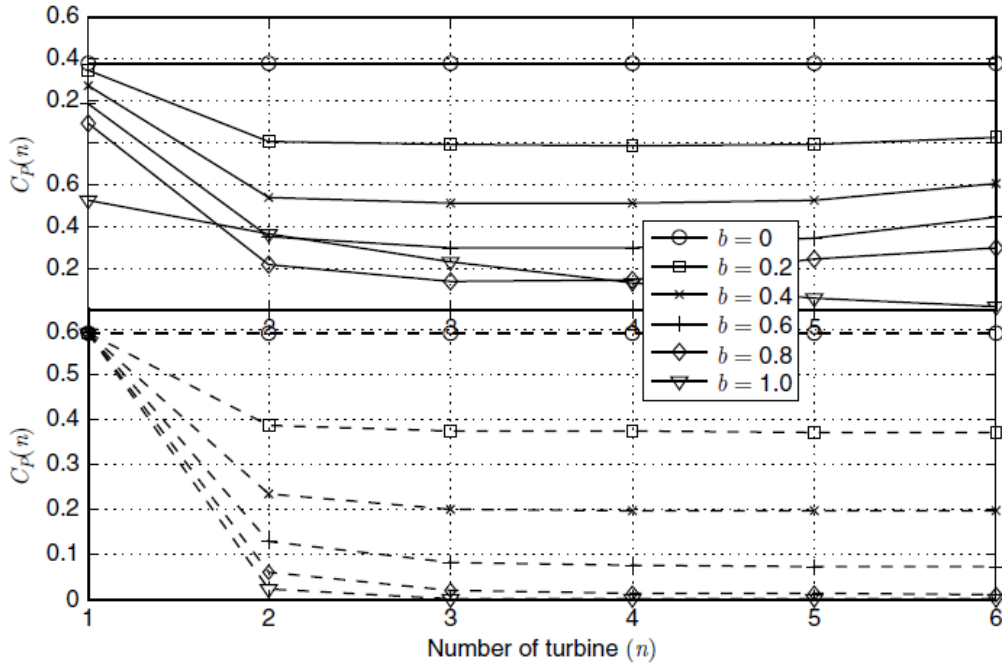


Figure 3.5: Individual turbine power output for $N = 6$ and b as indicated for co-operative (top Figure) and individual (bottom Figure) optimization. Value of b indicated in legend.

The two optimization cases for $N \leq 12$ were programmed in Matlab using routine *gamultiobj* which implements a non-dominated sorting genetic algorithm, [15]. The N -dimensional problem

of Case 1 was always evaluated with larger error than Case 2. For the latter, *gamultiobj* with the default parameters and a population size of 100 gave results so close to those from the present theory, that there would be no point in displaying them. Since co-operative optimization is the much more likely goal of wind farm layout design and subsequent operation, this is highly desirable result.

3.6 Modeling Turbines In Line with Changing Wind Speed

We now extend the analysis to include topographical effects modelled as changes in the mean wind speed along the line of turbines. Although the analysis is straightforward, it quickly becomes complicated for more than two turbines. We therefore consider co-operative and selfish optimization of only two turbines in line for either increasing wind speed (if, say, one turbine was below a hill and the second on the crest) or decreasing wind speed (if, say, the first is at the crest of a hill followed by a plateau). It is shown that co-operative optimization is superior and for increasing wind speed it is beneficial to switch off the first turbine even when the increase is small.

It is simple to extend Equation (3.24) to the situation where the wind speed at the n^{th} turbine is a factor k_n times the reference speed, say at the first turbine. With wake recovery, the power coefficient based on the reference wind speed is

$$C_{P,n} = \frac{1}{2} [k_n(1 - b_n a_{n-1}) + (1 - a_n)]^2 [k_n(1 - b_n a_{n-1}) - (1 - a_n)] \quad (3.33)$$

The topography of a wind farm sets the values of k_n . The wake model and turbine spacing determine the values of b_n , so the optimization of power output then depends only on a_n as for the situations considered previously.

An example estimation of k_n comes from Mohamed & Wood [16] who computed the wind profile above the crest of two-dimensional hills and compared the results with measurements in a wind tunnel. They developed an empirical expression for the modification of the logarithmic law with the principal aim of improving the vertical extrapolation of wind speeds. The expression was then extended to include a plateau starting at the crest by matching the wind tunnel results of Røkenes & Krogstad [17]. Equation (25) of Mohamed & Wood [16] gives the ratio of the wind speed at the crest ($x = 0$) or on the plateau ($x > 0$) to that before the hill as

$$k(x) = 1 + \frac{(H/h)^{0.12} - 0.505}{0.034(R + 98x)/H} \quad (3.34)$$

where H is the height of the crest with a radius of curvature R . h is the turbine hub height and all lengths are in m . If there is one turbine before the hill and one on the crest, and we take typical values of $h = H$ and $R/H = 9$, then Equation (3.34) gives: $k_2 = 2.6$. Reducing R obviously increases k so large values of k_2 are possible. If the first turbine is on the crest, then $k_2 = k(x)/k(x = 0) < 1$.

Equation (3.33) gives the power output of the two turbines, C_P , as

$$\begin{aligned} \sum C_P &= C_{P,1} + C_{P,2} = \\ &= \frac{1}{2} a_1 (2 - a_1)^2 + \frac{1}{2} [k(1 - b_2 a_1) + (1 - a_2)]^2 [k(1 - b_2 a_1) - (1 - a_2)] \end{aligned} \quad (3.35)$$

where k_2 is written as k and $k_1 = 1$. For co-operative optimization

$$\frac{\partial \sum C_P}{\partial a_1} = \frac{\partial \sum C_P}{\partial a_2} = 0 \quad (3.36)$$

From the first derivative in Equation (3.36):

$$4 - 8a_1 + 3a_1^2 + (a_2 - 1)^2 bk - 2(a_2 - 1)(a_1 - 1)bk^2 - 3b(ba_1 - 1)^2 k^3 = 0 \quad (3.37)$$

and from the second:

$$[(a_1 - 1) + (ba_1 - 1)k] \left[3a_2 - 3 - \frac{ba_1 - 1}{k} \right] = 0 \quad (3.38)$$

The first root in Equation (3.38) makes $a_2 > 1$ in some cases and must be rejected. Therefore

$$a_2 = 1 + \frac{(ba_1 - 1)k}{3} \quad (3.39)$$

which reduces to Equation (3.25) when $k = 1$, and

$$a_1 = \frac{16b^2k^3 - 18 + 3\sqrt{9 + (24 - 64b + 32b^2)bk^3}}{16b^3k^3 - 27/2} \quad (3.40)$$

In the spirit of the previous section note that if a_2 is replaced by a_n and a_1 by a_{n-1} , Equation (3.39) remains valid. It is therefore possible to analyze N turbines in line in a straightforward manner but the variation in k_n would probably preclude simple analytical results of any use. It is unlikely that situations where k_n is constant for $N > 2$ are ever likely to be important.

The argument of the square root in Equation (3.40) must be non-negative. For it to be zero:

$$k = \frac{-9}{\sqrt[3]{(24 - 64b + 32b^2)b}} \quad (3.41)$$

Even with a real root, it is possible for a_1 to be zero. This occurs when

$$k = \frac{1}{2} \sqrt[3]{9/b} \quad (3.42)$$

for which the denominator of Equation (3.40) is always positive. The other value of k for which the numerator of Equation (3.40) is zero also makes the denominator zero and the factors cancel. k from Equation (3.42) is always less than, or equal to that from Equation (3.41) with the equality occurring only at $b = 1$. Thus, Equation (3.42) gives the maximum possible value of k for each b for which a_1 is non-negative. Larger values of k are only possible if $a_1 = 0$. This constraint has no effect if $k < 1$ but clearly limits the range of optimal operating conditions for $k > 1$, especially

at large b because Equation (3.42) gives $k = 1.04$ at $b = 1$. Before elaboration, the conditions for selfish optimization are established.

The first term on the right of Equation (3.35) is the output from the first turbine, which depends only on a_1 . Thus, selfish optimization requires operation at the Betz-Joukowsky limit with $a_1 = 2/3$. Equation (3.39), which is valid for both types of optimization, then gives $a_2 = 1 - k/9$ and Equation (3.35) can be evaluated easily. Figure 3.6 shows Equation (3.35) as a function of k for selected values of b for co-operative and selfish optimization. The total power coefficient is divided by $2(1 + k_3)$ so the maximum normalized total power is $16/27$ if both turbines operate at the Betz-Joukowsky limit, which occurs for all k when there is full wake recovery ($b = 0$) for both types of optimization. For other values of b , co-operative optimization, shown as dotted lines, always produces equal, or greater, power than selfish optimization shown as the solid lines. In particular, the curve $k_3/(1 + k_3)$ (heavy dashed lines) indicates that the second turbine is operating at the Betz-Joukowsky limit and the first is shut down. All the co-operative maxima follow this curve at sufficiently large k , showing that there is a large range of operating conditions where it is optimal to shut down the first turbine. This subset of co-operative optimization will be called “sacrificial” optimization. Not surprisingly, Figure 3.6 shows that sacrificing the first turbine is optimal only when $k > 1$. It is also not surprising that sacrificing the first turbine eventually becomes optimal as k increase above unity, but what is surprising is that it becomes optimal at remarkably small values of k : for no wake recovery, sacrificial optimization should be used when $k \geq 1.04$ from Equation (3.42). Even when $b = 0.4$, sacrificial optimization is superior for $k \geq 1.41$.

Numerical optimization using the Matlab routine *gamultiobj* gave results that were indistinguishable from the analytic solutions for a wide range of b and k .

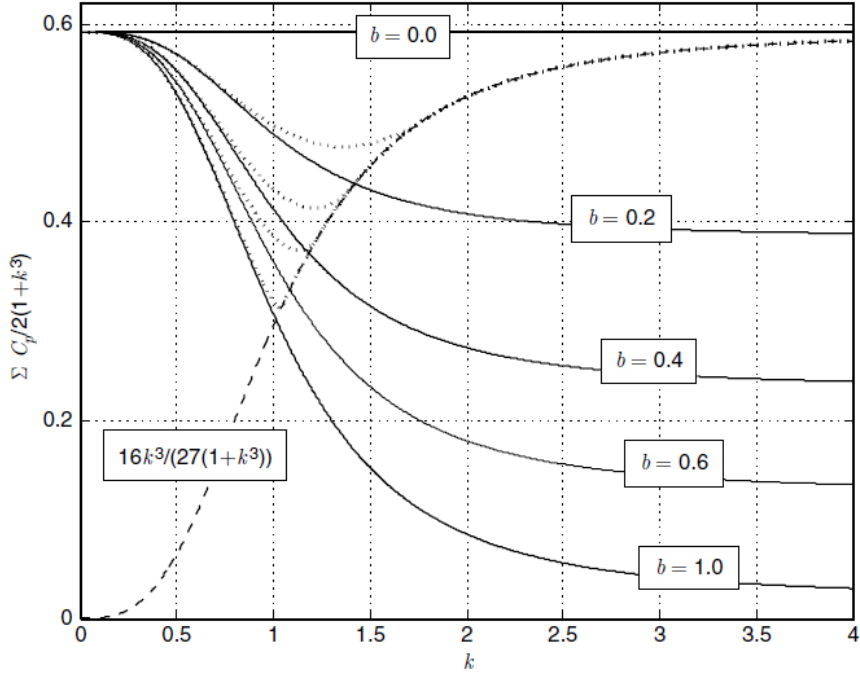


Figure 3.6: Maximum power output of two turbines for selfish (solid lines) and co-operative (dotted lines) optimization for a range of k . The value of b is indicated on each curve. The heavy dashed line indicates the power output with the first turbine shut down.

3.7 Conclusions

We have solved three simple models for output power optimization when an arbitrary number of turbines are in a straight line aligned with the wind direction, so that the wake of upwind turbine(s) can significantly reduce the power output of all downwind ones. The first model, taken from Hancock [9], has no wake recovery. It was solved exactly for any number of turbines. The second

model, also from [9], includes a simple measure of wake recovery by entrainment of external air which causes partial re-energization. The extent of the recovery is set by the factor b . The third model includes topographical effects by allowing the wind speed at the second and subsequent turbines to vary by a factor k from the reference value at the first turbine. Exact solutions were obtained for two turbines for both increasing and decreasing k and for any value of b .

The second model cannot be solved exactly for an arbitrary number of turbines, but an iterative method was developed to solve it to any level of accuracy. When $b = 1$, the first model is recovered and when $b = 0$ the turbines act independently. If the turbine output is optimized individually or selfishly, the total power output never exceeds that for co-operative optimization of the entire line of turbines. The advantage of co-operative optimization is significant in the range of turbine spacings that is common in wind farm practice. For the third model, co-operative optimization continued to be superior, to the extent that the first turbine should be shut down for surprisingly small values of k greater than unity.

Co-operative optimization is the easiest to program because it is one-dimensional. Calculations using Matlab routine *gamultiobj* for up to twelve turbines showed good agreement with the analytic solutions for all models.

ACKNOWLEDGMENTS

The work of Arman Kiani was supported by the University of Calgary's Institute for Sustainable Energy, Environment and Economy (ISEEE), that of David Wood by the NSERC Industrial Research Chairs program and the ENMAX Corporation, and Mamdouh Abdulrahman acknowledges the award of an Egyptian Government scholarship.

3.8 References

1. Elkinton, C., Manwell, J., McGowan, J. (2006). Offshore wind farm layout optimization (OWFLO) project: preliminary results. in 44th AIAA Aerospace Sciences Meeting and Exhibit.
2. Gonzlez, J., Rodriguez, A., Morac, J., Santos, J., Payan, J. (2010). Optimization of wind farm turbines layout using an evolutive algorithm. Renewable Energy, vol. 35, no. 8, pp. 1671-1681.
3. Grady, S., Hussaini, M., Abdullah, M. (2005). Placement of wind turbines using genetic algorithms. Renewable Energy, vol. 30, no. 2, pp. 259–270.
4. Sisbot, S., Turgut, O., Tunc, M., Camdali, U. (2009). Optimal positioning of wind turbines using multi-objective genetic algorithm. Wind Energy, vol. 13, no. 4, pp. 297–306.
5. Mosetti, G., Poloni, C., Diviacco, B. (1994). Optimization of wind turbine positioning in large wind farms by means of a genetic algorithm. Journal of Wind Engineering and Industrial Aerodynamics, vol. 54, no. 1, pp. 105–116.
6. Chowdhury, S., Zhang, J., Messac, A., Castillo, L. (2012). Unrestricted wind farm layout optimization (UWFLO): Investigating key factors influencing the maximum power generation,” Renewable Energy, vol. 38, pp. 16–30.
7. Jensen, N. O. (1983). A note on wind turbine interaction. Technical Report, Risø-M-2411, Risø National Laboratory, Denmark.
8. Katic, I., Hojstrup, J., Jensen, N. O. (1986). A simple model for cluster efficiency. In European Wind Energy Conference and Exhibition.
9. Hancock, P. (2013). Wind turbines in series: a parametric study. Wind Engineering, 37(1), pp. 37–58.

10. Okulov, V., van Kuik, G. (2012). The Betz-Joukowsky limit: On the contribution to rotor aerodynamics by the British, German and Russian scientific schools. *Wind Energy*, 15(2), pp. 335–344.
11. Herbert-Accro, J.-F., Franco-Acevedo, J.-R., Valenzuela-Rendon, M., Probst- Oleszewski, O. (2009). Linear wind farm layout optimization through computational intelligence. In *MICAI 2009, LNAI 5845*.
12. Majdian, D., Rantzer, A. (2011). A stationary turbine interaction model for control of wind farms. In *18th IFAC World Congress*.
13. Marden, J., Ruben, S., Pao, L. (2012). Surveying game theoretic approaches for wind farm optimization. In *Proceedings of the AIAA Aerospace Sciences Meeting*.
14. Crasto, G., Castellani, F. (2013). Wakes calculation in an offshore wind farm. *Wind Engineering*, 37(3), pp. 269–280.
15. Deb, K. (2001). *Multi-objective optimization using evolutionary algorithms*. John Wiley & Sons.
16. Mohamed, M., Wood, D. (2013). Vertical wind speed extrapolation using the k– ε turbulence model. *Wind Engineering*, 37(1), pp. 13–36.
17. Røkenes, K., Krogstad, P. (2009). Wind tunnel simulation of terrain effects on wind farm siting. *Wind Energy*, 12(4), pp. 391–410.

Chapter 4 : Some Effects of Efficiency on Wind Turbine Interference and Maximum Power Production

Abstract

The effects of finite efficiency on wake interference and power output are studied for identical horizontal-axis wind turbines in line with the wind. Interference occurs whenever turbines reduce the power available to any turbines downwind of them. The analysis uses wake models that are commonly employed in wind farm layout design. The aerodynamic efficiency is varied from 75% to 100% for six identical hypothetical turbines in line parallel to the wind direction with spacing from four to six rotor diameters. Selfish optimization of the power output of individual turbines and co-operative optimization of the total power are considered. For selfish control, all turbines operate at the maximum possible local C_P , based on the aerodynamic efficiency. For co-operative optimization, each turbine operates at a C_P value between zero and the selfish value, and the total power is optimized numerically. The results show that at low efficiency, there is little difference in total power output between the two strategies. As efficiency increases, co-operative optimization produces increasingly more power. As turbine spacing increases, the difference between the strategies decreases. There is, however, a realistic range of efficiencies and spacing over which more power is delivered by co-operative optimization. The simplest form of co-operative optimization requires reducing the power output of the most upwind turbine to allow increased performance from those downwind. This should be an easy strategy to implement in wind farm control.

Keywords: Layout optimization, Co-operative optimization, Selfish optimization, Turbines in-line, Wind farm control.

4.1 Introduction

One of the main challenges in designing a wind farm layout is the minimization of turbine wake interference. Any upwind turbine necessarily reduces the energy available to any turbine in its wake, and this interference is obviously maximized when turbines are in line in the direction of the wind. Hancock [1] formulated the problem of identical ideal turbines in line using two models, the first from actuator disk theory (ADT) which is the simplest possible, and the second was a modification that allowed wake recovery. Kiani et al. [2] derived explicit solutions for similar models and found, for example, that an infinite array of ideal wind turbines can produce only 12.5% more power than a single turbine operating at the Betz-Joukowsky limit. It was also found that co-operative optimization of all turbines always produced more power than selfish (or individual) optimization of each turbine. This is, potentially, a valuable result as the current paradigm in wind farm control is selfish optimization. To justify a move towards co-operative optimization, it must be demonstrated to be superior for more realistic wake models. Further, it is necessary to account for the effects of turbine efficiency on the energy remaining in the wind and, therefore, the performance of the downwind turbines. Efficiency in this context has two components, the first being the aerodynamic efficiency, η_a , which relates the extracted (aerodynamic) power coefficient, $C_{P,a}$, to that obtained from the ADT analysis at the same C_T . It is maximized at the Betz-Joukowsky limit and defined as

$$\eta_a = \frac{\text{aerodynamic power}}{\text{ADT power}} = \left(\frac{C_{P,a}}{C_{P,ADT}} \right)_{C_T} \quad (4.1)$$

Second, the available power curves of commercial turbines give the electrical output power whose ratio to the extracted power is the efficiency of power conversion. The conversion efficiency, η_c , is defined as

$$\eta_c = \frac{\text{converted electrical power}}{\text{aerodynamic power}} = \left(\frac{C_{P,c}}{C_{P,a}} \right)_{C_T} \quad (4.2)$$

In this paper the two power coefficients, $C_{P,a}$ and $C_{P,c}$, and the corresponding thrust coefficient, C_T , are based on the local wind speed of the turbine. The total power coefficient of the turbines in line based on the undisturbed wind speed, U_0 , is denoted $C_{P,O}$.

Only horizontal-axis wind turbines (HAWTs) are considered in this paper. They have complex wakes whose interaction with downwind turbines is even more complex, e.g. [3]. Many studies of interfering wind turbines have used sophisticated methods to solve the wake flow, such as large eddy simulation, which is computationally expensive even on powerful computer clusters, e.g. [4,5,6,7]. Such models are obviously unsuitable for optimization with present computational resources. They represent the other extreme from the models used by [1,2]. A satisfactory compromise that is accurate and useful for control will lie somewhere between these extremes. This paper attempts to move towards that satisfactory model by using a wake model that is a common component of current wind farm layout software.

In the next section, the mathematical formulation of the chosen wake model is described. The determination of the major operational parameters (C_P , C_T , and a) is discussed briefly in section 4.3. Section 4.4 gives the remaining details of the simulations. The results are presented and discussed in section 4.5, and finally the major conclusions are collected in section 4.6.

4.2 Wake Model

Among many wake models that have been developed during the last four decades, Jensen's is one of the oldest, simplest, and most accurate, e.g. [8,9]. According to Barthelmie et al. [10], who evaluated it along with other commonly used wake models: “*Overall, it is not possible to establish any of the models as having individually superior performance with respect to the measurements.*”

Further the model “*has proven to be reliable for long-term power predictions in small to medium size wind farms, but tends to underestimate wake losses for large wind farms*” [11], especially in the first few rows, [12]. This model, originally proposed by Jensen [13], was developed further by Katic et al. [14] and Frandsen [15].

The wake diameter, D_w , and wind speed, U_w , can be estimated at any downstream location, x , as function of an expansion constant, k , and the blade local axial induction factor, a , as:

$$D_w = D_{exp} + 2kx \quad (4.3)$$

$$U_w = U \left\{ 1 - \frac{2a}{[1 + 2k \cdot x/D_{exp}]^2} \right\} \quad (4.4)$$

$$D_{exp} = D \left[\frac{1-a}{1-2a} \right]^{1/2} \quad (4.5)$$

where $a = 1 - \frac{U_b}{U}$, D is the rotor diameter, D_{exp} is the downstream diameter immediately after the initial wake expansion [15], U is the turbine's upstream wind speed, and U_b is the wind speed at the rotor plane. The value of k is taken as 0.075 as recommended by WAsP [16] and WindPro [17] for onshore wind farms.

Each turbine (except the most upstream) is assumed to be effected by all the upwind ones. The total velocity deficit of the i^{th} turbine is approximated as

$$\delta U_i = \sqrt{\sum_{j=1}^{j=i-1} \delta U_{ij}^2} \quad (4.6)$$

where the contribution of the j^{th} turbine ($j < i$) is

$$\delta U_{ij} = \frac{2a_j}{\left[1 + 2k\Delta x_{ij}/D_{exp,j}\right]^2} \quad (4.7)$$

and Δx_{ij} is the distance between the i^{th} and j^{th} turbines. Thus, the velocity immediately upwind of turbine i is

$$U_i = U_0(1 - \delta U_i) \quad (4.8)$$

where U_0 is the undisturbed wind speed well upwind of the turbine line.

4.3 Determining the Induction Factor

Wake models normally use the turbine thrust coefficient, C_T , to establish the value of a . Further, most optimization studies assumed a fixed value for C_T , typically 0.88, e.g. [18,19,20,21,22], which is not generally accurate. On the other hand, Acero et al. [23] used the manufacturer's data for C_T for the commercial turbine that they considered. Alternatively, Frandsen [24] proposed a generic formula for C_T as function of wind speed:

$$C_T = \frac{3.5(2U - 3.5)}{U^2} \quad (4.9)$$

For an isolated turbine, Figure 4.1 demonstrates that neither $C_T = 0.88$ nor Equation (4.9) match the available manufacturers' data for commercial turbines, as documented in the Appendix.

The thrust data from Figure 4.1 is re-plotted in Figure 4.2 as a function of C_P along with the relation inferred from the basic ADT equations, e.g. [25]:

$$C_P = 4a(1 - a)^2 \quad (4.10)$$

$$C_T = 4a(1 - a) \quad (4.11)$$

Equation (4.10) was used by [1,2], to determine a . This over-estimates the power output for a turbine as well as the available power for the downwind ones. The thrust coefficient for three turbines (turbines 1-3) was given in terms of $C_{P,a}$ while for the other five (turbines 4-8) was based on $C_{P,c}$.

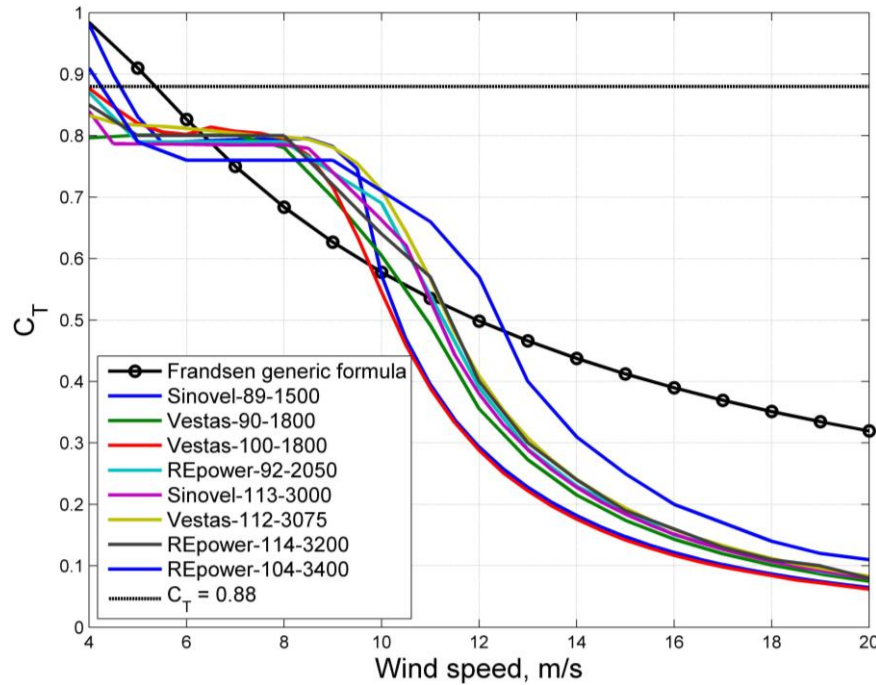


Figure 4.1: C_T vs U for the 8 wind turbines described in the Appendix compared with Equation (4.9) and $C_T = 0.88$.

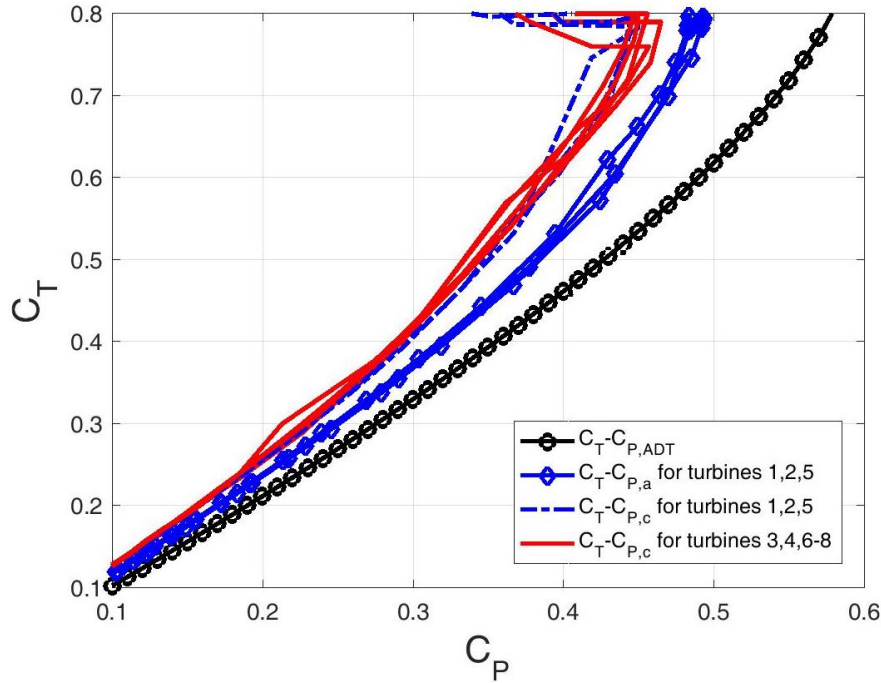


Figure 4.2: C_T vs C_P for the 8 wind turbines described in the Appendix compared to that from Equations (4.10) and (4.11).

4.4 Details of the Simulations

Figure 4.3 shows the two efficiencies for turbines 1-3. Since the wake development depends only on the aerodynamic efficiency, we decided to simplify the analysis by using only that efficiency. The wake development and interference were computed for a range of η_a ($0.75 \leq \eta_a \leq 1.0$) that exceeds the range shown in Figure 4.3. In other words, a was determined from Equation (4.10) using $C_P = C_{P,a}/\eta_a$, and no use was made of the thrust data for the wake calculations.

It was decided to study six turbines in line as this is typical of wind farm arrangement and large enough to display the major effects of interference, e.g. [14,26,27]. Calculations were done for turbine spacings of 4, 5, and 6 rotor diameters on the grounds that interference is greater for smaller distances and 4 is approximately the minimum used for wind farms.

MATLAB scripts were used to obtain the optimum solution for co-operative operation using the genetic algorithm solver, *ga*. The decision variable was the local aerodynamic power coefficient and the objective function for co-operative optimization was the total power. The population size was 60, and the computations were allowed to evolve for a maximum of 300 generations. The termination criterion in *ga*, TolFun, defines the tolerance on the converged solution. It was set at 10^{-15} , which is significantly smaller than the default value of 10^{-6} , in an attempt to get accurate differences between selfish and co-operative power output when the difference was very small. Typically, 200 to 250 generations were required for termination. No optimization algorithm was needed for selfish cases as the local $C_{P,a}$ for all turbines were set to the maximum value of $16 \eta_a / 27$.

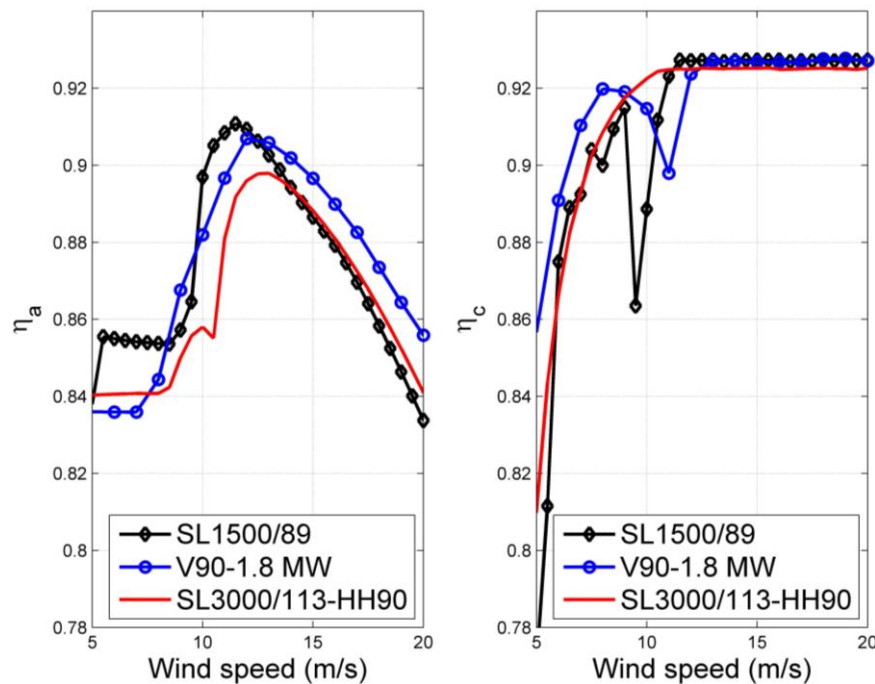


Figure 4.3: Comparison of the two efficiencies for turbines 1-3. The left Figure shows η_a and the right η_c .

4.5 Results and Discussion

Figure 4.4 and Figure 4.5 present the optimal distribution of $C_{P,a}$ and a , respectively, for all cases. For the lowest efficiency, $\eta_a = 0.75$, there is very little difference between selfish and co-operative optimizations. The differences increase with increasing η_a and are maximized for ideal turbines with $\eta_a = 1.0$, as studied by [2]. The main difference between the two optimizations occurs for the first turbine: if it operates co-operatively, then its power output is reduced to increase that of the downwind machines. As the efficiency increases, the power output of the first turbine rises, but very slightly. In all cases, the second turbine has the minimum power coefficient, and the last turbine has the same power coefficient independently of the optimization. As expected, there is an increase in power output as turbine spacing increases as this increases wake recovery.

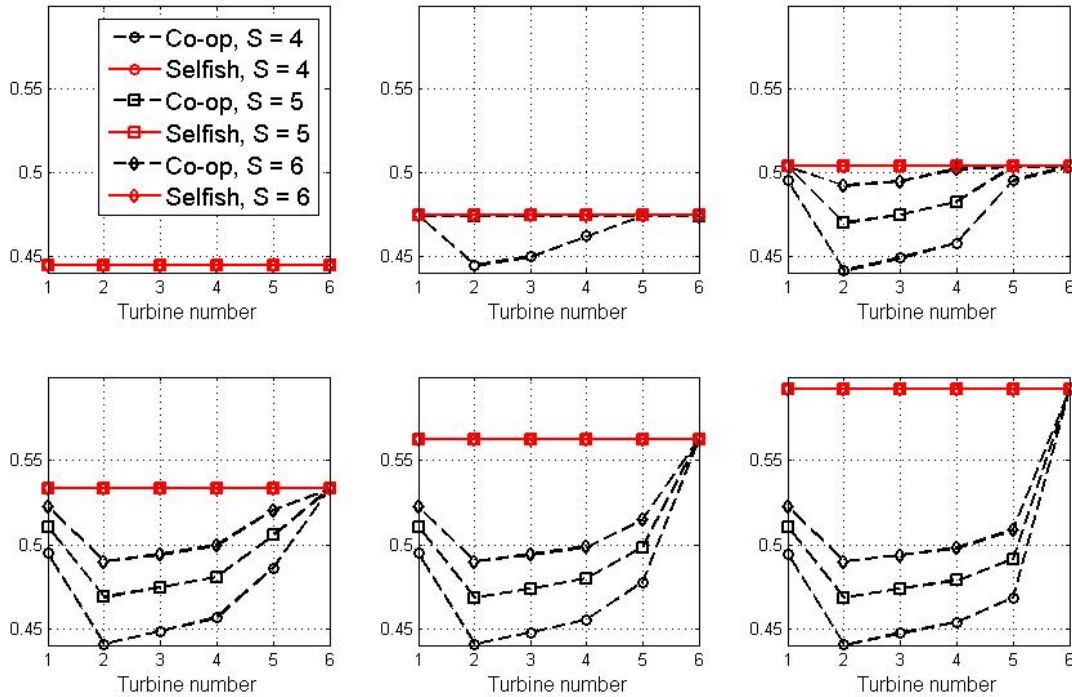


Figure 4.4: The local aerodynamic power coefficient for co-operative and selfish cases. From the top left Figure the values of η_a are 0.75, 0.80, and 0.85. From the bottom left Figure the values of η_a are 0.90, 0.95, and 1.0.

Figure 4.6 shows the contribution of each turbine to the total power output as measured by $C_{P,O}$, and Figure 4.7 and Figure 4.8 show the sum of the power coefficients. The difference between the two optimizations is negligible at the lowest efficiency but becomes significant as efficiency increases. In all cases of co-operative optimization, the first turbine reduces its output so the subsequent turbines can produce more. There is almost constant power produced by the second to sixth turbines, which agree with many experimental and theoretical data, e.g. [26,27]. This leads, as seen in Figure 4.9, to co-operative optimization generally producing more power than selfish optimization.

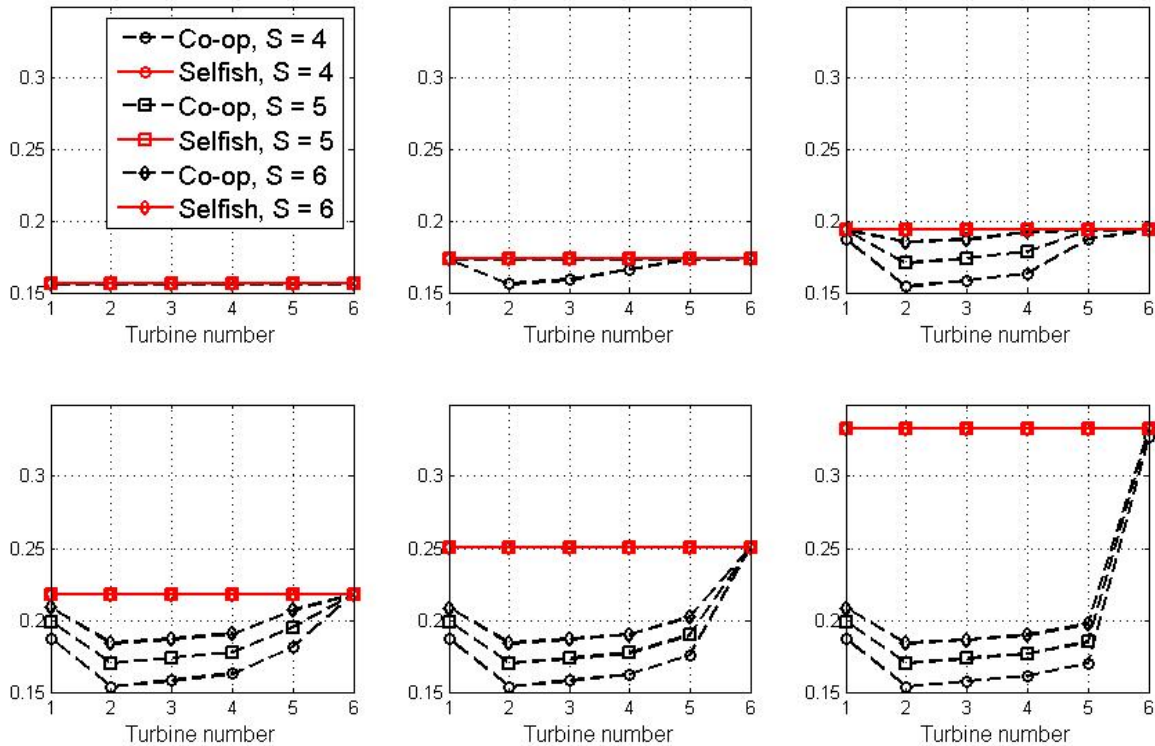


Figure 4.5: The local blade axial induction factor for co-operative and selfish cases. From the top left Figure the values of η_a are 0.75, 0.80, and 0.85. From the bottom left Figure the values of η_a are 0.90, 0.95, and 1.0.

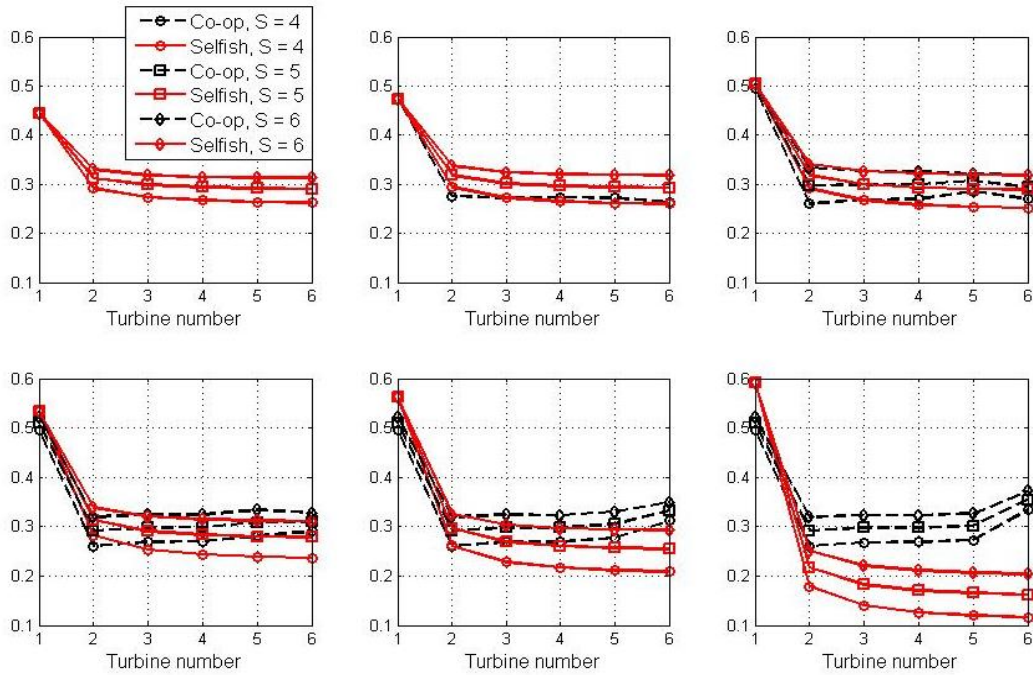


Figure 4.6: The global aerodynamic power coefficient for co-operative and selfish cases. From the top left Figure the values of η_a are 0.75, 0.80, and 0.85. From the bottom left Figure the values of η_a are 0.90, 0.95, and 1.0.

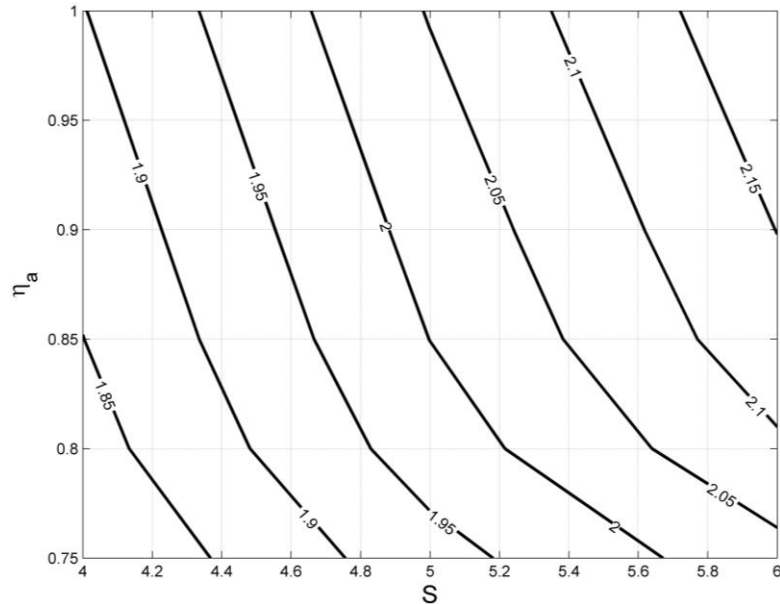


Figure 4.7: The sum of the global power coefficients for the co-operative cases.

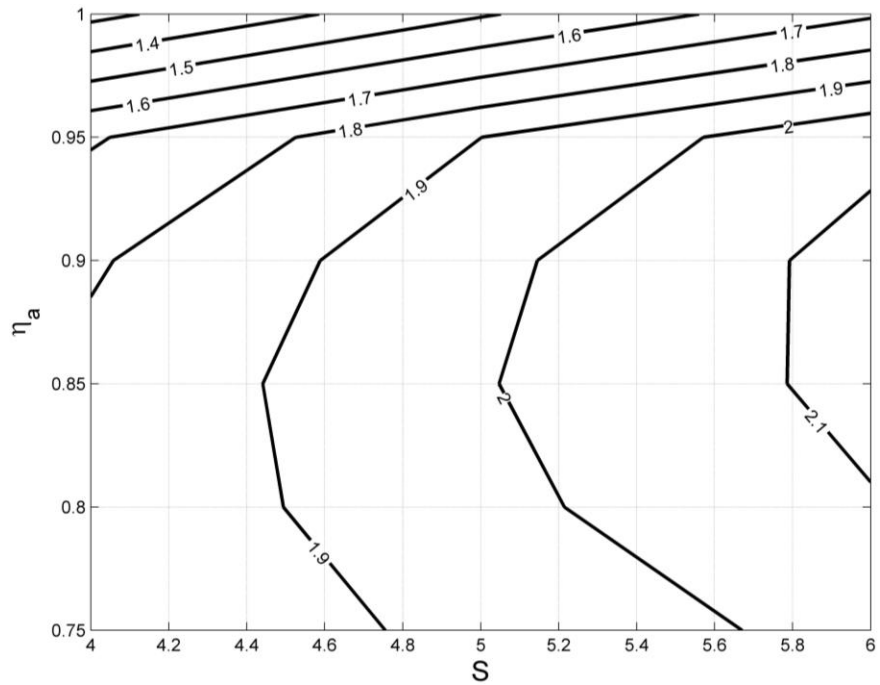


Figure 4.8: The sum of the global power coefficients for the selfish cases.

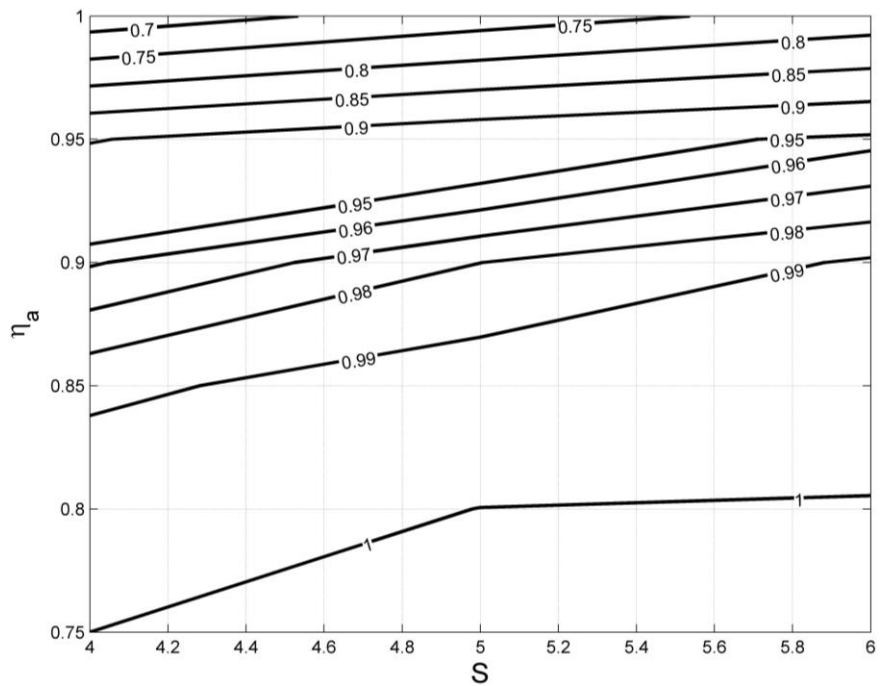


Figure 4.9: The ratio of selfish to co-operative total power.

4.6 Conclusions

This paper considers methods to optimize the power output from a straight line of HAWTs parallel to the wind direction by modelling the significant interference of downwind turbines by upwind ones. This problem was investigated by [1,2] who assumed ideal turbine behaviour and simple wake models. They found that co-operative optimization of the total power output always produced more power than selfish optimization of the individual turbines.

The main aim of this paper was to compare the optimization methods for the more realistic situation of non-ideal turbines using a wake model that is used in commercial wind farm layout software. A consideration of the available thrust data for commercial HAWTs showed that it was preferable to base the wake calculations on the aerodynamic parameters. The aerodynamic efficiency varied from 0.75 to 1.0, with the upper limit corresponding to an ideal turbine as defined by standard actuator disk theory.

All calculations were done for six turbines in line at spacing of 4, 5, and 6 rotor diameters on the grounds that these were representative values. Co-operative optimization can be done analytically only for simpler wake models than those used here, so we used MATLAB's genetic algorithm solver, *ga*, to perform such. On the other hand, selfish control was computed by adapting all the N turbines to work at the maximum possible $C_{P,a}$. The main results were:

1. At low efficiency, there is little difference in total power output between the two strategies,
2. As efficiency increases, co-operative optimization produces increasingly more power,
3. As turbine spacing increases, the difference between the two strategies decreases, and
4. There is a realistic range of efficiencies and spacing over which more power is delivered by co-operative optimization.

5. Co-operative optimization requires reducing the power output of the most upwind turbine to allow increased performance from those downwind. This should be an easy strategy to implement.

Acknowledgments

This research is part of a programme of work on renewable energy funded by the Natural Science and Engineering Council (NSERC) and the ENMAX Corporation.

Appendix to Chapter 4: The technical specifications for the 8 commercial turbines.

S/N	Manufacturer	Turbine designation	D (m)	Rated power (MW)	Rated speed (m/s)
1	Sinovel	SL1500/89	89.42	1.5	11.5
2	Vestas	V90-1.8	90	1.8	13
3	Sinovel	SL3000/113-HH90	113.3	3	11
4	Vestas	V100-1.8	100	1.815	11.5
5	REpower	MM92	92.5	2.050	13
6	Vestas	V112-3.0	112	3.075	13
7	REpower	3.2M114	114	3.17	12
8	REpower	3.4M104	104	3.37	14

- 1- Sinovel (2012). Technical specification SL 1500/89 (CC-60Hz). Sinovel wind group Co.,Ltd.

<https://www.edockets.state.mn.us/EFiling/edockets/searchDocuments.do?method=showPoup&documentId=%7B00FEBE64-5230-48BF-B68F-96EE5AA5EF09%7D&documentTitle=20124-74025-04> [accessed March 2015].

- 2- Vestas (2010). General Specification V90–1.8/2.0 MW 50 Hz VCS, Vestas Wind Systems A/S.

http://ventderaison.eu/gembloux/eie_ABO-WIND/Annexes/Annexe_N_1_Courbe_acoustique_V90.pdf [accessed March 2015].

- 3- Sinovel (2011). Specification SL3000 series wind turbine SL3000/113-HH90 (60Hz). Sinovel wind group Co.,Ltd.

<http://www.greenextreme.se/wp-content/uploads/2013/08/Bilagor.pdf> [accessed March 2015].

- 4- Vestas (2010). General Specification V100–1.8 MW VCUS, Vestas Wind Systems A/S.
<http://www.opsb.ohio.gov/opsb/assets/File/12-0160-12-0160-Vestas%20V100.PDF>
[accessed March 2015].
- 5- Repower (2011). Power Curve & Sound Power Level REpower MM92 [2050 kW], REpower Systems AG.
http://www.sholland.gov.uk/PublishedRecords/PBC/DC/APP/4/H19-0081-11-H19-0081-11_V1014400702052013_4DOCS.pdf [accessed March 2015].
- 6- Vestas (2010). General Specification V112–3.0 MW 50/60 Hz, Vestas Wind Systems A/S.
<http://documents.dps.ny.gov/public/Common/ViewDoc.aspx?DocRefId=%7B15E6A798-4D37-488D-A150-BD6CE70359CE%7D> [accessed March 2015].
- 7- Repower (2011). Power Curve & Sound Power Level REpower 3.2M114[3.2M/114/50Hz], REpower Systems SE.
http://ventderaison.eu/honnelles/eie_eneco_2013/annexes/annexe_F.pdf [accessed March 2015].
- 8- Repower (2011). Power Curve & Sound Power Level REpower 3.4M104[3.4M/104/50Hz], REpower Systems SE.
http://ventderaison.eu/honnelles/eie_eneco_2013/annexes/annexe_F.pdf [accessed March 2015].

4.7 References

1. Hancock, P. (2013). Wind turbines in series: A parametric study, *Wind Engineering*, 37(1), pp. 37-58.
2. Kiani, A., Abdulrahman, M., Wood, D. (2014). Explicit solutions for simple models of wind turbine interference. *Wind Engineering*, 38(2), pp. 167-180.
3. Adaramola, M.S., Krogstad P.-Å. (2011). Experimental investigation of wake effects on wind turbine performance. *Renewable Energy*, 36, 2078-2086.
4. Sanderse, B., van der Pijl, S., Koren, B. (2011). Review of computational fluid dynamics for wind turbine wake aerodynamics. *Wind Energy*, 14, pp. 799-819.
5. Vogstad, K., Bhutoria, V., Luns, J.A., Ivanell, S., Uzunoglu, B. (2012). Instant wind - Model reduction for fast CFD computations, Elforsk rapport V-366.
6. Porte-Agel, F., Yu, Y.T., Chen, C-H (2013). A numerical study of the effects of wind direction on turbine wakes and power losses in a large wind farm. *Energies*, 6, pp. 5297-5313.
7. Annoni, J., Seiler, P., Johnson, K., Fleming, P., Gebraad, P. (2014). Evaluating wake models for wind farm control. *American Control Conference*, pp. 2517-2523.
8. Sørensen, T., Nielsen, P., Thøgersen, M. L. (2006). Recalibrating wind turbine wake model parameters – Validating the wake model performance for large offshore wind farms. EMD International A/S.
9. Sørensen, T., Thøgersen, M. L., Nielsen, P., Jernesvej, N. (2008). Adapting and calibration of existing wake models to meet the conditions inside offshore wind farms. EMD International A/S. Aalborg.

10. Barthelmie, R.J., Folkerts, L., Larsen, G.C., Rados, K., Pryor, S.C., Frandsen, S.T., Lange, B., Schepers, G. (2006). Comparison of wake model simulations with offshore wind turbine wake profiles measured by SODAR. *Journal of Atmospheric & Oceanic Technology*, 23(7), pp. 888-901.
11. Schlez, W., Neubert, A. (2009). New developments in large wind farm modelling. *Proceedings of the EWEC*, Marseille, France.
12. Beaucage, P., Robinson, N., Brower, M., Alonge, C. (2012). Overview of six commercial and research wake models for large offshore wind farms. *Proceedings of the EWEA conference*, Copenhagen.
13. Jensen, N.O. (1983). A note on wind generator interaction. Risø-M-2411, Risø National Laboratory.
14. Katic, I., Hojstrup, J., Jensen, N.O. (1986). A simple model for cluster efficiency. In *Proceedings of the European Wind Energy Association Conference and Exhibition*, pp. 407–410.
15. Frandsen, S. (1992). On the wind speed reduction in the center of large clusters of wind turbines. *Journal of Wind Engineering and Industrial Aerodynamics*, 39, pp. 251-265.
16. Mortensen, N.G., Heathfield, D.N., Myllerup, L., Landberg, L., Rathman, O. (2005). Wind atlas analysis and application program: WAsP 8 help facility. Risø National Laboratory, Roskilde, Denmark. ISBN 87-550-3457-8.
17. Nielsen, P. (2006). The WindPRO manual, edition 2.5, EMD International A/S.
18. Mosetti, G., Poloni, C., Diviacco, B. (1994). Optimization of wind turbine positioning in large windfarms by means of a genetic algorithm. *Journal of Wind Engineering and Industrial Aerodynamics* 51(1), pp. 105-116.

19. Grady, S.A., Hussaini, M.Y., Abdullah, M.M. (2005). Placement of wind turbines using genetic algorithms. *Renewable Energy* 30(2), pp. 259–270.
20. Marmidis, G., Lazarou, S., Pyrgioti, E. (2008). Optimal placement of wind turbines in a wind park using monte carlo simulation. *Renewable Energy*, 33, pp. 1455–1460.
21. Emami, A., Noghreh, P. (2010). New approach on optimization in placement of wind turbines within wind farm by genetic algorithms. *Renewable Energy*, 35, pp. 1559–1564.
22. Chen, Y., Li, H., Jin, K., Song, Q. (2013). Wind farm layout optimization using genetic algorithm with different hub height wind turbines. *Energy Conversion and Management*, 70, pp. 56–65.
23. Acero, J., Acevedo, J., Rendon, M., Oleszewski, O. (2009). Linear wind farm layout optimization through computational intelligence. *Proceedings of 8th Mexican International Conference on Artificial Intelligence*, pp. 692–703.
24. Frandsen, S. (2007). Turbulence and turbulence-generated structural loading in wind turbine clusters. Risø-R-1188(EN), Risø National Laboratory.
25. Burton, T., Sharpe, D. (2011). Wind energy handbook. John Wiley & Sons Ltd, ISBN 0-471-48997-2, Chichester, 2nd edition.
26. Crespo, A., Hernandez, J., Frandsen, S. (1999). Survey of modelling methods for wind turbine wakes and wind farms. *Wind Energy*, 2, pp. 1–24.
27. Frandsen, S., Barthelmie, R., Pryor, S., Rathmann, O., Larsen, S., Højstrup, J., Thøgersen, M. (2006). Analytical modelling of wind speed deficit in large offshore wind farms. *Wind Energy*, 9, pp. 39–53.

Chapter 5 : Investigating the Power-COE Trade-Off for Wind Farm Layout Optimization

Considering Commercial Turbine Selection and Hub Height Variation

Abstract

New aspects were added to the wind farm layout optimization problem by including commercial turbine selection and a realistic representation for the thrust coefficient. The available manufacturers' data were used to develop generic representation for the thrust coefficient, on which the wake and power calculations mainly depend. A simple field-based cost model was implemented. The optimization was performed for onshore and offshore conditions using MATLAB genetic algorithm, *ga*, solver for two simple test cases. Three objective functions were considered, individually: (1) the output power, (2) the capacity factor, and (3) the cost per output power.

The results showed that the flexibility of using different turbines and hub heights can provide a useful trade-off between power and cost. The trade-off was found to be wider in offshore cases, which means that the optimization is more useful in such conditions. The optimization for maximum capacity factor acts as a mid-point between the two design extremes of maximizing power and minimizing the cost of energy. Almost all turbines were selected at least once in an optimum layout. However, the priority in selection was for the turbines that have bigger diameter and/or lower rated speed amongst the other turbines of the same rated power.

Keywords: Wind farm layout optimization, Genetic algorithm, Commercial turbine selection, Wind turbine thrust, Hub height variation.

5.1 Introduction

The expanding wind power market faces several technical and financial challenges related to output power maximization and cost of energy (COE) minimization. Moreover, many restrictions have been put on wind farm installations because of environmental impact in the form of noise, visual effects, and bird and bat interactions. All these factors increase the need for Wind Farm Layout Optimization (WFLO) which investigates the design of wind farms in order to optimize the value of one (or more) objective function(s) while satisfying one (or more) constraint(s). The classical WFLO literature deals mainly with placing identical turbines to maximize energy production, minimize COE, maximize profit, or a combination of them [1].

Mosetti et al. [2] introduced the WFLO problem. They considered 10×10 square cells of 200 m sides, in which identical 40 m diameter turbines were to be placed. A constant thrust coefficient, $C_T = 0.88$, as well as simple cubic power curve were assumed. Jensen's analytical wake model [3,4] was used to assess turbine interference and a Genetic Algorithm (GA) was implemented to maximize a combined objective function including the total power and the inverse of the cost of energy, using arbitrary weighting factors.

For the following decade, no significant contribution was made to WFLO. New aspects were then implemented; either to the design variables, constraints, objective functions, and/or to the optimization methodology. Many researchers have analyzed the problem proposed by Mosetti et al. in order to obtain better layouts and/or reduce the computational time, either with some improvements to the GA, e.g. [5,6,7,8] or by implementing other optimization strategies, e.g. [9,10,11,12,13].

Very few studies have considered non-identical turbines and/or varying hub heights; these will be reviewed in more detail in the next section. The motivation and the aims of the proposed

research are stated at the end of section 5.2. The proposed methodology is explained in detail in section 5.3. Finally, the primary results for the test cases as well as the major conclusions are the topics of sections 5.4 and 5.5, respectively.

5.2 Literature Review

Herbert-Acero et al. [14] maximized the power production by a line of turbines in the wind direction using both Simulated Annealing and a GA implemented in MATLAB. They used the technical data for the REpower, MD77 turbine with rotor diameter, $D = 77$ m. Two values of hub height (H) were used, 50 m and 85 m, to reduce the effect of wake overlap. The design parameters were the number of turbines, locations, and the individual H , while fixing the line length at 1,550 m ($20.13 D$). The optimum number of turbines was 6 or 7, which results in average spacing of 4 D and $3.35 D$, respectively. The results showed that the placement of wind turbines with different heights could increase the power generation in a straight line layout for a single wind speed and two opposite wind directions along the line.

Most actual wind farms employ identical turbines (one model and one H) even if the installation was done in several stages. It is worth noting, however, that a typical major wind farm owner owns up to several thousand turbines with a wide range of models and H [15]. For example, the European fleet maintained directly by EDPR (one of the major owners in Europe) includes 32 turbine models with a wide range of H [16]. In this context, a change from the current situation of companies owning a large number of farms with identical turbines to varying models and H in each farm, does not seem like a big change.

Chowdhury et al. [17,18] applied their Unrestricted Wind Farm Layout Optimization (UWFLO) simultaneously with the appropriate selection of turbines in terms of D (while fixing

H), in order to maximize the total power generation. Three different cases were considered: (1) wind farm with identical turbines, (2) wind farm with differing D , and (3) wind farm with identical turbines that can adapt to wind conditions (axial induction factor varying on the wind speed) which can be done for commercial turbines. They found that an optimal combination of wind turbines with differing rotor diameters can appreciably increase the farm power generation. They mentioned that a more practical wind farm optimization requires the treatment of rotor diameters as discrete design variables, as there is only a limited choice of commercial wind turbines.

Chowdhury et al. [19] significantly improved their UWFLO, enabling it to simultaneously optimize the placement and the selection of turbines for commercial-scale wind farms to minimize the COE. The number of turbines and the farm size were assumed to be fixed at the values for the particular wind farm that they studied. They considered the GE 1.5 xle-82.5 as the reference turbine and normalized the manufacturer's power curve with respect to the general specifications (rated power, P_r , cut-in and rated speeds, U_{in} and U_r , respectively). This curve was assumed to be valid for all commercial turbines and scaled to represent the power curve for any turbine (in the range $0.6 < P_r < 3.6$ MW) as long as the general specifications are defined. The results showed that simultaneous optimization of the layout and the turbine selection increased the capacity factor by 2% more than that accomplished by layout optimization alone. The optimum layout contained turbines with $1.8 < P_r < 3$ MW, $90 < D < 110$ m, and $80 < H < 120$ m.

Chen et al. [20] investigated the use of different H in a small wind farm layout optimization using GA in MATLAB. They first conducted the layout optimization of a 500 m square wind farm. Enercon E40m-600kW turbines were used with two values of H (50 and 78 m) and the minimum turbine proximity of 100 m ($2.5 D$). Then a larger wind farm (2800 m x 1200 m) with larger wind turbine (GE 1.62-100) was analyzed to further examine the benefits of using different hub heights

(80 and 100 m) in more realistic conditions. The minimum turbine proximity was set as 400 m (4 D). Different cost models were used in the analysis, and results showed that different hub height wind turbines can increase the power production and/or reduce the COE.

By reviewing the WFLO literature, three deficiencies were identified and led to the research objectives of the present work:

- (5) Selection among the available commercial turbines,
- (6) Developing realistic evaluation for commercial turbines' C_T , and hence the wake development, and
- (7) Investigating the trade-off range between total farm power and COE.

This was done for the basic layout of 6 Turbines In Line (TIL) with the wind as this maximizes turbine interference, and for a small wind farm (SWF) array consists of 18 turbines. Both typical onshore and offshore cases were simulated.

5.3 Methodology

In this section, the proposed methodology is presented in detail. In subsection 5.3.1, the wake model is described first and then the wake interference calculations are formulated. In subsection 5.3.2, the commercial turbines included in the proposed analysis are mentioned and the power calculations are presented, while subsection 5.3.3 presents the general C_T representation for commercial turbines. The investigated range of hub heights is given and justified in subsection 5.3.4, the cost analysis is discussed in subsection 5.3.5, the test cases are described in subsection 5.3.6, and the optimization methodology is illustrated in subsection 5.3.7.

5.3.1 Wake model and interference calculations.

Among many wake models that have been developed over the last four decades, Jensen's analytical wake model is one of the oldest, simplest, and most accurate in estimating both velocity and power deficits within wind farms, e.g. [21,22,23,24]. It was also implemented in the majority of WFLO literature as well as the major WFLO software packages, such as WAsP [25] and WindPro [26]. This model, originally proposed by Jensen [3], was developed by Katic et al. [4] and further by Frandsen [27]. Referring to Figure 5.1, the wake calculations are as follows:

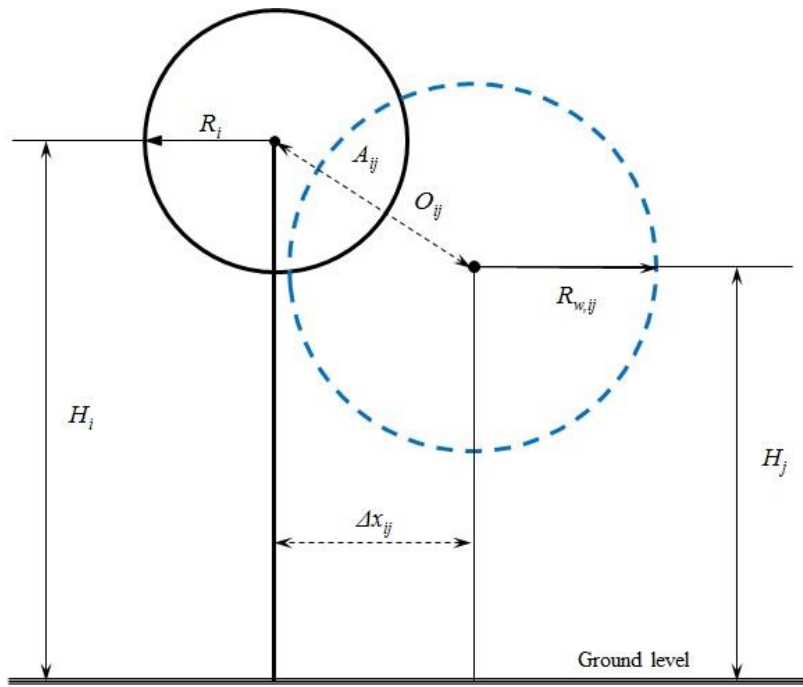


Figure 5.1: A front view (parallel to wind direction) illustrates the overlap of the upwind turbine wake (the dashed circle) with the downwind turbine rotor (the solid circle). The Y co-ordinate is into the page.

The wind blows in the positive Y direction, and the turbines were sorted in ascending order according to their Y coordinates. For example: the most upwind turbine, which has the least Y -coordinate, was designated 1, while the most downwind one was N (the total number of turbines). Accordingly, except the most upstream turbine, each turbine i in the farm, $2 < i < N$, is potentially affected by the wake of every upwind turbine j , $1 < j < i-1$.

In Figure 5.1, a schematic of the wake interference between upwind and downwind turbines is given. H_i and H_j are the hub heights for the downwind and upwind turbines, respectively, R_i is the downwind turbine rotor radius, and $R_{w,ij}$ is the radius of the j^{th} turbine wake when it reaches the i^{th} turbine [27]

$$R_{w,ij} = R_{exp,j} + \alpha_j \Delta y_{ij} \quad (5.1)$$

where

$$R_{exp,j} = R_j \sqrt{(1 - a_j)/(1 - 2a_j)} \quad (5.2)$$

- α_j is the wake expansion coefficient for the j^{th} turbine, which is given in terms of the hub height, H_j , and the site roughness length, z_o , as [27]

$$\alpha_j = 0.5 / \ln \left(\frac{H_j}{z_o} \right) \quad (5.3)$$

- $\Delta y_{ij} = y_i - y_j$, is the Y -distance between the two turbines, not shown in Figure 5.1.
- The velocity deficit for the i^{th} turbine that caused by the wake of the j^{th} turbine, δU_{ij} , is approximated as

$$\delta U_{ij} = \left\{ \frac{1 - \sqrt{1 - C_{T,j}}}{[1 + \alpha_j \Delta y_{ij} / R_{exp,j}]^2} \right\} \left(\frac{A_{ij}}{A_i} \right) \quad (5.4)$$

where A_{ij} is the overlap of the j^{th} turbine wake with the downwind turbine rotor, A_i .

- The cumulative velocity deficit ahead of the i^{th} turbine caused by all upwind turbines is [4]

$$\delta U_i = \sqrt{\sum_{j=1}^{j=i-1} (\delta U_{ij})^2} \quad (5.5)$$

The effective wind speed immediately upwind of the i^{th} turbine is given in terms of the cumulative velocity deficit and the undisturbed wind speed at H_i , $U_{o,i}$ as [3,4]

$$U_i = U_{o,i}(1 - \delta U_i) \quad (5.6)$$

The following assumptions were made:

(1) The wind has constant speed, direction, and density, $\rho = 1.225 \text{ kg/m}^3$. Three values were used ($U_{ref} = 8, 10, \text{ and } 12 \text{ m/s}$ at $H_{ref} = 60 \text{ m}$).

(2) The roughness length, z_o , was taken as 0.3 m for onshore and 0.0002 m for offshore farms.

These values are widely accepted in the WFLO literature.

(3) The log law [28] was used to extrapolate wind speed from the reference height in order to estimate the undisturbed wind speed at any height, $H_{min} \leq H_i \leq H_{max}$

$$U_{o,i} = U_{ref} \left[\frac{\ln(H_i/z_o)}{\ln(H_{ref}/z_o)} \right] \quad (5.7)$$

For each U_{ref} the electrical power output of any turbine depends on its location relative to all its upwind turbines, the type, H , and C_T for all upwind turbines, and its type (in terms of its power curve) and H .

The wake model was validated against the energy production data for Horns Rev 1 offshore wind farm (as one of the most famous large wind farms worldwide). The farm layout and turbines' power curve are available in [29], wind resource assessment over three years for the farm site (before installation) is available in [30], while the details of farm energy production are found in

[31]. Figure 5.2 presents the estimated annual energy production using Jensen wake model, based on the available wind resource assessment and $z_0 = 0.0002$ m, compared with the recorded farm production between 2005-2015. Three-year-average energy production is also provided for comparison.

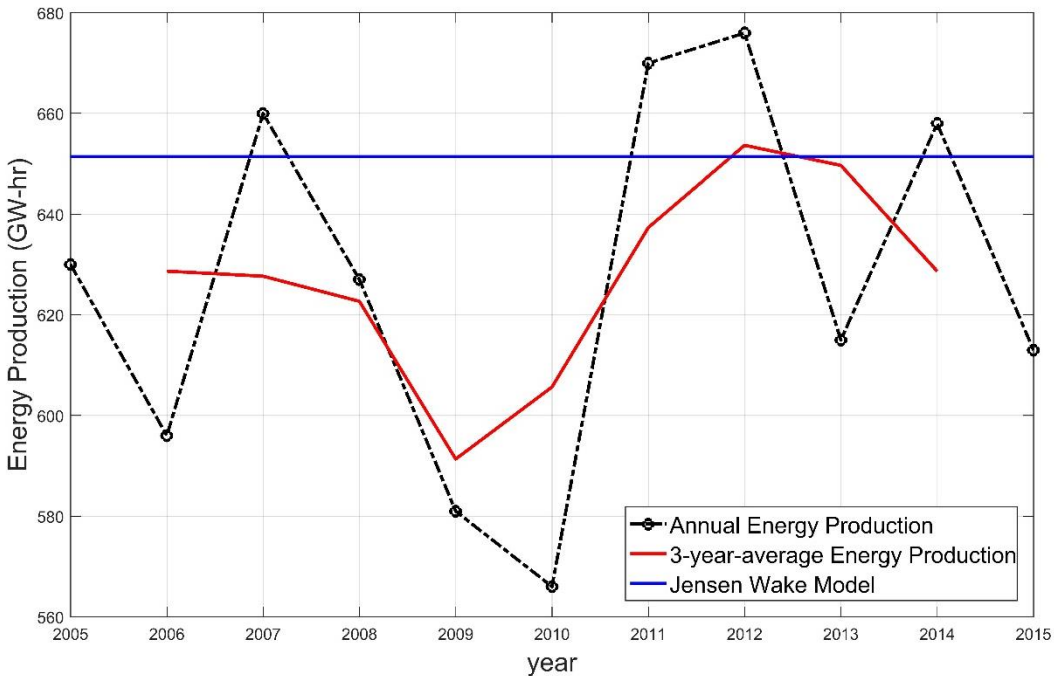


Figure 5.2: Validation of Jensen wake model against data from Horns Rev 1 offshore wind farm.

5.3.2 Commercial Turbines and Power Calculations

Part of the novelty in the present work is the use of the manufacturers' power curves for commercial turbines. The majority of manufacturers provide a graph of the output electrical power, P_e , as a function of U , rather than numerical values. A few manufacturers provide tabulated values at the standard air density, $\rho = 1.225 \text{ kg/m}^3$, while only Vestas gives these data for different air densities. Among more than one thousand turbine models [32], about one hundred numerical power curves could be obtained. However, it was decided to focus on the commercial turbines that

fall in the most popular range of rated power ($1.5 < P_r < 3.0$ MW). To this end, 61 commercial turbines from 15 manufacturers in 8 countries were included in the analysis. The selected turbines cover a wide range of rotor diameter ($66 \text{ m} \leq D \leq 115 \text{ m}$) and rated speed ($11 \text{ m/s} \leq U_r \leq 17 \text{ m/s}$). The 61 curves were fitted by a 5th degree polynomial, and the coefficients were used to estimate the power developed by each turbine at any wind speed between U_{in} and U_r . For wind speeds above rated speed, the power output was taken as the rated value. Note that no simulations were done for wind speeds greater than the cut-out speed. Accordingly, the power developed by the i^{th} turbine based on its type and the effective wind speed, U_i determined as per the previous section, is estimated as

$$P_i = c_{i0} + c_{i1}U_i + c_{i2}U_i^2 + c_{i3}U_i^3 + c_{i4}U_i^4 + c_{i5}U_i^5 = \sum_{k=0}^{k=5} c_{ik}U_i^k \quad (5.8)$$

The total farm output power is simply the sum of the individual powers from the N turbines

$$P = \sum_{i=1}^N P_i = \sum_{i=1}^N \sum_{k=0}^{k=5} c_{ik}U_i^k \quad (5.9)$$

and the farm capacity factor (CF) is defined as

$$CF = \frac{\text{Output Power}}{\text{Rated Power}} = \frac{\sum_{i=1}^N \sum_{k=0}^{k=5} c_{ik}U_i^k}{\sum_{i=1}^N P_{r,i}} \quad (5.10)$$

5.3.3 Commercial Turbine Coefficients

The major wind turbine operational parameters are the power and thrust coefficients. As shown by Equation (5.4), C_T is required for wake analysis, however, thrust data is rarely available and one of the greatest challenges in WFLO is the lack of accurate C_T , e.g. [19]. For this reason, many WFLO analyses assumed a fixed value for C_T , usually 0.88, e.g. [2,5,9,7,20]. However, it is not

accurate in comparison with the available C_T curves for commercial turbines, [33]. It was found by simple calculations that an underestimation of C_T by 0.1 typically results in a significant underestimation in δU_{ij} by about 2-3 %, which overestimates the power output of a downstream turbine by 6-10 %. In order to obtain a general and practical representation for the thrust coefficient, the available C_T data for thirteen commercial turbines (eight from Vestas, three from REpower, and two from Sinovel) were used to develop two general representations for C_T in terms of the aerodynamic and the electric power coefficients, $C_{P,a}$ and $C_{P,e}$, respectively. The electric power is simply the turbine output power given by the manufacturer as function of the approaching wind speed, while the aerodynamic power is defined as the turbine output power if the mechanical and conversion losses are neglected. These two generic curves are given in Figure 5.3 along with the results obtained by WT_Perf BEM theory code for NREL 5 MW reference turbine for different values of pitch angle, β [34]. It is clear that the $C_T-C_{P,a}$ curve matches well with that for NREL turbine at different pitch angles, which give confidence to the proposed generalization. Finally, the $C_T-C_{P,e}$ (the dashed line in Figure 5.3) was fitted by a 5th degree polynomial and used to estimate the thrust coefficient for any turbine once the electric power coefficient is evaluated.

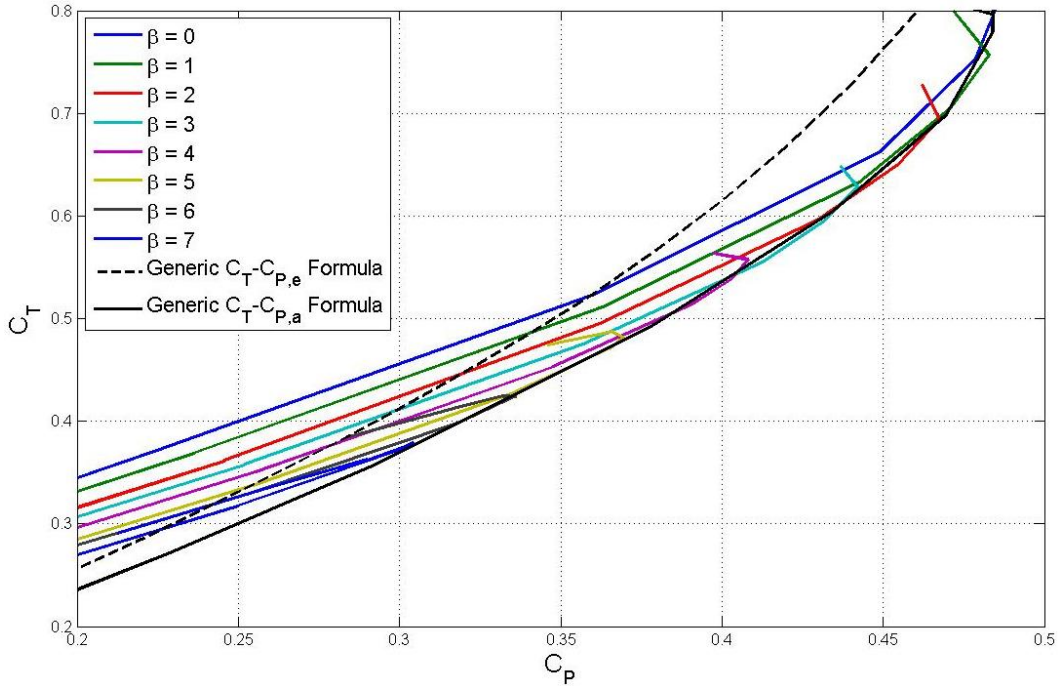


Figure 5.3: General representation for the thrust coefficient, C_T , vs the aerodynamic and the electric power coefficients, $C_{P,a}$ and $C_{P,e}$, respectively, compared with $C_T - C_{P,a}$ curves obtained for NREL 5 MW reference turbine at different values of pitch angle, β .

5.3.4 Hub Height Variation

It is essential to specify the minimum and maximum H (H_{min} and H_{max}) to be investigated. For H_{min} , the “minimum ground clearance” recommendations were taken into account, while H_{max} should be set by the technology available to install and operate turbines on tall towers. The ground clearance of a commercial turbine is the height of the blade tip at its lowest position (when the blade is vertically down). The minimum practical value was taken as 75 ft. (22.86 m), e.g. [35]. Accordingly, H_{min} for the largest rotor diameter included in the current study ($D_{max}=115$ m) is $H_{min} = (115/2) + 22.86 = 80.36$ m.

On the other hand, taller towers are usually employed to avoid the large wind shear and high turbulence level at relatively low heights caused partly by the topography, [36]. Engström et al. [36] described welded steel shell towers for large turbines and concluded that the available technology can provide towers up to 150 m for 3 MW turbines. Moreover, many operating turbines were installed with $H > 140$ m, e.g. [37]. To this end, the lower and upper limits for H in the analysis were taken as 80 m and 140 m, respectively.

5.3.5 Simple Cost Model

Since the pioneering work by Mosetti et al., many cost models have been developed in order to implement the COE as an objective function in WFLO [38,1]. The majority of these models were based on assumptions, local experience, and/or limited available data. The cost of wind farm installation as well as COE varies significantly over time and location, e.g. [39]. The number of turbines, the distance from the manufacturer, the cost of land and infrastructure, material and labor costs, etc. significantly affect the total farm cost as well as the COE. Accordingly, it was decided to simplify the cost analysis by parameterization in terms of the main design variables (P_r and H) as far as possible. The major wind power cost reports were reviewed and the following conclusions were drawn:

- i. The Capital Cost (CC) is the major component of the Total Cost (TC) of a wind power project. Its fractional contribution ranges from 0.70 - 0.83 of the Levelized Cost of Electricity (LCOE) in the major European countries to 0.89 in USA [40].
- ii. The operations and maintenance (O&M) costs of wind power can be represented in \$/kW, \$/kW-yr, \$/MW-h, or as a percentage of the LCOE, e.g. [40,41,42].

- iii. The average cost/kW for offshore wind farms is almost double that for onshore ones, also the O&M cost share ($C_{O\&M}$) is larger in offshore projects, e.g. [40,41].
- iv. The turbine capital cost represents about 0.68 of the CC for onshore and about 0.32 for offshore projects. The tower cost share (C_{tower}) represents approximately 0.12 and 0.0565 of the CC for onshore and offshore projects, respectively [43].

In order to develop a simple and general cost model, the following assumptions were made:

- a. Turbine cost was assumed to be determined by the rated power and hub height only. Also the turbines were assumed equally available everywhere, accordingly the factor of proximity from the manufacturers was disregarded.
- b. The CC was represented in terms of the turbines' rated power and hub height, while the O&M costs were determined as a fraction of the TC over the entire lifespan, and independent of layout.
- c. It was decided to set $C_{O\&M}$ as 0.15 and 0.25 of the TC over the entire lifespan for onshore and offshore farms, respectively.
- d. The minimum H ($H_{min} = 80$ m) was assumed to be the reference tower height, which also matches with the common practice for multi-MW turbine towers.
- e. The CC of 1.0 MW at H_{min} was taken as the unit cost and was denoted by Capital Cost Index (CCI).
- f. The increase in H was assumed to be added linearly to the CCI, i.e. each increase of 1.0 m above H_{min} adds 1/80 of the contribution of the tower cost to the CC.

Accordingly, the Total Cost Index (TCI) was calculated using the general formula

$$TCI = \frac{CCI}{1 - C_{O\&M}} = \left(\frac{1}{1 - C_{O\&M}} \right) \sum_{i=1}^N P_{r,i} \left[1 + \frac{C_{tower}}{H_{min}} (H_i - H_{min}) \right] \quad (5.11)$$

where $P_{r,i}$ is the rated power of the i^{th} turbine (in MW).

It is worth noting here that “total” in TCI is strictly not correct, as the financial and balance of system costs are not included in Equation (5.11). However, the effect on the calculation is negligible because these costs depend mainly on the turbines citing which was assumed fixed in the SWF cases and slightly changes along a specified line length in the TIL ones.

Finally, the Total Cost Index per Output Power (TCIOP) as the TCI divided by the output power (similar to the COE) is the third objective function.

5.3.6 Test cases

Before applying the proposed optimization methodology to real wind farms, it was decided to consider simpler test cases in order to examine the effect of the investigated parameters on the different optimum designs. Two arrangements were analyzed (1) turbines in line with the wind direction, and (2) a small wind farm. For all cases, the wind direction was in the direction of the turbines in Figure 5.4a. This Figure shows the simplest wind farm layout, the turbine in line, and the extreme case of wake interference [44,33]. This simple arrangement is suitable for examining the effect of turbine selection and hub height variation on the different optimum layouts. $N = 6$ is typical of wind farm rows and large enough to display the major effects of interference, e.g. [4,45,46,44,1]. The total length of the line, L_Y , was specified based on N , an arbitrary spacing multiplier, S , and nominal diameter, $D_{nominal}$. The nominal diameter was taken as the diameter of the largest rated power turbine in the dataset used in this work, which has a rated power of 3.075 MW and 112 m rotor diameter.

$$L_Y = (N - 1) SD_{nominal} \quad (5.12)$$

Three values of S were investigated (4, 5, and 6), giving three values for L_Y : 2.24, 2.80, and 3.36 km, respectively. The reason for using fixed N and L_Y was to allow later comparison among the different optimum layouts and a reference (un-optimized) design. The reference design was simply N equally spaced turbines of largest rated power installed at maximum investigated height ($H = 140$ m). It is important to emphasize here that S was used initially to specify the line length. Except of the reference design, the turbines can be located anywhere along the line during the optimization as long as the minimum turbine proximity constraint is satisfied.

The second test case was for small wind farm array of m columns parallel to the wind and n rows normal to the wind direction, where $m = 3$ and $n = 6$ (so $N = 18$). The same values for S , L_Y , and U_{ref} (as given in TIL test case) were investigated. The spacing multiplier in the crosswind direction was 3, fixed in all optimizations, so the farm crosswind length was fixed ($L_X = 672$ m). It was decided to fix the turbine locations during the optimizations in order to direct the optimization towards the turbine selection (which is the main aspect) as well as H variation. However, two common configurations were used (array and staggered) as shown in Figure 5.4b and Figure 5.4c, respectively. Again, the reference design for each configuration contains 18 largest turbines at $H = 140$ m.

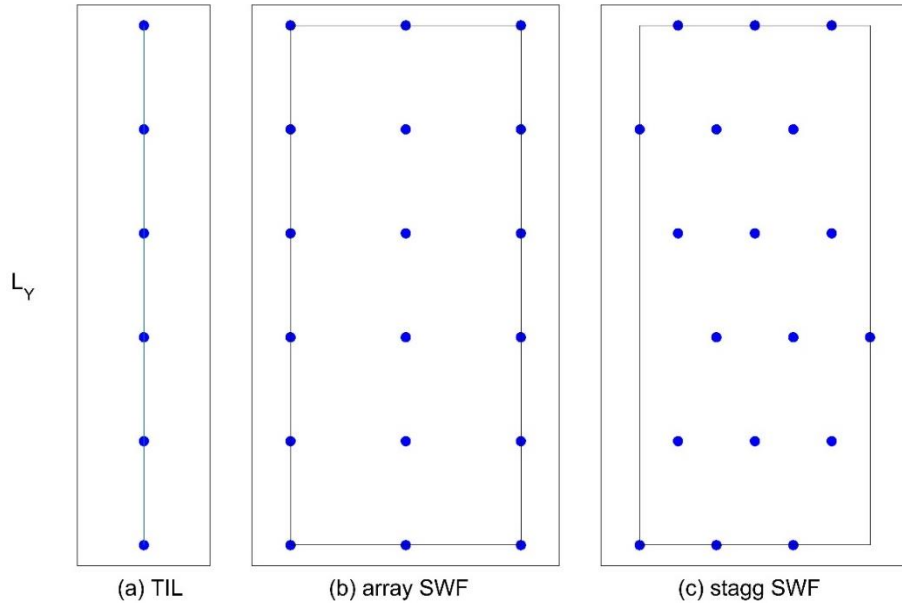


Figure 5.4: Reference TIL, array, and staggered SWF layouts.

5.3.7 Optimization

Any optimization problem, including the WFLO, consists of four fields: the design variable(s), the constraint(s), the optimization objective(s), and the optimization technique, e.g. [38,1]. In this subsection, the treatment of these four parts in the proposed methodology is explained.

5.3.7.1 Design Variables.

The design (or decision) variable is a parameter that needs to be determined (adjusted) in order to achieve the optimum solution. The design variables must have upper and lower limits within which the feasible solutions could be obtained. For the first test case, three variables are to be evaluated for each turbine: location Y , type, and H , while the turbine locations for the second test case are fixed. Accordingly, the number of design variables are 18 and 36 for TIL and SWF, respectively.

5.3.7.2 Constraints

Optimization problems are usually subjected to restrictions (constraints), and hence not all solutions are feasible. The upper and lower limits for the design variables are the simplest form of constraints, and the integer constraint is another example, in which one (or more) of the variables is (are) necessarily integer. The following constraints were involved in the proposed problem:

- The location of any turbine, i , ($1 \leq i \leq N$) in the TIL case was bounded by the line length (linear constraint)

$$0 \leq y_i \leq L_Y \quad (5.13)$$

- The hub height for any turbine was bounded by the minimum and maximum investigated value of H (linear integer constraint)

$$H_{min} \leq H_i \leq H_{max} \quad (5.14)$$

- The selection among the commercial turbines is a linear integer constraint. The 61 turbines were sorted based on the rated power in an ascending order. The turbines then coded and any turbine in the farm was allowed to take any integer value from 1 to 61.

$$1 \leq code_i \leq 61 \quad (5.15)$$

- The minimum turbine proximity was used for TIL optimizations, in which the minimum distance between any two turbines was set as $3D_{nominal}$. Accordingly, the following condition was applied

$$\Delta y_{ij} = y_i - y_j \geq 3D_{nominal} \quad (5.16)$$

where, $1 \leq i, j \leq N$ and $i \neq j$; which results in $\sum_{k=2}^N k = 20$ linear constraint equations.

5.3.7.3 Optimization objectives

The objective (fitness) function is simply the variable to be optimized (maximized or minimized). As mentioned before, three objective functions were considered, individually, in this work: total power, Equation (5.9), farm capacity factor, Equation (5.10), and total cost index per output power, determined from Equation (5.11) divided by Equation (5.9).

5.3.7.4 Optimization technique

The best optimization technique depends mainly on the nature of the problem as well as the constraints. The present optimization problem is discrete, non-linear, non-convex (as it has many local minima), of very high dimension (each turbine has 61 probabilities in both turbine selection and H), and mixed integer. GAs have been proven a powerful tool for such complex problems, e.g. [47]. For this reason, a GA was implemented in the majority of the WFLO literature, although it is slow compared with the other optimization methods [38,1]. GAs are computer programs that mimic the processes of biological evolution in order to solve problems and to model evolutionary systems [48]. The solution is obtained by moving from one population of chromosomes (feasible solutions) to a new population by using a kind of natural selection (random search) together with the genetics-inspired operators of crossover, mutation, inversion, etc. Each chromosome consists of a number of genes that are the possible values of the design variables. The selection operator chooses those chromosomes in the population that will be allowed to reproduce, and on average the fitter chromosomes produce more offspring than the less fit ones [48].

The MATLAB *ga* solver was used to obtain the optimum layouts. The population size (number of feasible solutions) was set as large as possible to widen the random search in order to increase the probability of finding the global optimum solution instead of local optima. The chromosomes

were allowed to evolve up to 3,000 generations unless the algorithm stops because the average relative change in the best fitness function value is less than or equal to an arbitrary value called *TolFun*. This value was set as low as 10^{-15} compared with the default value, 10^{-6} , in order to ensure that the solution is optimal. The stopping criterion was satisfied (and hence the algorithm was terminated and the optimum solution was obtained) after 1,500 to 2,500 generations in the majority of the test cases presented in this paper. A flowchart is given in Figure 5.5 for the GA procedure.

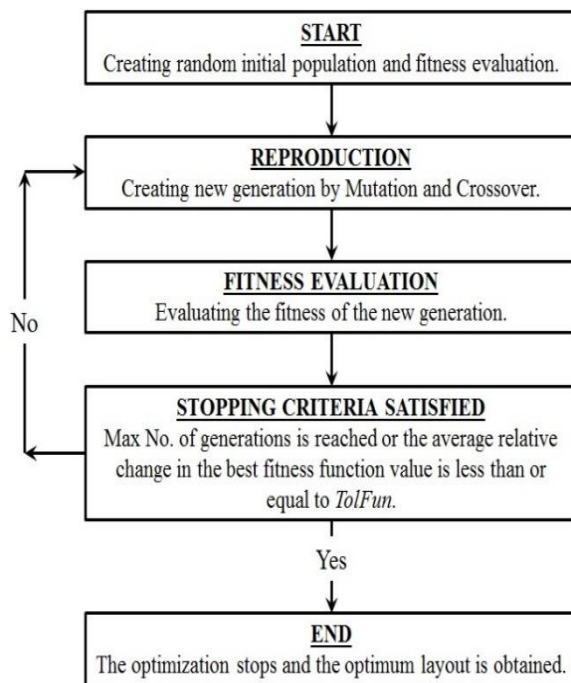


Figure 5.5: Flowchart for Genetic Algorithm.

5.4 Results, and Discussion

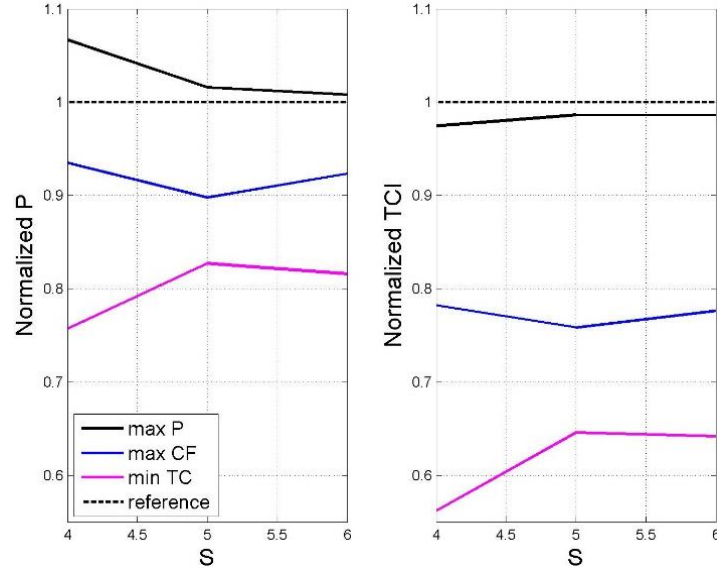
In this section the results are presented and analyzed and the major findings are discussed. The power output and the total cost index of the un-optimized design will be referred as “reference

power” and “reference cost”, respectively. The optimization for minimum TCIOP will be referred as “min TC ” for brevity.

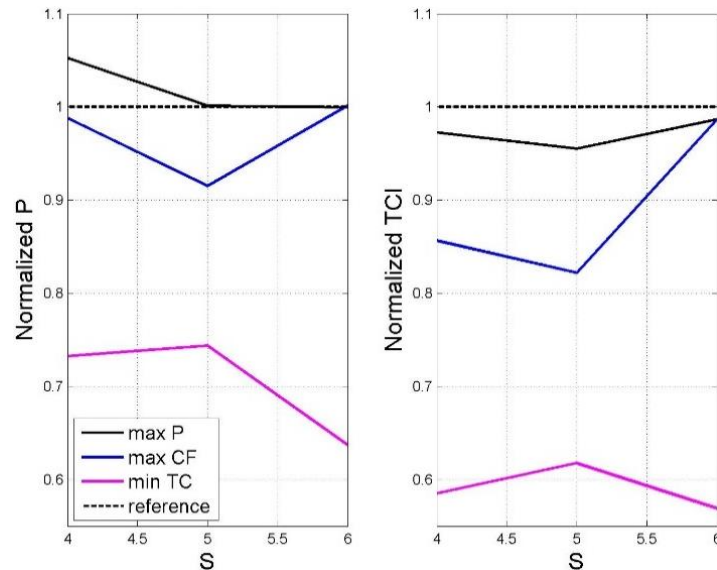
Figure 5.6a, b, and c present the results for the onshore TIL optimizations for $U_{ref} = 8, 10$, and 12 m/s , respectively, while Figure 5.7a, b, and c are for the offshore ones. The total power, P , and the total cost index, TCI , are normalized with respect to that for the corresponding reference layout in order to get clear comparisons. The main results are summarized as:

1. The reference cost was always the maximum cost, as it contains the largest turbines and max H . However, the reference power was not the maximum, except for the onshore conditions at high wind speed at which P from all optimizations, except min TC , collapse to the reference power.
2. As expected; the optimization for max P and min TC are two design extremes. The optimization of max CF gives results between these extremes, except for high wind speed conditions when it tends to collapse to the max P optimization.
3. Between the two design extremes there is a relatively wide band of both P and TCI which is, in all cases, shifted up for normalized P compared with that for normalized TCI . These two observations are very important and beneficial. The existence of the two bands gives many feasible designs for the $P-TCI$ trade-off. Moreover, the upward shift of normalized P implies that lower cost well-designed layouts can develop equal to (or even higher than) power that can be developed by higher cost improperly designed ones.
4. For the same U_{ref} , N , and farm area the onshore cases developed power up to double that of the offshore ones (especially at low U_{ref}), however, the latter gave higher normalized power as well as wider trade-off range. These two observations have the same origin which can be explained as follows: the onshore roughness length, z_0 , is much larger, which cause more wind shear. As the reference wind speed was given at a particular height, the wind speed was higher

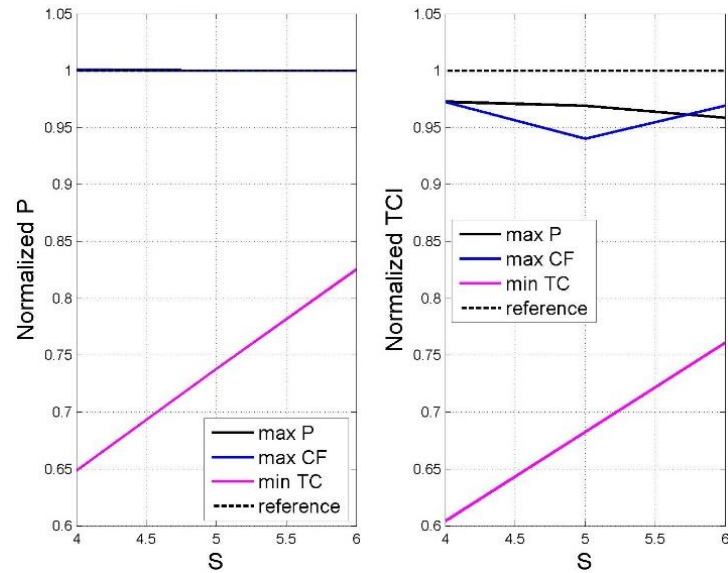
for the larger z_0 at higher H . Moreover, the larger the z_0 the higher the entrainment and the wake velocity through the wake, according to Equations (5.3) and (5.4), respectively. All these reasons make the onshore cases develop much more power and, in the same time, make the optimization more effective in the offshore cases (especially at lower U_{ref} and/or S).



(5.6a) $U_{ref.} = 8 \text{ m/s.}$

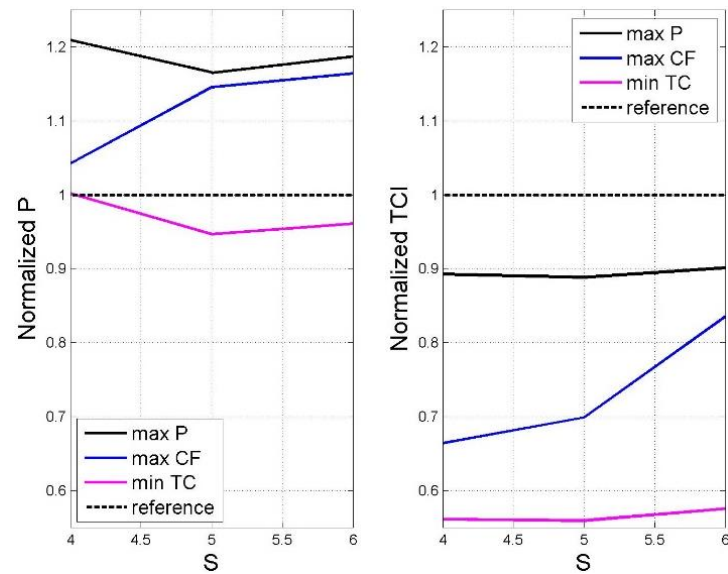


(5.6b) $U_{ref.} = 10 \text{ m/s.}$



(5.6c) $U_{ref.} = 12 \text{ m/s.}$

Figure 5.6: Normalized P and TCI to the reference layout for onshore TIL as a function of S .



(5.7a) $U_{ref.} = 8 \text{ m/s.}$

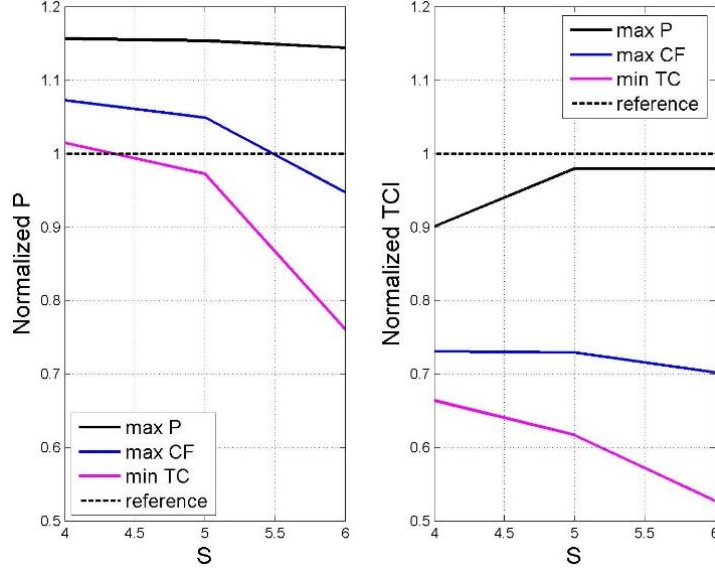
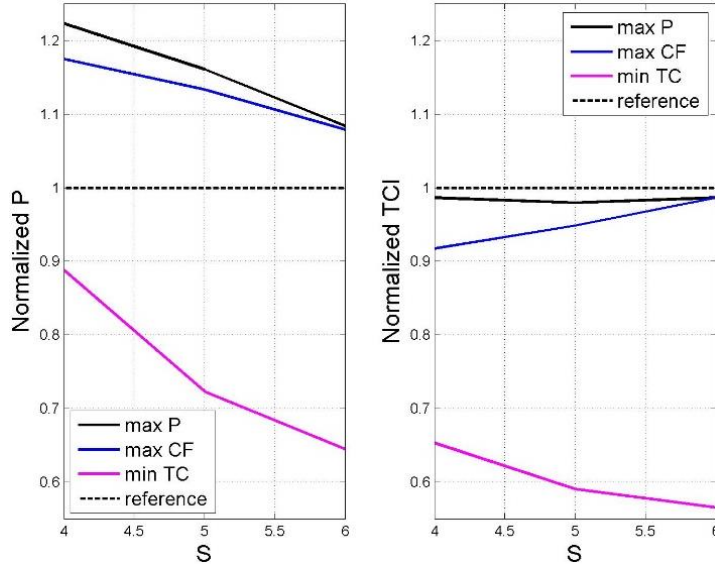
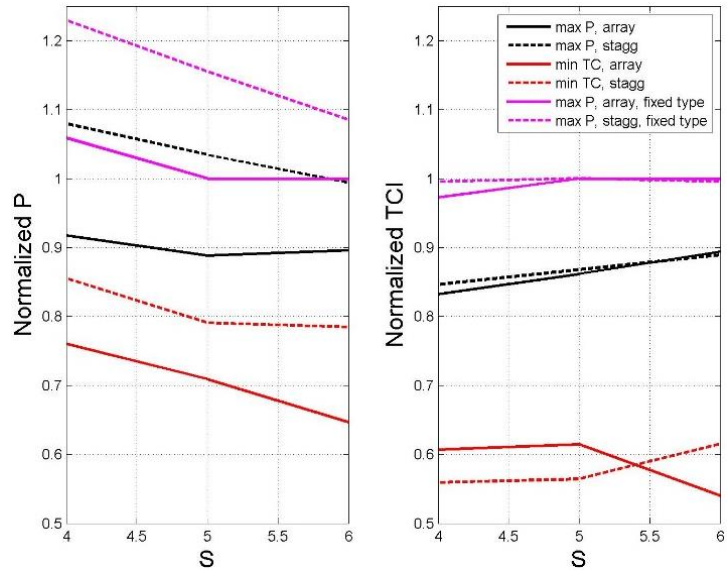
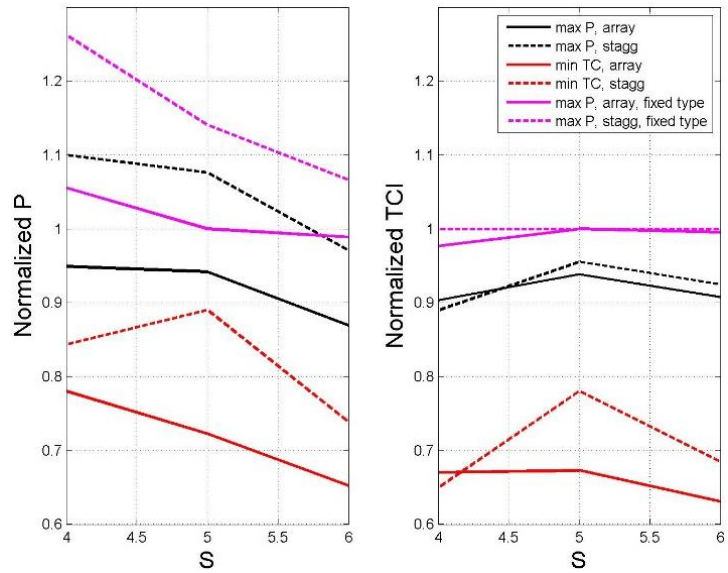
(5.7b) $U_{ref} = 10 \text{ m/s.}$ (5.7c) $U_{ref} = 12 \text{ m/s.}$ Figure 5.7: Normalized P and TCI to the reference layout for offshore TIL as a function of S .

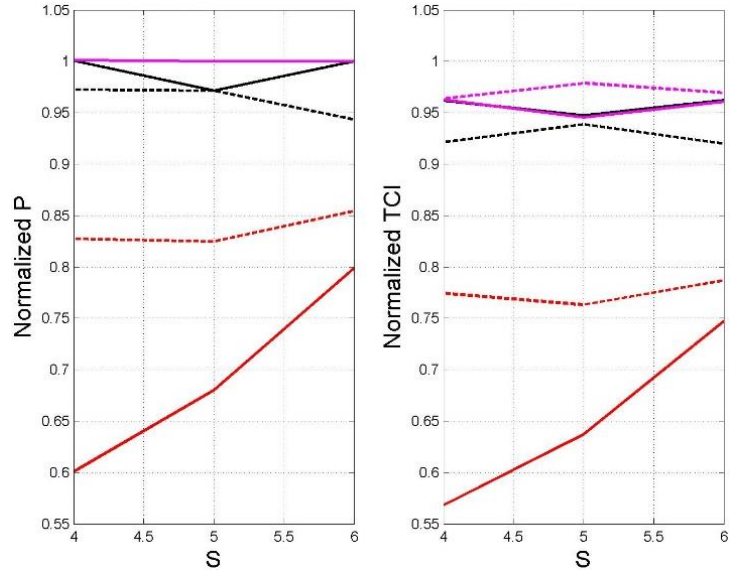
Figure 5.8a, b, and c present the onshore SWF optimizations for $U_{ref} = 8, 10$, and 12 m/s , respectively, while Figure 5.9a, b, and c are for the offshore condition. As mentioned earlier, the

turbine locations were fixed as one of the two configurations in Figure 5.4 (b and c). Moreover, it was decided to exclude the max CF optimization results in order to keep the Figures clear and understandable. Layouts with fixed turbine type with variable H are also provided for both array and staggered configurations in order to present the effect of H variation. Again, P and TCI for array and staggered configurations are normalized relative to that for the un-optimized array layout.

The general trends for SWF results are quite similar (qualitatively) to those for the TIL ones, the other findings are summarized below:

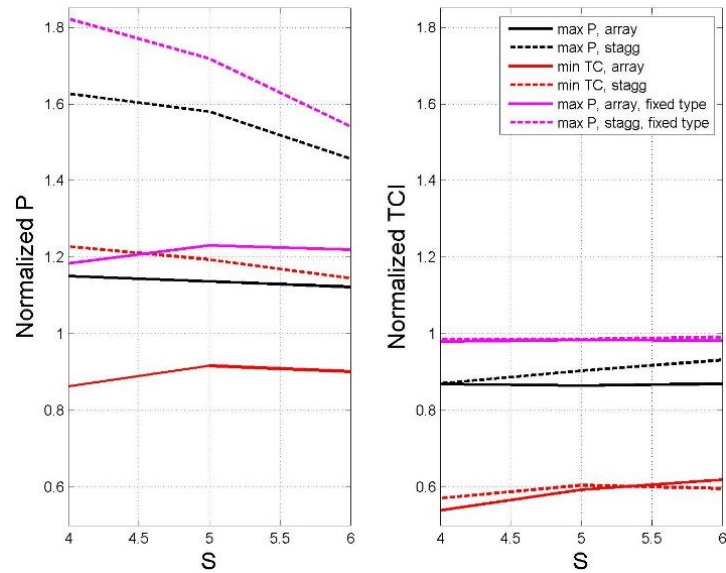
1. As expected, the staggered configuration was superior; it can develop power up to 1.15 and 1.4 times the array one for onshore and offshore conditions, respectively.
2. The staggered SWF has the widest $P-TCI$ trade-off band, especially for the offshore conditions, the TIL comes second, while the array SWF offers a relatively narrow band.
3. The hub height variation was very efficient in optimization, especially for staggered offshore conditions with low U_{ref} and/or S , with the maximum normalized power of 1.82, at $S = 4$, with almost the same reference cost, as seen in Figure 5.9a.

(5.8a) $U_{ref} = 8$ m/s.(5.8b) $U_{ref} = 10$ m/s.

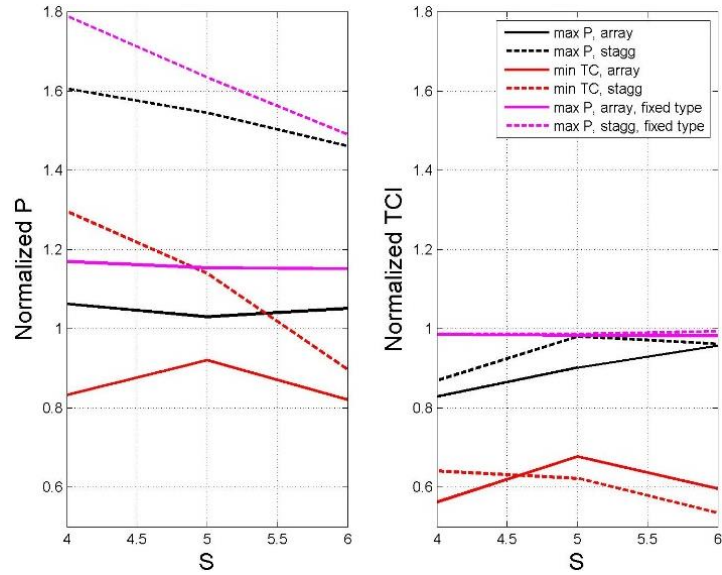
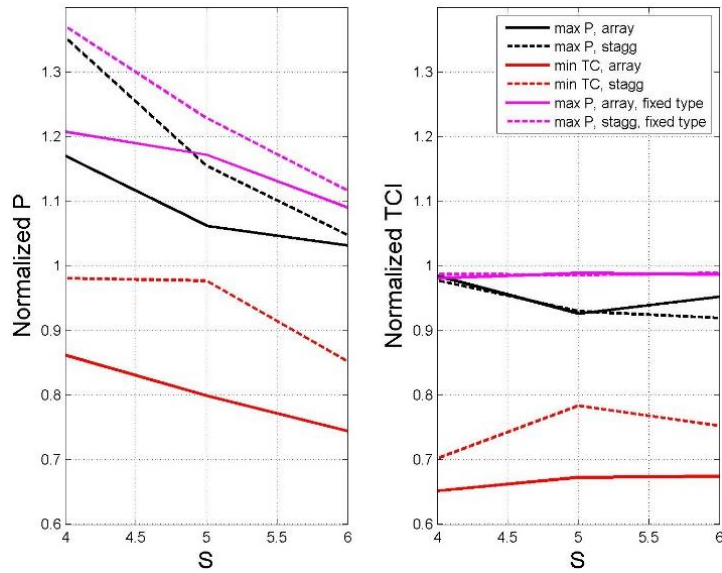


(5.8c) $U_{ref} = 12 \text{ m/s.}$

Figure 5.8: Normalized P and TCI to the reference layout for onshore SWF as a function of S .



(5.9a) $U_{ref} = 8 \text{ m/s.}$

(5.9b) $U_{ref} = 10 \text{ m/s.}$ (5.9c) $U_{ref} = 12 \text{ m/s.}$ Figure 5.9: Normalized P and TCI to the reference layout for offshore SWF as a function of S .

For the sake of brevity and as the P-COE trade-off is the main aspect, it was decided not to present the resulted optimum layouts for the test cases in detail. However, the frequency of turbine and H selection for TIL optimizations are given in Figure 5.10, the technical data for the six most selected turbines is provided in Table 5.1. Finally, general remarks about turbine selection for all cases are given below

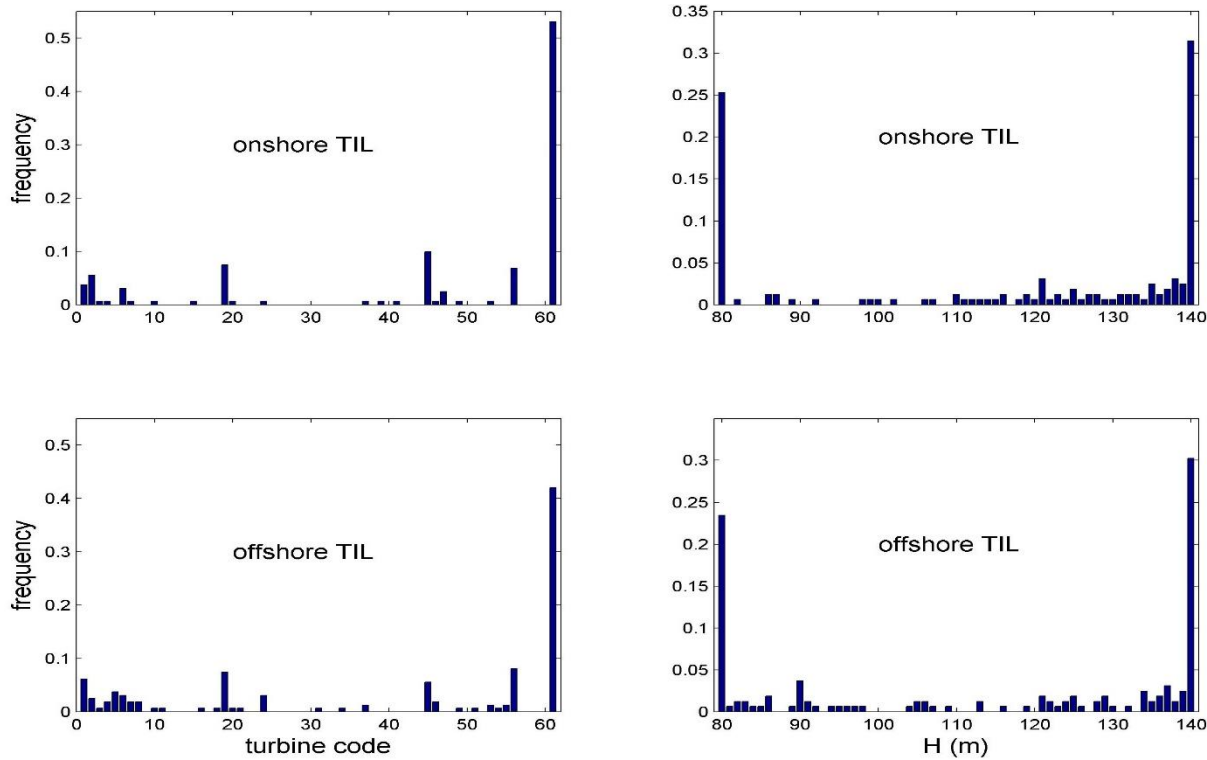


Figure 5.10: Frequency of turbine and H selection for TIL cases.

Turbine code	Rated power (MW)	Diameter (m)	Rated speed (m/s)
61	3.075	112	13
56	3.0	112	12
19	1.8	100	12
45	2.5	115	12
1	1.5	77	13
6	1.5	82	12

Table 5.1: Technical data for the six most selected turbines in decreasing order.

1. Almost all the investigated turbines were selected at least once in an optimum design (only two turbines were never selected). This confirms that any commercial turbine could be used somewhere in the farm at certain conditions to obtain an optimum farm design based on the desired objective(s).
2. The superior turbines (those selected most often) have lower U_r and larger D amongst the turbines of the same rated power. These turbines develop higher power at any wind speed so the selection for max P optimizations was entirely among them. The second group of turbines selected in many layouts were those with large D but higher U_r . The turbines that have lower U_r and smaller D came third, while those of higher U_r combined with smaller D were rarely selected.
3. At low wind speeds, the CF optimizations tend to mix medium and large size turbines providing that the CF is kept high but the total power falls between P and TC optimizations. As the wind

speed increases, the medium turbines are replaced by larger ones as they can operate at high CF , this results in increasing the power output to approach the max P optimizations at higher wind speeds.

4. The max P optimizations generate feasible layouts by using larger turbines as well as elevated heights in order to increase the power output. At some locations (especially at lower U_{ref} and/or S) the higher heights cause accumulation of wake deficits so one turbine should have a lower H in order to allow the wakes to recover for the rest of the downwind turbines.
5. The min TC optimizations have the opposite trend, with smaller to medium size turbines with low H being in the majority. At some locations some turbines should escape from the wake accumulation by having higher H in order to increase the power to reduce the overall TCI . The chosen turbines, usually of low to medium size also reduce the tower cost, as it depends on the turbine size.
6. At higher wind speeds and/or S , larger turbines can be used in many places for max CF and even for min TC optimizations as long as CF kept high and TC kept low, respectively.

5.5 Conclusions

Based on the proposed approach for optimizing the layout of wind farms, and by analyzing the results for the test cases; we conclude:

1. The analysis provides strong reasons to suggest that wind farm design with identical turbines should be abandoned in favour of using a range of commercial turbines and hub heights.

2. The optimization for maximum power and minimum cost of energy are the extreme designs bounding a wide band of optimum designs. Maximizing the capacity factor is one example between the extremes.
3. Taller towers are needed, not only to reach higher wind speeds, but also to reduce wake effects, especially in compact wind farm layouts, by exploiting hub height variation.
4. The optimization is more effective in offshore wind farms because of the low entrainment which delays the wake recovery.
5. The diversity of the 61 commercial turbines used in his study is found to be beneficial in optimizing the wind farm design, as each turbine could be the optimum selection somewhere inside the farm at a particular hub height.
6. The priority in selection among commercial turbines having the same rated power (and the same cost as well) is the larger diameter combined with lower rated speed, followed in order by larger diameter with higher rated speed, the smaller diameter with lower rated speed, and finally the smaller diameter combined with higher rated speed.

ACKNOWLEDGEMENTS

This research is part of a program of work on renewable energy funded by the Natural Science and Engineering Council (NSERC) and the ENMAX Corporation. The first author also acknowledges the Egyptian Government and Prof. El-Adl El-Kady for sharing the fund and supervision during the early (and the important) part of this work.

5.6 References

1. Tesauro, A., Réthoré, P-E, Larsen, G.C. (2012). State of the art of wind farm optimization. Proceedings of European Wind Energy Conference & Exhibition, European Wind Energy Association (EWEA 2012), Copenhagen, Denmark.
2. Mosetti, G., Poloni, C., Diviacco, B. (1994). Optimization of wind turbine positioning in large wind farms by means of a genetic algorithm. *Journal of Wind Engineering and Industrial Aerodynamics*, 51, pp. 105-116.
3. Jensen, N.O. (1983). A note on wind generator interaction. Risø-M-2411, Risø National Laboratory.
4. Katic, I., Hojstrup, J., Jensen, N.O. (1986). A simple model for cluster efficiency. In Proceedings of the European Wind Energy Association Conference and Exhibition, pp. 407–410.
5. Grady, S.A., Hussaini, M.Y., Abdullah, M.M. (2005). Placement of wind turbines using genetic algorithms. *Renewable Energy*, 30(2), pp. 259-270.
6. Hou-Sheng, H. (2007). Distributed genetic algorithm for optimization of wind farm annual profits. International Conference on Intelligent Systems Applications to Power Systems, ISAP 2007, Kaohsiung, Taiwan.
7. Emami, A., Noghreh, P. (2010). New approach on optimization in placement of wind turbines within wind farm by genetic algorithms. *Renewable Energy*, 35, pp. 1559–1564.
8. Chen, L., MacDonald, E. (2012). Considering landowner participation in wind farm layout optimization. *Journal of Mechanical Design*, 134, 084506-1:6.
9. Marmidis, G., Lazarou, S., Pyrgioti, E. (2008). Optimal placement of wind turbines in a wind park using monte carlo simulation. *Renewable Energy*, 33, pp. 1455–1460.

10. González, J.S., Gonzalez Rodriguez, A.G., Mora, J.C., Santos, J.R., Payan, M.B. (2010). Optimization of wind farm turbines layout using an evolutive algorithm. *Renewable Energy*, 35(8), pp. 1671-1681.
11. Ituarte-Villarreal, C.M., Espiritu, J.F. (2011). Wind turbine placement in a wind farm using a viral based optimization algorithm. *Procedia Computer Science*, 6, pp. 469–474.
12. Turner, S.D.O., Romero, D.A., Zhang, P.Y., Amon, C.H., Chan, T.C.Y. (2014). A new mathematical programming approach to optimize wind farm layouts. *Renewable Energy* 63(c), pp. 674–680.
13. Zhang, P.Y., Romero, D.A., Beck, J.C., Amon, C.H. (2014). Solving wind farm layout optimization with mixed integer programming and constraint programming. *EURO Journal on Computational Optimization*, 2(3), pp. 195-219.
14. Herbert-Acero, J-F., Franco-Acevedo, J-R., Valenzuela-Rendon, M., Probst-Oleszewski, O. (2009). Linear wind farm layout optimization through computational intelligence. *Proceedings of 8th Mexican International Conference on Artificial Intelligence*, pp. 692–703.
15. http://www.thewindpower.net/owners_en.php [last access: August 2016].
16. Sierra, A. H., Pérez, E. G. (2013). Wind farm owner's view on rotor blades – from O&M to design requirements IQPC - Advances in Rotor Blades for Wind Turbines, Bremen, Germany.
17. Chowdhury, S., Messac, A., Zhang, J., Castillo, L., Lebron, J. (2010). Optimizing the unrestricted placement of turbines of differing rotor diameters in a wind farm for maximum power generation. *ASME 2010 International Design Engineering Technical Conferences*

- and Computers and Information in Engineering Conference, Paper No. DETC2010-29129, pp. 775-790.
18. Chowdhury, S., Zhang, J., Messac, A., Castillo, L. (2012). Unrestricted wind farm layout optimization (UWFLO): Investigating key factors influencing the maximum power generation. *Renewable Energy*, 38(1), pp. 16–30.
 19. Chowdhury, S., Zhang, J., Messac, A., Castillo, L. (2013). Optimizing the arrangement and the selection of turbines for wind farms subject to varying wind conditions. *Renewable Energy*, 52, pp. 273-282.
 20. Chen, Y., Li, H., Jin, K., Song, Q. (2013). Wind farm layout optimization using genetic algorithm with different hub height wind turbines. *Energy Conversion and Management*, 70, pp. 56–65.
 21. Sørensen, T., Nielsen, P., Thøgersen, M.L. (2006). Recalibrating wind turbine wake model parameters – Validating the wake model performance for large offshore wind farms. EMD International A/S.
 22. Sørensen, T., Thøgersen, M.L., Nielsen, P., Jernesvej, N. (2008). adapting and calibration of existing wake models to meet the conditions inside offshore wind farms. EMD International A/S.
 23. Barthelmie, R.J., Folkerts, L., Larsen, G.C., Rados, K., Pryor, S.C., Frandsen, S.T., Lange, B., Schepers, G. (2006). Comparison of wake model simulations with offshore wind turbine wake profiles measured by SODAR. *Journal of Atmospheric & Oceanic Technology*, 23(7), pp. 888-901.

24. Beaucage, P., Robinson, N., Brower, M., Alonge, C. (2012). Overview of six commercial and research wake models for large offshore wind farms. Proceedings of the EWEA conference, Copenhagen.
25. Mortensen, N.G., Heathfield, D.N., Myllerup, L., Landberg, L., Rathman, O. (2005). Wind atlas analysis and application program: WAsP 8 help facility. Risø National Laboratory, Roskilde, Denmark.
26. Nielsen, P. (2006). The WindPRO Manual Edition 2.5, EMD International A/S.
27. Frandsen, S. (1992). On the wind speed reduction in the center of large clusters of wind turbines. *Journal of Wind Engineering and Industrial Aerodynamics*, 39, pp. 251-265.
28. Oke, T.R. (1987). Boundary layer climates. 2nd Edition, Methuen, London.
29. Jensen, L., Mørch, C., Sørensen, P., Svendsen, K. H. (2004). Wake measurements from the Horns Rev wind farm, EWEC 2004, 22-25, London, United Kingdom.
30. Sommer, A., Hansen, K. (2002). Wind resources at Horns Rev. Tech-Wise A/S, Eltra PSO-2000 Proj. NR. EG-05 3248, Report no. D-160949, Project no. 11746.01.06, p. 69.
31. <http://www.ens.dk/node/2233/register-wind-turbines> [last accessed: August 2016].
32. <http://www.thewindpower.net> [last accessed: August 2016].
33. Abdulrahman, M., Wood, D. (2015). Some effects of efficiency on wind turbine interference and maximum power production. *Wind Engineering*, 39(5), pp. 495-506.
34. <https://wind.nrel.gov/forum/wind/viewtopic.php?t=582> [last accessed: August 2016].
35. Oteri, F. (2008). An overview of existing wind energy ordinances. National Renewable Energy Laboratory Technical Report, NREL/TP-500-44439.

36. Engström, S., Lyrner, T., Hassanzadeh, M., Stalin, T., Johansson, J. (2010). Tall towers for large wind turbines. Report from Vindforsk project V-342 Höga torn för vindkraftverk. Elforsk rapport 10:48.
37. <http://www.abo-wind.com/com/wind-energy/reference-list.html> [last accessed: August 2016].
38. Samorani, M. (2010). The wind farm layout optimization problem, Technical Report, Leeds School of Business, University of Colorado.
39. Tegen, S., Lantz, E., Hand, M., Maples, B., Smith, A., Schwabe, P. (2013). 2011 Cost of wind energy review. NREL Report No. TP-5000-56266.
40. Schwabe, P., Lensink, S., Hand, M. (2011). IEA wind task 26: multi-national case study of the financial cost of wind energy. Work Package 1, Final Report, NREL Report No. TP-6A20-48155.
41. IRENA Working Paper (2012). Renewable energy technologies: Cost analysis series, Volume 1: Power Sector, Issue 5/5, Wind Power.
42. Manwell, J.F., McGowan, J.G., Rogers, A.L. (2009) Wind energy explained: Theory, Design and Application, Second Edition, John Wiley & Sons, Ltd, Chichester, UK.
43. Moné, C., Smith, A., Maples, B., Hand, M. (2015). 2013 Cost of wind energy review. Technical Report, NREL/TP-5000-63267.
44. Kiani, A., Abdulrahman, M., Wood, D. (2014). Explicit solutions for simple models of wind turbine interference. Wind Engineering, 38(2), pp. 167-180.
45. Crespo, A., Hernandez, J., Frandsen, S. (1999). Survey of modelling methods for wind turbine wakes and wind farms. Wind Energy, 2, pp. 1–24.

46. Frandsen, S., Barthelmie, R., Pryor, S., Rathmann, O., Larsen, S., Højstrup, J., Thøgersen, M. L. (2006). Analytical modelling of wind speed deficit in large offshore wind farms. *Wind Energy*, 9, pp. 39–53.
47. Kwong P., Zhang P.Y., Romero D.A., Moran J., Morgenroth M., Amon C.H. (2012). Wind farm layout optimization considering energy generation and noise propagation. In Proceedings of the ASME International Design Engineering Technical Conferences.
48. Melanie, M. (1999). An introduction to genetic algorithms, 5th Printing, MIT Press, Cambridge, Massachusetts, USA.

Chapter 6 : Large Wind Farm Layout Upgrade Optimization

Abstract

The problem of increasing the size of existing wind farms has not been practically investigated in the literature. In this paper, a proposed wind farm layout upgrade optimization by adding non-identical (in type and/or hub height) commercial turbines to an existing farm is introduced. A number of proposed locations were selected to add more turbines, either inside or outside the existing farm area. The manufacturer's power curve and a general representation for thrust coefficient are used in power and wake calculations, respectively. A simple field-based model was implemented and both offshore and onshore conditions were considered. A Random Independent Multi-Population Genetic Algorithm was used for optimization and three objective functions were considered, individually: (1) annual energy production, (2) cost of added energy, and (3) cost of total energy.

Two proposed upgraded (inside and outside) layouts were determined for the Horns Rev 1 wind farm. The results showed a wide range of suitable upgrade scenarios depending on the upgraded layout and the optimization objective. The farm energy production was increased by 190 - 336% with an increase in the total cost by 147 – 720 %. The Random Independent Multi-Population technique significantly increased the Genetic Algorithm optimization efficiency.

Keywords: Wind farm layout upgrade optimization, Multi-population genetic algorithm, Commercial turbine selection, Hub height variation.

6.1 Introduction

Wind energy has become one of the most competitive sources of electricity, not only among renewable energy sources but also compared with conventional fossil fuels [1]. The global cumulative installed wind capacity exceeded 432 GW by the end of 2015 [2], which represents about 6 % of the global electricity capacity [3] and about 3.22 % of the global electricity generation [4] of all energy sources.

The energy demand for human activities increases rapidly, which requires usage optimization for conventional and renewable energy sources. For wind power, the feasible sites for new projects that have promising wind resources are limited. Moreover, wind energy is facing many restrictions because of environmental impact in the form of noise, visual effects, and bird and bat interactions, e.g. [5]. As a result, Wind Farm Layout Optimization (WFLO) became an essential part of wind farm planning, in order to maximize the Annual Energy Production (AEP) and/or minimize the Cost Of Energy (COE) or any undesired environmental impact. The first WFLO study was published in 1994 by Mosetti et al. [6] for a very simple problem. The classical era of WFLO extended up to the end of the first decade in the 21st century. The vast majority of wind farms designed in this era could be characterized by:

- Identical turbines.
- Relatively low area utilization (large distance among turbines).
- Average tower height, H , of about 80 m [7].
- Average rotor diameter, D , of about 85 m [7].
- Average rated power, P_r , of about 1.8 MW [7].

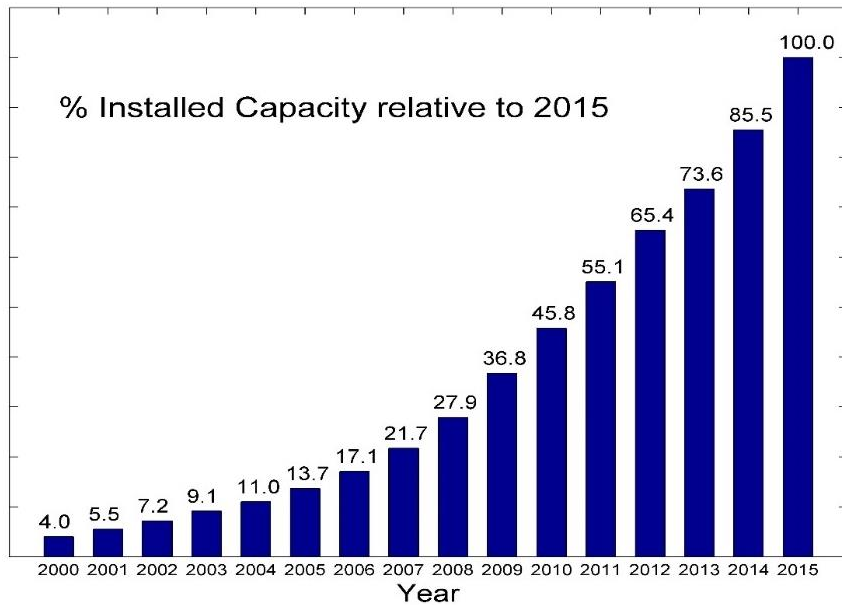


Figure 6.1: The percentage global cumulative installed wind capacity, relative to 2015, adapted from Ref. [2].

Taking into account that designing, ordering, installing, and testing turbines for a large wind farm takes more than two years, e.g. [8], this simply means that the majority of the wind farms that have been installed by the end of 2012 were not thoroughly optimized, based on the recent research findings for WFLO. Increasing wind energy production to meet the global demand requires new farms. This should be done side by side with increasing the performance of the existing ones in order to reduce the technical, financial, and environmental challenges facing the installation of new farms. One way to improve the power output and utilization of existing wind farms is by “upgrade”; that is, to add new turbines to an existing farm.

In order to understand the need for Wind Farm Layout Upgrade Optimization (WFLUO), the 2000-2015 global cumulative installed wind capacity [2] was normalized as a percentage of the 2015 value and presented in Figure 6.1, from which the following statistics could be drawn:

- 96 % of current wind farms were installed during the last 15 years, 86.3 % during the last decade.
- 65.4 % of the wind farms have been installed by the end of 2012.

The majority of current wind farms may benefit from upgrading, without re-locating or replacement of the existing turbines as they are in the first half of their lifespan (which is commonly 20 - 30 years, e.g. [9]).

In this paper, the problem of WFLUO is introduced for the first time in the literature, an upgrade methodology is proposed and applied to Horns Rev 1 offshore wind farm as a case study. In section 6.2, the case study is highlighted and justified. The proposed upgrade methodology is given in section 6.3. The results and discussions are the topic of section 6.4, while the most useful conclusions are listed in section 6.5.

6.2 Horns Rev 1: Background and Reasons for Its Selection

Horns Rev1 is one of the most famous wind farms worldwide. It has received great interest since commencing power production in 2002 because of many reasons, which can be summarized as:

1. The installed capacity is 160 MW, which made it the world's largest offshore wind farm when installed and for several years thereafter.
2. Throughout its 13 years of operation it has produced more than 8 TW-hr [10].
3. Three years of detailed wind resource assessment data taken prior to the installation are publically available [11].
4. Detailed operational measurements are also publically available, e.g. [12].

Accordingly, the farm performance and wake measurements were used in many wake model validations and wind farm layout optimization studies e.g. [12,13,14,15,16,17,18].

Many investigators have computationally improved the Horns Rev 1 performance by relocating the turbines within the farm area. Rivas, et al. [19] applied the Simulated Annealing Algorithm to solve the Turbine Positioning Problem in order to maximize the AEP. They concluded that the AEP could be increased up to 1%. Vezyris [20] applied deterministic, semi-stochastic, and stochastic approaches in order to minimize the Levelized Production Cost (cents/kWh). The results showed that a decrease in the Levelized Production Cost by ~1 % combined with an increase in the AEP with ~1 % could be achieved by re-optimizing the farm layout. Park and Law [21] derived a continuous and smooth wind speed profile that allowed the wind farm power function to be expressed as a smooth (differentiable) function of wind turbine location variables. The wind farm power function then optimized using a gradient-based optimization algorithm. The minimum turbine proximity was fixed at $5D$ and the results suggested an increase in the farm output power by 7.3 %, without providing with any cost calculations.

Horns Rev 1 wind farm is a matrix of 80 identical turbines (8 East to West rows by 10 North to South columns). The columns are aligned approximately 7.2° West of North, forming a parallelogram. The turbines are all Vestas V80-2.0 with $D = 80$ m and P_r of 2 MW. The spacing between turbines in both the rows and columns is $7D$, as indicated in Figure 6.3. The tower height is 70 m and the power curve is specific for the turbines delivered to this wind farm and may not apply to other V80 turbines [12].

Apart from the availability of performance and other data that was noted above, Horns Rev 1 was chosen as a case study as an example of middle-aged non-optimized wind farm, based on the recent findings. It is slightly more than 13 years old, it contains identical turbines, the turbine P_r and H are below the recent average values for offshore farms [7], and finally the turbines spacing is $7D$ in both directions, which is significantly larger than in more recent farms.

The references quoted above optimized the farm performance by computationally re-locating the turbines, but this is clearly not feasible for most existing wind farms. The present work aims to give a practical solution for the WFLUO, for the first time in the literature, by not changing the existing farm layout. The proposed methodology is based on commercial turbine selection and hub height variation that introduced and tested in [22].

Understanding and analyzing the wind data is an essential task in any wind power project. As mentioned earlier, three years of wind measurements were made prior to Horns Rev 1 installation. The wind data at 62 m height from June, 1st, 1999 to May, 31st, 2002 was averaged and Weibull parameters - scale and shape factors - were evaluated for 12 directional sectors (30 degrees each) [11]. Moreover, these parameters were extrapolated to the hub height of 70 m [23]. Figure 6.2 shows the frequency of occurrence, f , of each speed (at hub height) at different wind directions in contour format.

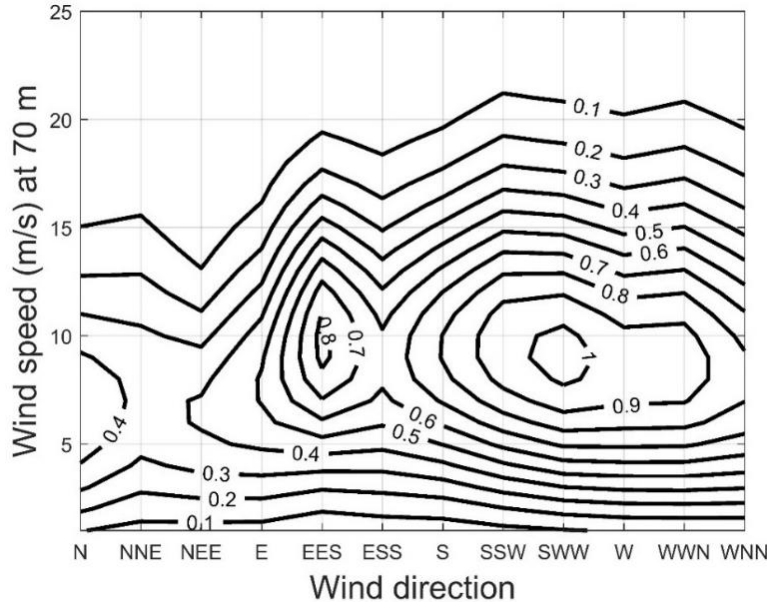


Figure 6.2: Frequency of occurrence, f , of wind speed and direction at hub height for Horns Rev 1, adapted from Ref. [23].

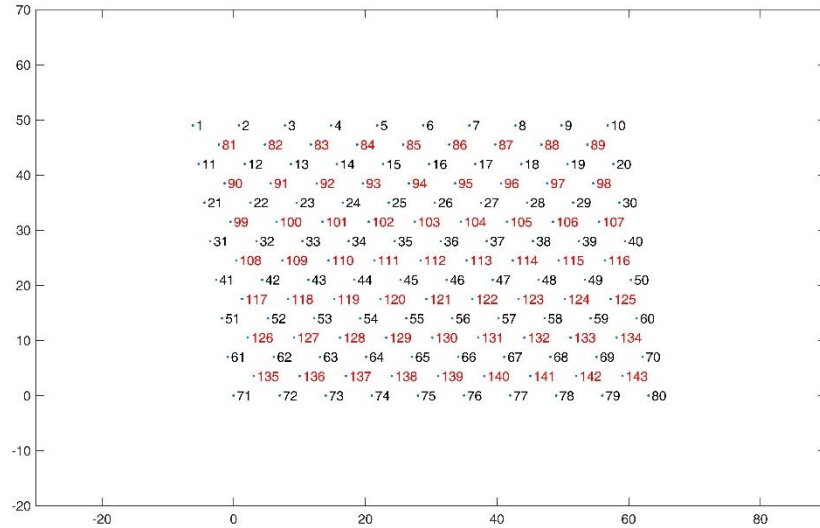
6.3 Upgrade Methodology

The proposed upgrade methodology is given in detail in this section. In subsection 3-1, the proposed upgraded layouts are illustrated. The wake model and wake interference calculations are described briefly in subsection 3-2. Subsection 3-3 describes the pool commercial turbines from which were chosen the turbines for the upgraded farm as well as the AEP calculations. The strategy of hub height variation is discussed in subsection 3-4. Finally, the cost analysis and the optimization methodology are the topics of subsections 3-5 and 3-6, respectively.

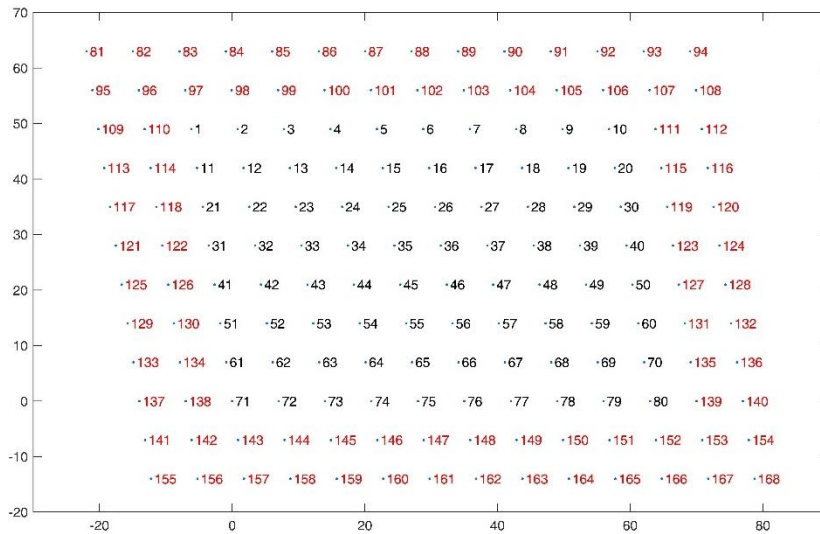
6.3.1 Proposed upgraded layouts.

The development of methodologies for multiple-turbine wind farm layouts (variable turbine size and/or hub height), e.g. [24,25,26,27,,22], allowed the turbine spacing to be reduced to $3.5D$. This recent finding provides compact farm designs with higher AEP, excellent area and height utilization, without severe wake loss, and hence lower COE. Accordingly, it was proposed to install new turbines either inside or outside the existing wind farm area, as illustrated in Figure 6.3a and b, respectively. For the inside upgrade, the farm area was kept unchanged and new turbines were installed in between the existing ones, in order to maximize the utilization of the farm space while reducing the added cost due to extra infrastructure. In the outside upgrade, the added turbines form four rows and four columns outside the existing area, in order to allow larger turbines to be installed with the least effect on the rest of the turbines. In all cases, Vestas turbines and the grid layout was considered as this manufacturer's turbines were used in the original farm. The number of turbines in the original farm denoted N ($N = 80$), while the number of the added turbines denoted M ($M = 63$ and 68 for the inside and outside layouts, respectively). In all cases, the existing turbines were numbered from 1 to N , while the added turbines were numbered from

$N+1$ to $N+M$. The vertical coordinate in Figure 6.3 indicates the North direction and the values in both vertical and horizontal directions are in terms of D .



(a)



(b)

Figure 6.3: Proposed upgraded layouts for Horns Rev 1 wind farm. (a): inside. (b): outside. The existing turbines are numbered from 1 to 80 (in black), while the added turbines are numbered from 81 (in red).

As shown in Figure 6.3, the original farm is a parallelogram of base $63D$ and height $49D$ which is unchanged in the inside case. However, the total outside area is a parallelogram of base $91D$ and height $77D$. Defining the Area Factor, AF , for the upgraded layout as the farm area divided by the original farm area, gives AF for the inside and outside upgrades of 1.0 and 2.27, respectively.

6.3.2 Wake model and interference calculations

Wake modelling is one of the first and most important steps in WFLO. The availability of the field measurements for some wind farms, especially Horns Rev 1 and Nysted, gave a great opportunity to validate the existing wake models and even develop new models. Because of many reasons mentioned in [28,29,30,31], the Jensen wake model was implemented in the present wake calculation. Ref. [22] demonstrated that the model lead to accurate estimates of the energy production data for Horns Rev 1 between 2005 and 2015, [31]. Originally proposed by Jensen [332], the model was developed by Katic et al. [433] and Frandsen [2734]. Full details of its implementation were given in [22]. Referring to Figure 6.3 and Figure 6.4 [22], the wake calculations were done as follows:

For each of twelve angles from North, $\theta = 0^\circ, 30^\circ, 60^\circ, \dots, 330^\circ$, the Y -axis used in the following description was rotated so that the wind was always in the positive Y -direction. The turbines then sorted in ascending order according to their Y coordinates. For example: the most upwind turbine, which has the least Y -coordinate, was designated 1, while the most downwind one was $N+M$ (the total number of turbines). Accordingly, each turbine i in the farm apart from the most upwind one, $2 < i < N$, is potentially affected by the wake of every turbine upwind of it: j , $1 < j < i-1$.

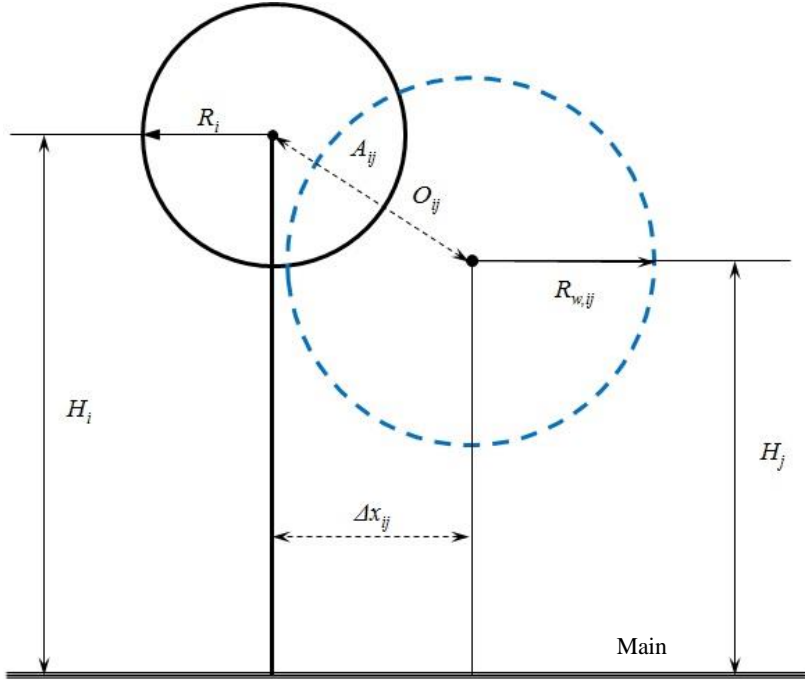


Figure 6.4: A front view (parallel to wind direction) illustrates the overlap of the upwind turbine wake (the dashed circle) with the downwind turbine rotor (the solid circle). The Y co-ordinate is into the page [22].

The roughness length, z_0 , is an essential parameter in Jensen wake model, on which the vertical wind profile and the wake entrainment greatly depend. The ambient roughness length for offshore farms was taken as 0.0002 m in [22] as it widely accepted for open sea, e.g. [35]. However, the upwind turbines increase the turbulence level within the farm, which in turn increases the effective roughness. Following many investigators, e.g. [36,37], z_0 was taken as 0.05 m in order to match the field measurement for velocity/power deficits and turbulence level.

The wake analysis used in the present work was described in Ref. [22] and the reader is referred to that particular reference for full details.

6.3.3 Commercial turbines and AEP calculations

In order to obtain practical upgraded layouts, it was decided to restrict the selection to available models from the same manufacturer as the existing turbines. To this end, the selection in the current optimization was among 19 Vestas turbines, the turbines were sorted in an ascending order according to the rated power and then according to the diameter. The turbine code, rated power, rotor diameter, and rated speed, U_r , are given in Table 6.1.

The manufacturer's power curves for the 19 turbines were fitted by a 5th degree polynomial and the coefficients were used to evaluate the power output from any turbine, i , as function of the effective hub height wind speed, U_i , [22] ahead of its rotor.

Accordingly, the power developed, P_i , by the i^{th} turbine based on its type and the effective wind speed, U_i , was estimated as [22]

$$P_i = c_{i0} + c_{i1}U_i + c_{i2}U_i^2 + c_{i3}U_i^3 + c_{i4}U_i^4 + c_{i5}U_i^5 = \sum_{k=0}^{k=5} c_{ik}U_i^k \quad (6.1)$$

the total farm output power for each wind speed, v , at each wind direction, θ , is simply the sum of the individual powers from all turbines

$$P_{(\theta,v)} = \sum_{i=1}^{N+M} P_i = \sum_{i=1}^{N+M} \sum_{k=0}^{k=5} c_{ik}U_i^k \quad (6.2)$$

and the AEP was calculated as

$$AEP = 8,766 \sum_{\theta=0}^{360} \sum_{v=4}^{25} f_{(\theta,v)} \cdot P_{(\theta,v)} \quad (6.3)$$

where 8,766 is the number of hours per year.

Turbine code	Rated power (kW)	Rotor diameter (m)	Rated speed (m/s)
1	1,815	90	13
2	1,815	100	11.5
3	2,000	80	14
4	2,000	90	13
5	2,000	100	12
6	2,000	110	11
7	2,600	100	15
8	3,000	90	16
9	3,000	112	12
10	3,000	126	10.5
11	3,075	112	13
12	3,300	105	13.5
13	3,300	112	12.5
14	3,300	117	13
15	3,450	105	13.5
16	3,450	112	12.5
17	3,450	117	11.5
18	3,450	126	11.5
19	3,450	136	11

Table 6.1: Code, rated power, rotor diameter, and rated speed for the turbines included in the selection.

6.3.4 Hub height variation

The hub height is one of the most important design parameters for a wind turbine, upon which power and cost greatly depend. The proper value of H for a specific turbine should consider the turbine diameter, rated speed, installation cost, wind resources, site restrictions, etc. Moreover, many recent WFLO studies, e.g. [38,39,22,40], suggest the implementation of individual values of H for the turbines within the farm, in order to minimize the wake interference, the installation cost, or a combination of them. In our previous work [22] it was decided to use common H limits ($80 \text{ m} \leq H \leq 140 \text{ m}$) for all turbines. However, in the present work, the investigated range of H was widened and made flexible (turbine-specific). The Maximum Tip Height (MTH) and the Minimum Ground Clearance (MGC) along with the turbine diameter were used to determine the individual H range for each turbine. The MTH and MGC are the blade tip height at its highest and lowest positions, respectively. The MTH was set as 230 m for Horns Rev wind farms [41], which matches the world's tallest installed wind turbine [42]. On the other hand, the recommended value for the MGC varied worldwide from 5 m to 23 m [35]. However, the rare combination of maximum wave height and tidal range at Horns Rev site is less than 7 m, the mean value is about 3 m [11]. To this end, the MTH and the MGC were taken as 200 m and 15 m, respectively. Accordingly, the individual turbine's H limits and Hub Height Range (HHR) for any turbine, i , based on its rotor diameter, D_i , as

$$H_{max,i} = MTH - \left(\frac{D_i}{2} \right) \quad (6.4)$$

$$H_{min,i} = MGC + \left(\frac{D_i}{2} \right) \quad (6.5)$$

$$HHR_i = H_{max,i} - H_{min,i} \quad (6.6)$$

Figure 6.5 shows H_{max} , H_{min} , and HHR as function of D in the investigated range ($80 \text{ m} \leq D \leq 136 \text{ m}$), as given in Table 6.1.

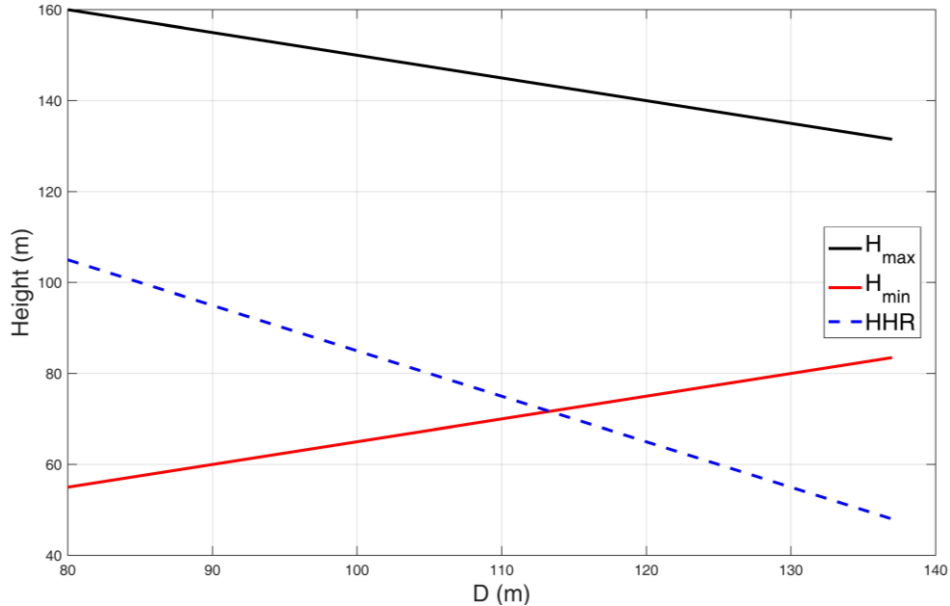


Figure 6.5: H_{max} , H_{min} , and HHR as function of D in the investigated range.

6.3.5 Modified simple cost model

The cost model used in this study is a modified version of the simple model introduced in detail in [22]. Only the major assumptions for offshore conditions along with the modifications that made based on the most recent cost reports, e.g. [44] will be given in this subsection.

1. The Total Cost of a wind farm is a combination of the Capital Cost, C_c and the Operation and Maintenance cost, O&M, Co&M. It was assumed that $C_c = 0.75$, while $C_{O\&M} = 0.25$.
2. The CC in turn is subdivided into the total turbine cost, $C_{turbine} = 0.329C_c$, and the remainder, $0.671C_c$, is the Financial & Balance of system costs, $C_{F\&B}$.
3. The tower cost, C_{tower} , is about 0.1831 of the $C_{turbine}$, or 0.06 of the C_c .

4. The $C_{F\&B}$ depends only on the farm area. In other words, if the turbines were added within the original farm area, the added C_C would comprise only $C_{turbine}$ while $C_{F\&B}$ were considered unchanged.
5. The cost of 1.0 MW at the corresponding H_{min} was taken as the unit cost and was denoted by Unit Cost Index, UCI. The corresponding capital and total costs were denoted Capital Cost Index, CCI, and Total Cost Index, TCI, respectively. Each 1 m increase of H_i over $H_{min,i}$ was assumed to add $\frac{C_{tower}}{H_{min,i}}$ to the CCI.

Accordingly, the added TCI as a result of the upgrade can be expressed as

$$TCI_a = \frac{AF}{(1 - C_{O\&M})(1 - C_{turbine})} \sum_{i=1}^M P_{r,i} \left[1 + \frac{C_{tower}}{H_{min,i}} (H_i - H_{min,i}) \right] \quad (6.7)$$

where $P_{r,i}$ and H_i are the rated power (in MW) and the hub height (in m) of the i^{th} turbine, respectively, while AF is the Area Factor as introduced in subsection 3-1.

Based on the above analysis, the TCI for the original farm, TCI_O is

$$TCI_O = \frac{1.0}{(1 - 0.25)(1 - 0.329)} \sum_{i=1}^{80} 2.0 \left[1 + \frac{0.06}{55} (70 - 55) \right] = 323 \text{ UCI} \quad (6.8)$$

Two useful quantities are defined; the Cost Of Added Energy Index (COAEI) and the Cost Of Total Energy Index (COTEI):

$$COAEI = \frac{TCI_a}{AEP - AEP_O} \quad (6.9)$$

$$COTEI = \frac{TCI_a}{AEP} \quad (6.10)$$

where $AEP_O = 715$ MW-hr is the estimated AEP for the original farm.

Finally, the three objective functions considered in the optimization are shown in Table 6.2.

<i>ObjFun#</i>	Optimizer	Equation
<i>ObjFun1</i>	max AEP	(6.3)
<i>ObjFun2</i>	min COAEI	(6.9)
<i>ObjFun3</i>	min COTEI	(6.10)

Table 6.2: Illustration of the three objective functions.

6.3.6 Optimization

Layout optimization for large wind farms with commercial turbine selection is one of the most complex optimization problems because it is discrete, non-convex, non-linear, and of high dimension. Genetic Algorithms (GA) are one of the most successful optimization methods for such problems that their capability has been proven over years, especially with WFLO, e.g. [45]. On the other hand, GA is slow compared with other optimization methods [45,46] as it depends basically on successive random search. The solution evolves from one generation of a fixed population size (PS) to the next generation. In general, the larger the PS the wider the search and the greater the probability of finding the global optima. On the other hand, very large PS requires large execution time and may disperse the conversion to the global optima, e.g. [47,48]. In general, the CPU time is nonlinear in PS and the proper choice of PS is greatly problem dependent. However, a simple test case from the current work showed that an increase in PS from 15 to 45 (300%) the execution time increased by about 390% (this relative increase would increase if PS were increased from 45 to 135 for example). Accordingly, it is very important to select the proper PS in order to increase the probability of finding the global optima while keeping the execution time reasonable, e.g. [49].

For both inside and outside layouts, two cases were investigated. Single turbine with variable H was the first with only $ObjFun1$. Multi-turbine with variable H and the three objective functions were then considered in turn.

Two significant modifications were made compared to what described in Ref. [22]. First, the H variation was treated for each turbine individually based on its D . Accordingly, the upper and lower bands for H were not the same for all turbines and the individual height was not included explicitly in the optimization design variables. Instead, a fractional parameter denoted “coefficient of height” was an optimization design variable with the same upper and lower bands (1.0 and 0.0, respectively) for all turbines. Once the coefficient of height, C_H , is selected (during the optimization) for a particular turbine, i , the corresponding value of H_i is calculated using Equation (6) as

$$H_i = H_{min,i} + C_H \cdot HHR_i \quad (6.11)$$

Second, as discussed earlier in this subsection, as the PS increases the execution time per generation increases significantly. A global optimization technique called “Random Independent Multi-Population Genetic Algorithm, RIM-GA” was applied to the GA used for the multi-turbine cases, as it has double the variables than the single turbine cases. The multi-population genetic algorithms (in general) have been proven as a powerful tool to enhance the GA optimization efficiency, e.g. [50]. An arbitrary number of independent populations, n , having relatively small population size, ps , were initiated and allowed to evolve over a small number of generations, g_1 . The final population from each run was stored, sorted based on the $ObjFun$ value. The fittest m individuals from each independent run were collected and assigned as the initial population for one last run for g_2 generations. Again, the effectiveness of this technique is problem dependent, however, RIM -GA was tested with some test cases and gave almost the same results but with 82

- 87 % of the execution time. The comparison was made against single runs having population size $PS = m \cdot n \cdot ps$ and number of generations, $G = g_1 + g_2$.

6.4 Results and Discussion

Two proposed upgraded layouts (inside and outside) were investigated. The existing 80 turbines were left unchanged, while suitable locations were specified for the new turbines. The selection was among 19 Vestas commercial turbines covering a rated power range of 1.8 – 3.45 MW and rotor diameter range from 80 – 136 m. MATLAB's genetic algorithm solver, *ga*, was employed for the optimization and three objective functions in Table 6.2 were considered individually.

AEP and the TCI were normalized with respect to the corresponding values for the original farm (AEP₀ and TCI₀, respectively), the two normalized quantities were denoted NAEF and NTCI, respectively. Moreover, the NTCI were divided by the NAEF, the resulted quantity called Normalized Cost Of Energy Index, NCOEI.

Figure 6.6 shows the NAEF, NTCI, and NCOEI for the single turbine cases and *ObjFun1*. In these cases, the M added turbines were assumed identical in type, but different in height. The major remarks are summarized below:

1. There is a wide range of feasible optimum upgrades providing a useful trade-off between AEP and COE.
2. The single turbine inside layouts produce a range of NAEF from 1.90 to 2.60 with a NTCI from 1.47 to 2.87, based on the turbine model and optimization objective.
3. The single turbine outside layouts gave NAEF from 2.23 to 3.36 with a NTCI from 3.81 to 7.20, based on the turbine model and optimization objective.

4. The inside layout produces a cheap added AEP if small turbines are used. The added AEP increases as the turbine size increases, but at a higher rate in the added cost. The reason is the limited wind resources which causes the increase in AEP to reduce as the turbine size (and hence the cost) increases.
5. As expected, the outside layout adds more AEP than the inside one, however, this increase in AEP is accompanied with very high cost as a consequence of adding area to the farm.
6. Both inside and outside layouts have the same trends in AEP and TCI (qualitatively), however, the latter has magnified scales, especially for the cost.
7. Both layouts confirm the superiority of using turbines with relatively large D and relatively low U_r (turbines number 2, 1, 6, 5, 4, and 3) than the opposite (turbines number 15, 8, 17, 16, and 12). This finding matches with that obtained in the previous research [22] and with others in the literature, e.g. [51].
8. The NCOEI for the inside layouts are usually close to unity, which means that the increase in added AEP coincides with a comparable increase in the TCI.

As the turbine type was fixed in these cases, the hub height variation (not presented here for the sake of brevity) plays the main role in both AEP maximization and COE minimization. For the max AEP optimization, the majority of turbines should be installed as high as possible in order to meet the highest possible wind speed, while the minimum height was required for the rest of turbines, especially in the middle of the farm, in order to allow wake recovery ahead of the exterior turbines.

For the min COE optimizations, heights close to H_{min} were dominant, and scattered values close to H_{max} were selected in order to capture the most power at a few locations and to allow

wake recovery for the rest of the turbines at lower heights in order to reduce the COE. In general, a wide range of H was used in order to compensate the absence of the turbine selection.

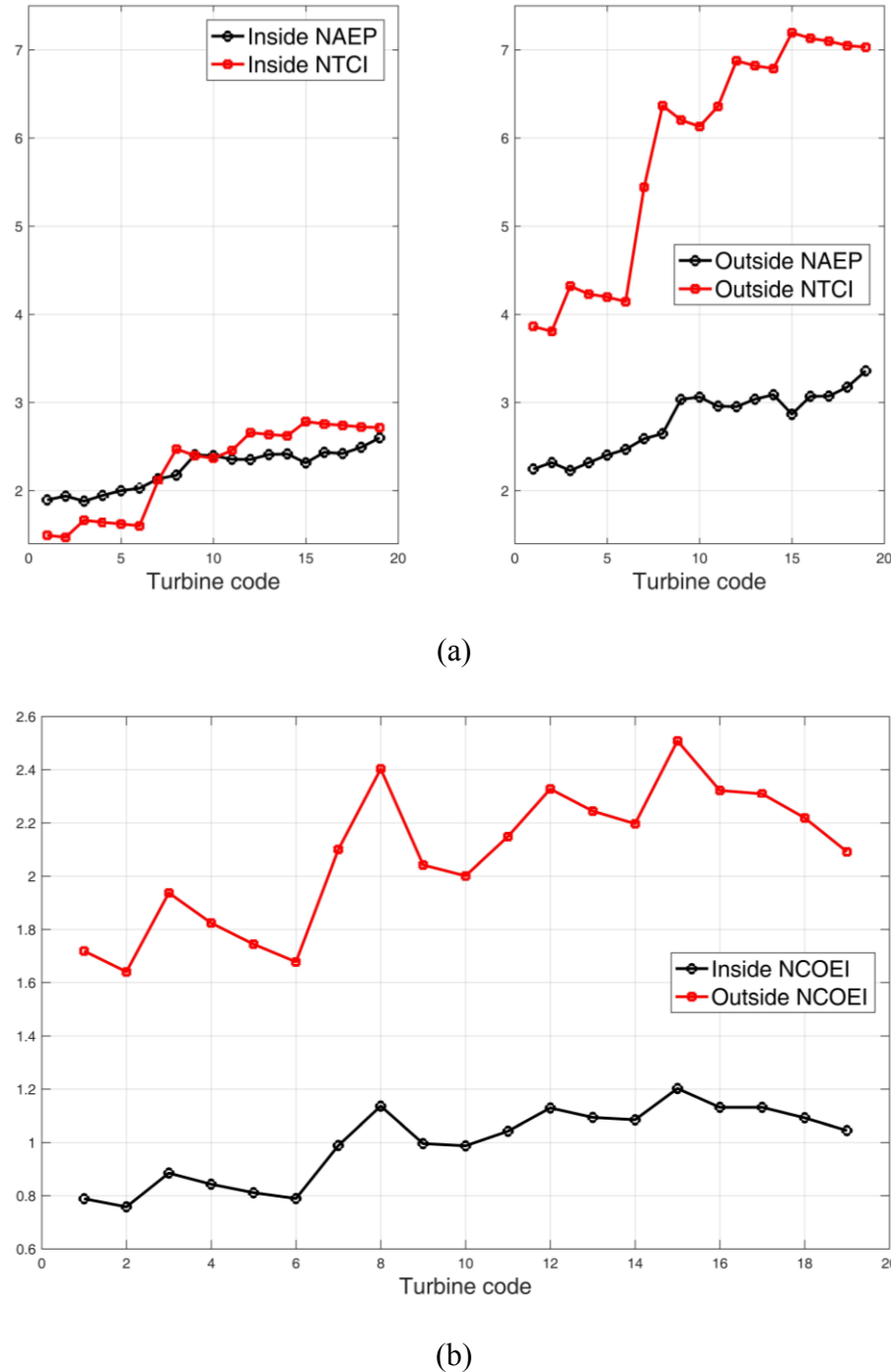


Figure 6.6: Normalized AEP, TCI, and COEI for single turbine layouts.

Figure 6.7 shows the NAEP, NTCI, and NCOEI for the multi-turbine layouts where the M added turbines could be different in both type and height. The rated power distribution for the selected turbines and the corresponding coefficient of height distribution are given in Figure 6.8 and Figure 6.9, respectively. In Figures 8 to 11, symbols (I) and (O) represent the inside and the outside layouts, respectively, while the number indicates the $ObjFun\#$ as given in Table 6.2. For example: I2 represents the Inside layout with $ObjFun2$.

Finally, the histogram of turbine and C_H selection frequencies for all multi-turbines cases are given in Figure 6.10 and Figure 6.11, respectively. Again, the outside layout gives significant more AEP but with a huge cost (Figure 6.7) because of the added area (and hence $C_{F&B}$) compared to the inside layout. The optimization for max AEP ($ObjFun1$) gave results close to those for the single-turbine case of larger size for both inside and outside layouts. This can be explained by the turbine selection distribution (Figure 6.8) which shows for maximum AEP regardless the cost, larger turbines should be used as much as possible. The resulting layouts usually have high total cost and COE. Similarly, but at the other extreme, the optimization for min COTEI ($ObjFun3$) gave results close to those for the single-turbine case of smaller size in both inside and outside layouts. This can be also explained by the turbine selection distribution (Figure 6.8) which shows for maximum COE, the selection should be among small size turbines in general. The larger turbines should be selected carefully in some places where the increase in power output dominates the corresponding increase in cost. The medium size turbines were rarely used, which means that the proper turbine selection should be, in general, among a few large turbines and a few small ones. The optimization for max AEP requires significantly wider range in both turbine size and H . On the other hand, the optimization for min COE requires a much smaller range of both turbine size and H .

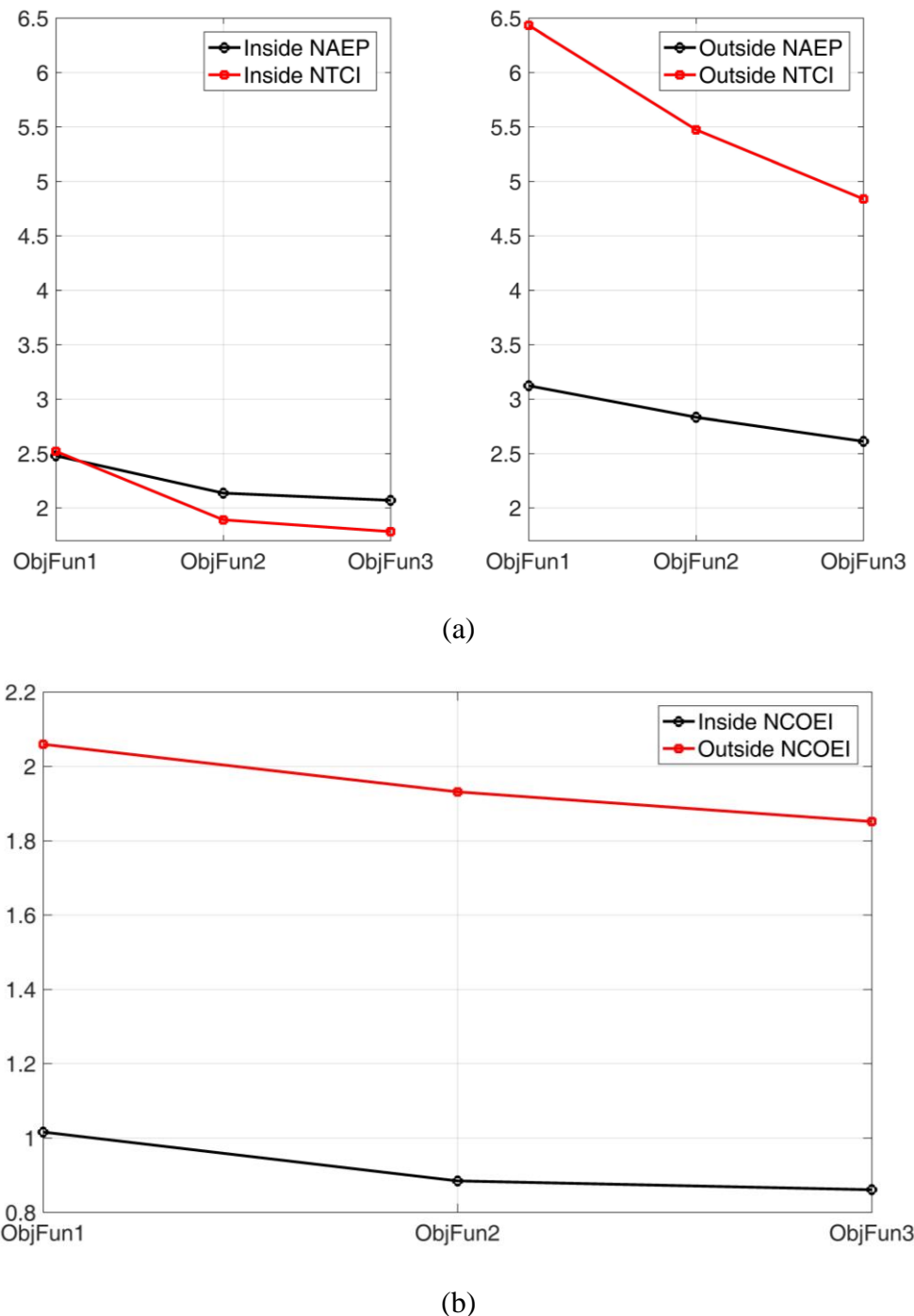


Figure 6.7: Normalized AEP, TCI, and COEI for multi-turbine layouts.

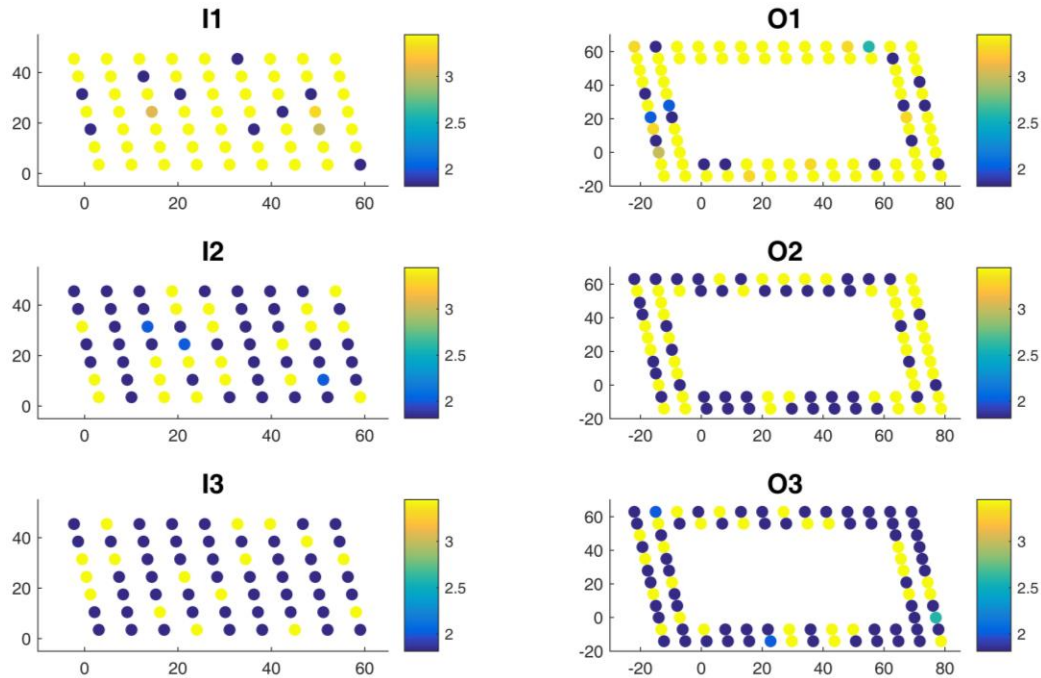


Figure 6.8: Rated power distribution for the selected turbines for all multi-turbine cases.

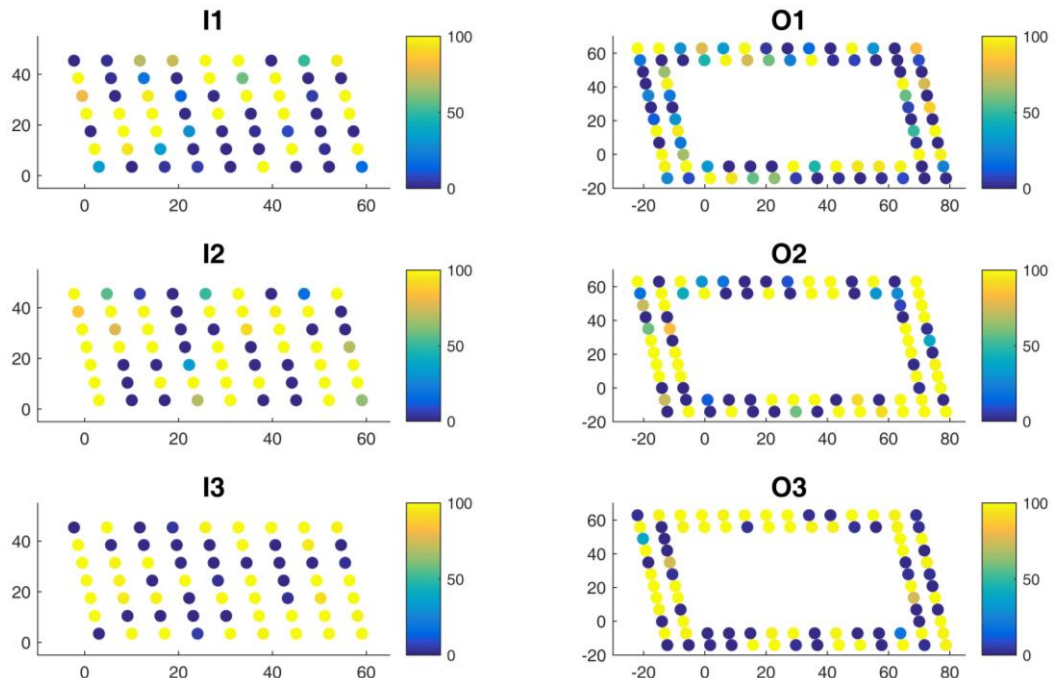


Figure 6.9: Coefficient of height, C_H , distribution for all multi-turbine cases.

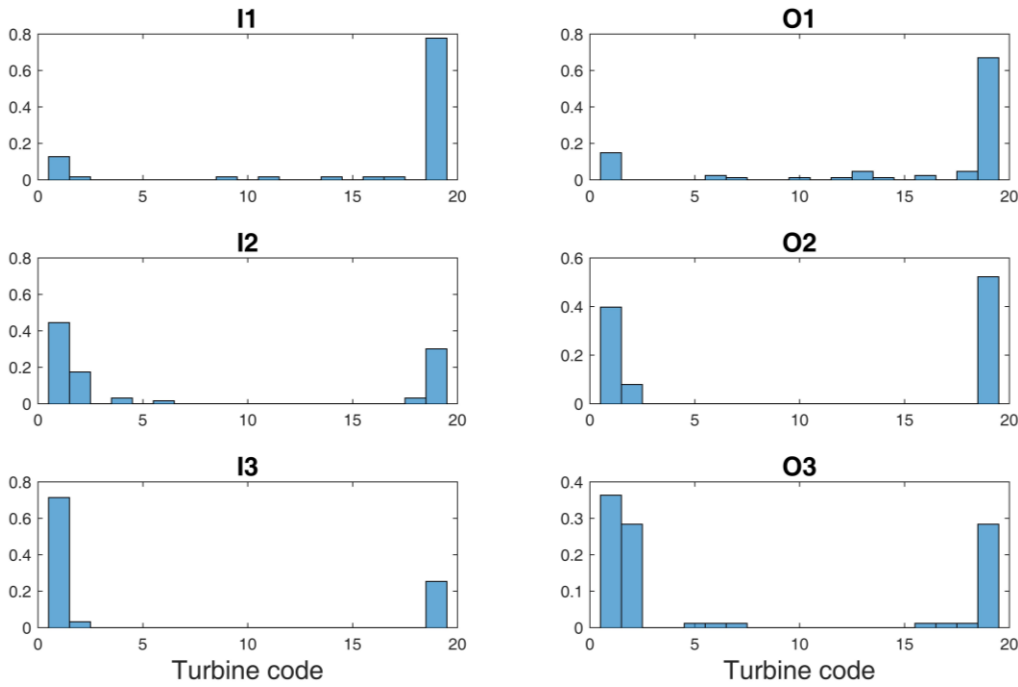


Figure 6.10: Frequency of turbine selection for multi-turbine cases.

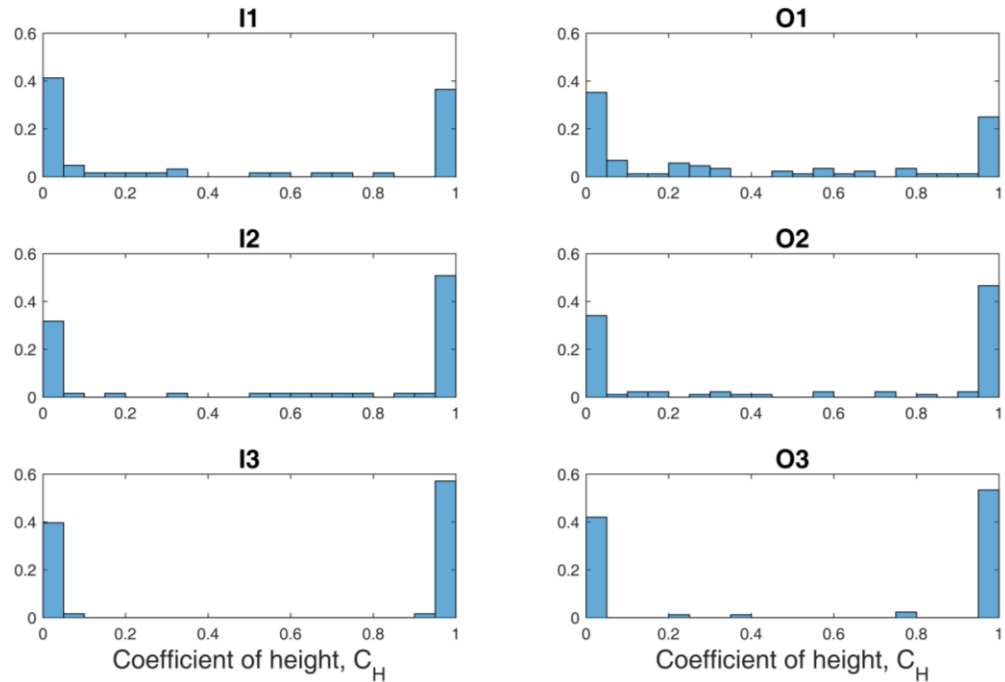


Figure 6.11: Frequency of C_H selection for multi-turbine cases, with bin width = 0.05.

6.5 Conclusions

In this paper, the large wind farm layout upgrade optimization problem was introduced. The proposed upgrade methodology was based on adding new non-identical turbines to the existing farm either within the farm area or as an extension. The famous Horns Rev 1 large offshore wind farm was taken as a case study. The existing 80 turbines were kept as they are while 63 and 88 turbines were added in the inside and outside upgraded layouts, respectively. 19 Vestas commercial turbines of rated power ranged from 1.8 to 3.45 MW were included in the selection.

The following are the implications of the findings of this paper:

1. Existing wind farms can be effectively upgraded by increasing the energy production by adding new turbines, while keeping the existing turbines unchanged.
2. Wind farm layout upgrade optimization for offshore farms is recommended if it is done within the original farm area and infrastructure. In this case, a significant increase in the energy production can be achieved while keeping the cost of energy in reasonable range.
3. Wind farm layout upgrade optimization is an efficient method to increase the utilization of the existing area instead of installing new costly farm(s).
4. Having a range of commercial turbines for selection as well as allowing variation in height is a powerful tool in wind farm layout upgrade optimization.
5. The optimum layouts are greatly dependent on the proposed upgraded layout as well as the optimization objective.
6. The hub height variation is beneficial not only to reduce the wake interference and hence increase the energy production, but also to reduce the total cost as well as the cost of energy.

7. By including a wide range of commercial turbines in the selection, a wide band of feasible optimum layouts is obtained which provide a trade-off between energy production and cost.
8. Among commercial turbines having the same rated power, the priority in selection should be biased towards the turbines with larger diameter and lower rated speed.
9. The random independent multi-population technique reduces the execution time for the genetic algorithm without compromising the outcomes.

ACKNOWLEDGEMENTS

This research is part of a program of work on renewable energy funded by the Natural Science and Engineering Council (NSERC) and the ENMAX Corporation. The first author also acknowledges the Egyptian Government and Prof. El-Adl El-Kady for support and supervision during the early (and the important) part of this work.

6.6 References

1. REN21. 2016. Renewables 2016 Global Status Report (Paris: REN21 Secretariat). ISBN 978-3-9818107-0-7.
http://www.ren21.net/wp-content/uploads/2016/06/GSR_2016_Full_Report.pdf [last accessed: July 2017].
2. Global wind report, Annual market update 2015, Global Wind Energy Council (GWEC), April, 2016.
3. <http://www.tsp-data-portal.org/Breakdown-of-Electricity-Capacity-by-Energy-Source#tspQvChart> [last accessed: July 2017].
4. <http://www.tsp-data-portal.org/Breakdown-of-Electricity-Generation-by-Energy-Source#tspQvChart> [last accessed: July 2017].
5. http://www.ucsusa.org/clean_energy/our-energy-choices/renewable-energy/environmental-impacts-wind-power.html#references [last accessed: July 2017].
6. Mosetti, G., Poloni, C., Diviacco, B. (1994). Optimization of wind turbine positioning in large wind farms by means of a genetic algorithm. Journal of Wind Engineering and Industrial Aerodynamics, 51, pp. 105-116.
7. 2014 Wind technologies market report highlights. Prepared for US Department of Energy, Wind and Water Power Technologies Office (Berkeley, CA: August 2015)
8. Lindvig, K. (2010). European forum for renewable energy sources the installation and servicing of offshore wind farms. CSO, A2SEA A/S 16th September 2010.
9. <http://www.ewea.org/wind-energy-basics/faq/> [last accessed: July 2017].
10. <http://www.ens.dk/node/2233/register-wind-turbines> [lase accessed: July 2017].

11. Sommer, A., Hansen, K., (2002). Wind resources at Horns Rev, Tech-Wise A/S, Eltra PSO-2000 Proj. NR. EG-05 3248, Report no. D-160949, Project no. 11746.01.06, p. 69.
12. Jensen, L., Mørch, C., Sørensen, P., Svendsen, K. H. (2004). Wake measurements from the Horns Rev wind farm, EWEC 2004, 22-25, London, United Kingdom.
13. Barthelmie, RJ, Hansen, K, Frandsen, ST, Rathmann, O, Schepers, JG, Schlez, W, Phillips, J, Rados, K, Zervos, A, Politis, ES, Chaviaropoulos, PK. (2009). Modelling and measuring flow and wind turbine wakes in large wind farms offshore. *Wind Energy* 2009, 12, pp. 431–444.
14. Rathmann, O, Barthelmie, RJ, Frandsen, ST. (2006). Wind turbine wake model for wind farm power production, European Wind Energy Conference, Athens.
15. Barthelmie, RJ, Pryor, S, Frandsen, ST, Hansen, KS, Schepers, JG, Rados, K, Schlez, W, Neubert, A, Jensen, LE, Neckelmann, S. (2010). Quantifying the impact of wind turbine wakes on power output at offshore wind farms. *Journal of Atmospheric and Oceanic Technology*, 27, pp. 1302-1317.
16. Frandsen, S, Barthelmie, R, Pryor, S, Rathmann, O, Larsen, S, Højstrup, J, Thøgersen, M. (2006). Analytical modelling of wind speed deficit in large offshore wind farms. *Wind Energy*, 9, pp. 39–53.
17. Frandsen, S, Rathmann, O, Barthelmie, R, Jørgensen, HE, Badger, J, Hansen, K, Ott, S, Rethore, P, Larsen, SE, Jensen, LE. (2008). The making of a 2nd generation wind farm model. Wake Meeting, Dong Energy, Copenhagen.
18. Beaucage, P., Robinson, N., Brower, M., Alonge, C. (2012). Overview of six commercial and research wake models for large offshore wind farms, EWEA Proceedings, 10 p., Copenhagen, Germany.

19. Rivas, R., Clausen, J., Hansen, K., Jensen, L., (2009). Solving the turbine positioning problem for large offshore wind farms by simulated annealing. *Wind Engineering*, 33(3), pp. 287-297.
20. Veziris, C. (2012). Offshore wind farm optimization investigation of unconventional and random layouts. MSc Thesis, TU Delft, Netherlands.
21. Park, J., Law, K. (2015). Layout optimization for maximizing wind farm power production using sequential convex programming. *Applied Energy*, 151, pp. 320–334.
22. Abdulrahman, M, Wood, D. (2017). Investigating the power-COE trade-off for wind farm layout optimization considering commercial turbine selection and hub height variation. *Renewable Energy*, 102(B), pp. 267-516.
23. Feng, Ju, and Wen Zhong Shen. (2015). Modelling wind for wind farm layout optimization using joint distribution of wind speed and wind direction. *Energies* 8.4, pp. 3075-3092.
24. Herbert-Acero, J-F., Franco-Acevedo, J-R., Valenzuela-Rendon, M., Probst-Oleszewski, O. (2009). Linear wind farm layout optimization through computational intelligence. *Proceedings of 8th Mexican International Conference on Artificial Intelligence*, pp. 692–703.
25. Tesauro, A., Réthoré, P-E, Larsen, G.C. (2012). State of the art of wind farm optimization. *Proceedings of European Wind Energy Conference & Exhibition*, European Wind Energy Association (EWEA 2012), Copenhagen, Denmark.
26. Chowdhury, S., Zhang, J., Messac, A., Castillo, L. (2013). Optimizing the arrangement and the selection of turbines for wind farms subject to varying wind conditions. *Renewable Energy*, 52, pp. 273-282.

27. Chen, Y., Li, H., Jin, K., Song, Q. (2013). Wind farm layout optimization using genetic algorithm with different hub height wind turbines. *Energy Conversion and Management*, 70, pp. 56–65.
28. Sørensen, T., Nielsen, P., Thøgersen, M.L. (2006). Recalibrating wind turbine wake model parameters – Validating the wake model performance for large offshore wind farms. EMD International A/S.
29. Sørensen, T., Thøgersen, M.L., Nielsen, P., Jernesvej, N. (2008). Adapting and calibration of existing wake models to meet the conditions inside offshore wind farms. EMD International A/S.
30. Barthelmie, R.J., Folkerts, L., Larsen, G.C., Rados, K., Pryor, S.C., Frandsen, S.T., Lange, B., Schepers, G. (2006). Comparison of wake model simulations with offshore wind turbine wake profiles measured by SODAR. *Journal of Atmospheric & Oceanic Technology*, 23(7), pp. 888-901.
31. Beaucage, P., Robinson, N., Brower, M., Alonge, C. (2012). Overview of six commercial and research wake models for large offshore wind farms. Proceedings of the EWEA conference, Copenhagen.
32. Jensen, N.O. (1983). A note on wind generator interaction. Risø-M-2411, Risø National Laboratory.
33. Katic, I., Hojstrup, J., Jensen, N.O. (1986). A simple model for cluster efficiency. In Proceedings of the European Wind Energy Association Conference and Exhibition, pp. 407–410.
34. Frandsen, S. (1992). On the wind speed reduction in the center of large clusters of wind turbines. *Journal of Wind Engineering and Industrial Aerodynamics*, 39, pp. 251-265.

35. Wieringa, J. (1992). Updating the davenport roughness classification. *Journal of Wind Engineering and Industrial Aerodynamics*, 41, pp. 357-368.
36. Port-Agel F, Wu Y-T, Chen C-H. (2013). A numerical study of the effects of wind direction on turbine wakes and power losses in a large wind farm. *Energies*, 6(10), pp. 5297–5313
37. Jensen, L., Wake losses and turbulence within the Horns Rev off-shore wind farm. Elsam Engineering A/S.
https://www.ieawind.org/task_23/Subtask_1S_docs/PPT_Risoe1205/Jensen.pdf [last accessed: July 2017].
38. Chowdhury, S., Zhang, J., Messac, A., Castillo, L. (2013). Optimizing the arrangement and the selection of turbines for wind farms subject to varying wind conditions. *Renewable Energy*, 52, pp. 273-282.
39. Chen, Y., Li, H., Jin, K., Song, Q. (2013). Wind farm layout optimization using genetic algorithm with different hub height wind turbines. *Energy Conversion and Management*, 70, pp. 56-65.
40. Chen, K., Song, M.X., Zhang, X., Wang, S.F. (2016). Wind turbine layout optimization with multiple hub height wind turbines using greedy algorithm. *Renewable Energy*, 96 (A), pp. 676- 686.
41. Horns Rev 3 - Technical project description for the large-scale offshore wind farm (400 MW) at Horns Rev 3. ENERGINET, Document no. 13/93461-2897, dated 28.04.2014.
42. http://www.nordex-online.com/en/news-press/news-detail.html?tx_ttnews%5Btt_news%5D=2772&cHash=5f3689a99a [last accessed: July 2017].

43. Oteri, F. (2008). An overview of existing wind energy ordinances. National Renewable Energy Laboratory Technical Report, NREL/TP-500-44439.
44. Christopher Moné, Tyler Stehly, Ben Maples, and Edward Settle, (2015). 2014 Cost of wind energy review. National Renewable Energy Laboratory (NREL).
45. Samorani, M. (2010). The wind farm layout optimization problem. Technical Report, Leeds School of Business, University of Colorado.
46. Tesauro, A., Réthoré, P-E, Larsen, G.C. (2012). State of the art of wind farm optimization. Proceedings of European Wind Energy Conference & Exhibition, European Wind Energy Association (EWEA 2012), Copenhagen, Denmark.
47. Goldberg, D.E. (1989b). Sizing populations for serial and parallel genetic algorithms. Proceedings of the Third International Conference on Genetic Algorithms, San Mateo, CA: Morgan Kaufman. pp. 70-79.
48. Deb, K., Agrawal, S. (1999). Understanding interactions among genetic algorithm parameters. Foundations of Genetic Algorithms V, San Mateo, CA: Morgan Kauffman, pp. 265–286.
49. Gotshall, S., Rylander, B. (2003). Optimal population size and the genetic algorithm. School of Engineering University of Portland, USA.
50. Kim, J. O. (1992). A multi-population genetic algorithm and its application to design of manipulators. In Proc. IEEE/RSJ Int. Conf. on Intelligent Robots and Systems, Raleigh, NC, 1992 (pp. 279-286).
51. Rehman, S., Khan, S. A. (2016). Fuzzy logic based multi-criteria wind turbine selection strategy - A case study of Qassim, Saudi Arabia, Energies 2016, 9, 872.

Chapter 7 : Conclusions and Suggestions for Further Investigations

7.1 Introduction

The thesis was organized in such a way to reflect both logical order and research time frame. In this chapter, the research sequence is illustrated, the chapters are connected, and the findings from the different papers are integrated. Finally, some further investigations are suggested.

7.2 Findings from “Explicit Solutions for Simple Models of Wind Turbine Interference”

In this paper, the selfish and co-operative optimization strategies were investigated analytically. The severe wake interference case of N turbines in-line with the wind was considered. The turbines were assumed identical and the design variable was the axial induction factor, a . Three simple models for output power optimization were applied, individually. The first model was with no wake recovery, the second model was an extension of the first model with including a simple wake recovery factor, b ($b = 1$ corresponds to no wake recovery, while $b = 0$ results in complete wake recovery). Topographical effects were included in the third model by allowing the wind speed at the second and subsequent turbines to vary by a factor k from the reference value at the first turbine.

The major outcome from this paper is the superiority of the co-operative optimization over the selfish (individual) one in all cases considered. The formal proof of this result for simple wake models is the first in the open literature. In other words; the upstream turbine(s) should not capture the maximum possible energy from the wind. Instead, more energetic wind should be left for the downstream turbines to increase the total power output. It was also proven that the degree of

performance reduction for the upstream turbine(s) increases as the number of turbines in the line increases and/or the turbines' proximity decreases.

The next step(s) were to examine these findings from analytic solutions of simple models on more realistic cases. i.e. real turbines, accurate wake model, and/or real wind farms.

7.3 Findings from “Some Effects of Efficiency on Wind Turbine Interference and Maximum Power Production”

The performance of the commercial turbines was compared with the actuator disk model (as a theoretical limit). Accordingly, new operational efficiencies (aerodynamic, conversion, and overall efficiencies) were defined. It was decided to investigate the effect of the turbine aerodynamic efficiency on the power production for both selfish and co-operative power maximization. All calculations were done for six turbines in line at spacing of 4, 5, and 6 rotor diameters on the grounds, as these were representative values. The classical Jensen's wake model was implemented and the turbines' performance was judged by the power coefficient and the blade axial induction factor. MATLAB's genetic algorithm solver, *ga*, was used to perform the optimization for the co-operative cases. On the other hand, selfish control was computed by adapting all the N turbines to work at the maximum possible individual power coefficient.

The results confirmed the superiority of the co-operative optimization over the selfish one. The difference between the two optimization strategies was found to increase as the turbines' efficiencies increase and/or the turbine spacing decreases.

The outcome from the first two papers has led to the fact that the operation of each turbine within the farm should be adapted (based on its location) to increase the total power. Thus, the non-identical turbine selection for wind farms was found to be more suitable than the classical use

of identical turbines. For example: it is more economical to install small turbines somewhere in the farm instead of installing larger (and hence more expensive) turbine while operating at very low power coefficient as suggested by the co-operative optimization.

Accordingly, it was decided to proceed for the next step by including co-operative optimization for non-identical turbines (different models with variable hub height).

7.4 Findings from “Investigating the Power-COE Trade-Off for Wind Farm Layout Optimization Considering Commercial Turbine Selection and Hub Height Variation”

The commercial turbine selection was added to the wind farm layout optimization problem for the first time. Generic realistic representation for the thrust coefficient in terms of the power coefficient were developed from the available commercial turbines’ data. Hub height variation and three optimization objectives (implemented individually) were also considered. Field-based cost model was developed to estimate the cost of the different layouts for both onshore and offshore conditions. Simple wind conditions and simple test cases were considered in order to investigate the effect of the turbine selection, hub height variation, and optimization objective on the optimal layouts.

The results showed strong reasons to suggest that wind farm design with identical turbines should be abandoned in favour of using a range of commercial turbines and hub heights. The resulted optimum layouts showed a wide range of power-cost of energy trade-off. Almost all the 61 turbines were selected at least once in one optimum layout. However, the priority in selection was biased towards the larger diameter combined with lower rated speed, followed in order by larger diameter with higher rated speed, the smaller diameter with lower rated speed, and finally

the smaller diameter combined with higher rated speed. The optimization was found more effective in offshore wind farms because of the low entrainment which delays the wake recovery.

It was decided to apply the previous research findings to a real case study. Instead of re-optimizing an existing wind farm, it was decided to investigate the upgrade possibilities while keeping the existing turbines. Finally, the offshore farms were preferred as it was found that the optimization is more efficient at such conditions.

7.5 Findings from “Large Wind Farm Layout Upgrade Optimization”

In this paper, the large wind farm layout upgrade optimization problem was introduced. It has not been studied previously in the literature. The proposed upgrade methodology was based on adding new and different turbines to the existing farm either within the farm area or as an extension. The famous Horns Rev 1 large offshore wind farm was taken as a case study. The existing 80 turbines were kept as they are while 63 and 88 turbines were added inside and outside the original farm area, respectively. Nineteen Vestas commercial turbines of rated power ranged from 1.8 to 3.45 MW were included in the selection. The following remarks summarize the output from this paper:

1. Existing wind farms can be effectively upgraded by increasing the energy production by adding new turbines, while keeping the existing turbines unchanged.
2. Wind farm layout upgrade optimization for offshore farms is recommended if it is done within the original farm area and infrastructure. In this case, a significant increase in the energy production can be added while keeping the cost of energy in reasonable range.
3. Wind farm layout upgrade optimization is an efficient solution to increase the utilization of the existing area instead of installing new costly farm(s).

4. Having a range of commercial turbines for selection as well as allowing variation in height is believed to be a powerful tool in wind farm layout upgrade optimization.
5. The resulted optimum layouts are greatly dependent on the proposed upgraded layout as well as the optimization objective.
6. The hub height variation is beneficial not only to reduce the wake interference and hence increase the energy production, but also to reduce the total cost as well as the cost of energy.
7. By including a wide range of commercial turbines in the selection, a wide band of feasible optimum layouts is obtained which provide a trade-off between energy production and cost.
8. Among commercial turbines having the same rated power, the priority in selection should be biased towards the turbines with larger diameter and lower rated speed.
9. The random independent multi-population technique reduces the execution time for the genetic algorithm without compromising the outcomes.

Subsequent to submitting Chapter 6 for publication, a formula was developed including the turbine technical data given in Table 6.1 to represent the resulted NCOEI (Figure 6.6b). The best fit, shown in Figure 7.1, was denoted Turbine COE Comparison Index (TCCI)

$$TCCI = \frac{P_r^{0.783}}{D^{0.527}} \quad (7.1)$$

Equation (7.1) has a maximum local deviation of 5.5 %. This formula should play an important role in comparing two or more turbines from the COE point of view. It is clear from Equation (7.1) that the turbine diameter has an important inverse effect while the rated power is dominant. The effect of the rated speed was found to be negligible, the reason is believed to be the relatively high wind speeds considered in the present work.

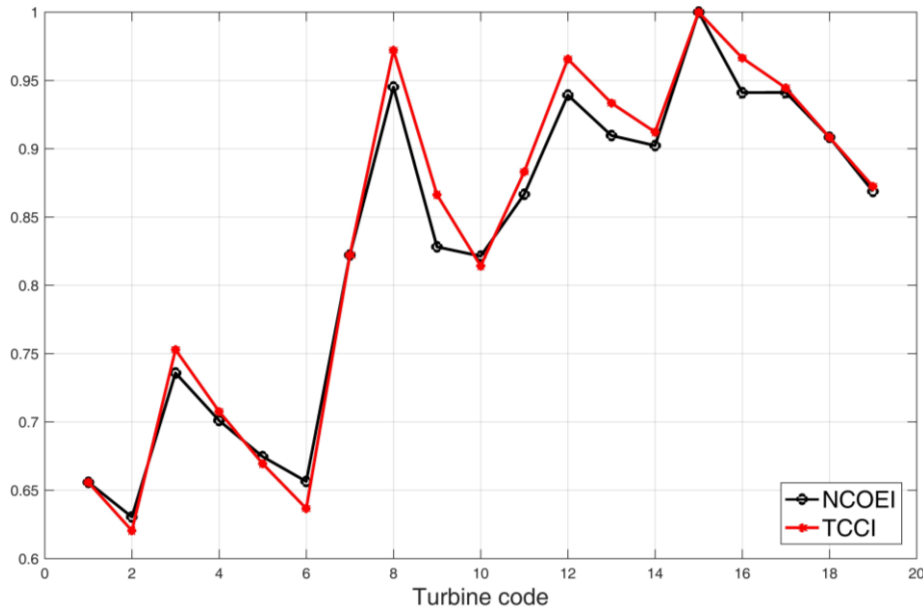
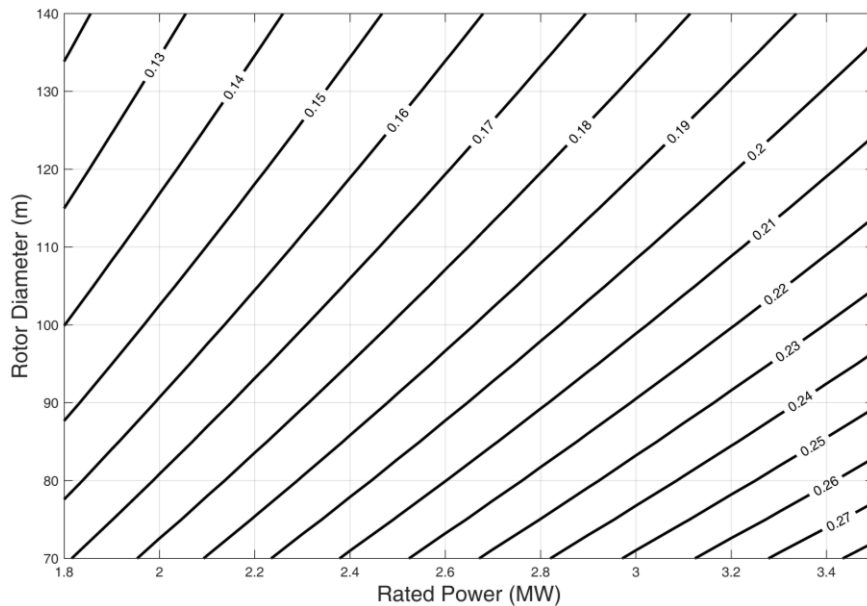


Figure 7.1: TCCI vs NCOEI.

Moreover, Figure 7.2 shows the dependence of TCCI on P_r and D according to Equation (7.1), within the investigated ranges. Beside the opposite effects of P_r and D on TCCI, Figure 7.2 also predicts that the use of large diameter is crucial for turbines with high rated power.

Figure 7.2: TCCI dependence on P_r and D .

7.6 Suggestions for Further Investigations

The present research used classical models of wind turbine wake, along with some simplified installations, i.e. offshore as they do not have complex topography, and some complex parameters were ignored. The following suggestions for further investigations address some of these issues:

1. The study of onshore sites with complex terrain, and hence more complex spatial variations in the wind speed.
2. Further improvement to the optimization performance for WFLO, either by GA or by considering new powerful optimization techniques.
3. Using different turbines and hub heights in the farm layout significantly increases the contribution of partial wake interference, which is believed to increase the dynamic loading on the rotor. The minimization of dynamic loading is suggested as a new aspect to WFLO.
4. For very large farms, the effect of wake meandering and yaw alignment delay on the energy production are suggested to be considered.
5. Continuous improvements on cost analysis is suggested in order to be more accurate while being simple and general. One area on which very little information was available was the dependence of tower cost on height. Improved estimates for this would be valuable given the demonstration of the importance of varying this height.
6. The collaboration between WFLO and Co-operative control is believed to be possible and beneficial. In other words, future WFLO should consider more than just turbine siting.